UNIVERSITY OF
BIRMINGHAM

THE BIOPHYSICAL EFFECTS OF LOW INTENSITY ULTRASOUND ON THE MORPHOLOGY, GROWTH AND DIFFERENTIATION POTENTIAL OF BONE MARROW-DERIVED MESENCHYMAL STEM CELLS

and

THE DYNAMIC CHANGES IN HISTONE MODIFICATIONS ON THE HOXB GENES THAT ACCOMPANY EMBRYONIC STEM CELL DIFFERENTIATION

By

Hafsa Munir

A thesis submitted to the University of Birmingham for the degree of

MASTER OF RESEARCH

Institute of Biomedical Research
College of Medical and Dental Sciences
University of Birmingham
August 2012

THE BIOPHYSICAL EFFECTS OF LOW INTENSITY ULTRASOUND ON THE MORPHOLOGY, GROWTH AND DIFFERENTIATION POTENTIAL OF BONE MARROW-DERIVED MESENCHYMAL STEM CELLS

By

Hafsa Munir

ACKNOWLEDGEMENT:

I would like to thank the supervisor for my first project Dr Ben Scheven for his support and enthusiasm throughout the project. I would also like to sincerely thank the technicians in the lab, Gay and Michelle who guided me through the practical aspects of the project. Furthermore, I would like to thank the PhD students in the Dental School for their friendly attitudes and help with the practical planning of the experiments. I would especially like to thank Upen Patel for teaching me how to use the ultrasound device despite being incredibly busy.

I would sincerely like to thank the supervisor for my second project Dr Laura O'Neill for her optimism, dedication and encouragement. I would also like to thank Professor Bryan Turner for his time and input to the project. I am grateful to the other members of the group particularly Dr John Halsall who guided and aided me in the day to day life in the lab. I would lastly like to thank Dr Karl Nightingale for always being there to offer advice.

ABSTRACT:

Mesenchymal stem cells (MSCs) are considered to be an attractive target for cell-replacement therapies due to their extensive self-renewal and multipotent differentiation capabilities. Applying ultrasound to soft tissue lesions and bone fractures has been shown to promote repair of damaged tissue. It was suggested that ultrasound stimulates repair by activating bone-marrow derived MSCs (BMSCs) to begin proliferating and differentiating to replenish the tissue. Therefore, the aim of the study was to analyse the biophysical effects of low-frequency, low-intensity ultrasound on the differentiation and colony forming unit ability of BMSCs. To test this colony forming unit assays were performed on ultrasound treated and untreated cells and cell staining was used to analyse the effects. Furthermore, to determine the intracellular response to ultrasound stimulation, the expression of ultrasound-sensitive genes was also analysed by reverse-transcriptase PCR.

The results obtained in this study showed that BMSCs treated with low-frequency, low-intensity ultrasound did not generate a greater number of colonies than untreated cells. Colony size was found to be unchanged by treatment. Furthermore, ultrasound treatment did not appear to enhance the differentiation potential of BMSCs down the osteogenic lineage. This data suggests that low-frequency, low-intensity ultrasound does not appear to activate BMSCs in culture.

Table of Contents

Table of Figures

1. INTRODUCTION:

1.1. The potential application of mesenchymal stem cells in regenerative medicine:

Mesenchymal stem cells (MSCs) are a rare population of multipotent cells that are capable of self-renewing and differentiating into several mesenchymal lineages namely osteocytes, chondrocytes, and adipocytes as well as various endodermal lineages such as neurones (Figure 1-1). MSCs were initially isolated from the bone marrow (BM) stroma, however several studies have shown that these cells are also present in the brain, spleen, dental pulp and umbilical cord [1, 2]. MSCs are activated following injury and subsequently migrate to the site of damage where they secrete trophic factors to modulate the immune system and stimulate the proliferation of local cells. During tissue repair these cells also undergo lineage-specific differentiation to regenerate the tissue following injury [3]. Due to their extensive self-renewal and regenerative capabilities, MSCs represent an attractive cell-based therapy for the treatment of degenerative diseases.

MSCs are generally isolated based on the ability to adhere to tissue culture plastic and must be expanded *in vitro* to obtain sufficient numbers for therapeutic applications. However several studies have shown that MSCs begin to lose their SC features and undergo senescence during prolonged culture [4]. Therefore, MSCs can only be used therapeutically at an early passage. To overcome these issues several studies have recently been conducted to increase the yield of MSCs in culture by either enhancing the initial isolation of cells from the BM or by optimising the conditions for MSC expansion *in vitro* [1]. Bianchi et al. (2003) showed that supplementing the culture medium with basic-fibroblast growth factor increased the life span of MSCs whilst maintaining their morphological features and differentiation potential [5]. Furthermore, it was found that coating flasks with components of the extracellular matrix

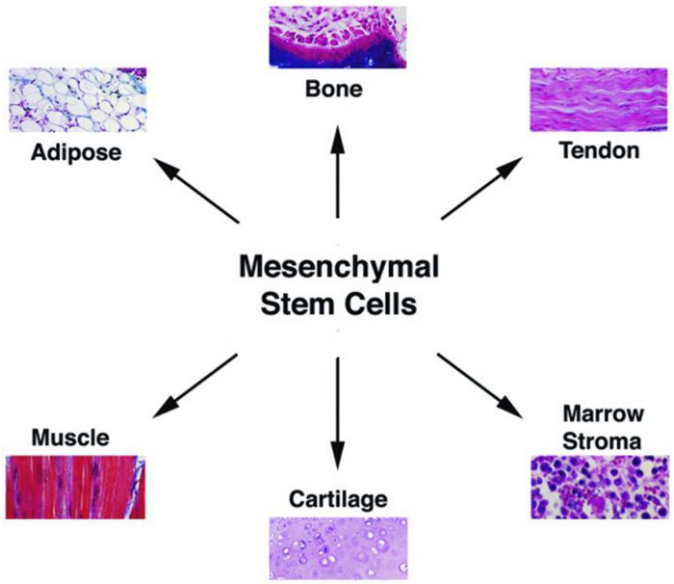

Figure 1-1: Multipotent differentiation potential of MSCs. Under appropriate culture conditions MSCs are able to differentiate into a number of different cell types including osteoblasts, chondrocytes, adipocytes and myocytes [31].

(ECM), including fibronectin and collagen, increased the yield of MSCs obtained from the BM [6]. This is likely due to an increase in the interaction with cell surface receptors such as integrins which mediate both attachment and proliferation of cells [7]. Similarly various types of mechanical stimuli such as shear stress and low intensity pulsed ultrasound (LIPUS) can influence cell proliferation, migration and adhesion. These mechanical stresses are thought to stimulate cell surface receptors and in turn activate downstream signalling pathways to induce these effects [8]. Therefore US is a promising intervention for increasing the therapeutic potential of MSCs.

1.2. Characteristics of therapeutic ultrasound:

US is an inaudible (high frequency) mechanical acoustic pressure that produces a range of effects when transmitted through biological tissues [9]. While US is mainly used clinically as a diagnostic tool, it is now recognised that US also has therapeutic benefit. US can facilitate the delivery of drugs (via contrast-enhanced US), the repair of soft tissue lesions and LIPUS has received FDA approval for the treatment of bone fractures [9]. US treatment distinguishes itself from other mechanical stimuli because it is both non-invasive and easy to administer with fewer side effects [10]. Therefore, therapeutic US has received attention for its potential applications in both tissue engineering and regenerative medicine.

The mechanical waves created by US transducers are generated by converting electrical energy into acoustic pressure. The waves in turn propagate through the biological tissue by causing collisions and vibrations with molecules in the sample. These progressively become attenuated during passage through the tissue as a result of absorption or dispersion of the waves [9]. Therefore the amount of energy produced by the US transducer that actually reaches the therapeutic site deep within the tissue is significantly lower than the amount of

energy initially applied. The intensity of energy that reaches the specific site within the tissue is dependent on a number of parameters including the amplitude, intensity and frequency of the US wave as well as the thickness of the tissue [9]. Therapeutic US is generally used at frequencies ranging from 1-3 MHz. Low frequency US (0.75-1 MHz) is normally recommended for bone fractures since the waves are able to penetrate deep into the tissue. Conversely high frequency (1.5-3 MHz) waves are generally used for more superficial injuries in easily accessible tissues (Figure 1-2) [11]. The dose of US can be adjusted depending on the type of injury sustained by altering the amplitude and intensity of the waves generated.

1.3. The biophysical effects of ultrasound:

US has been previously shown to exert both a thermal and non-thermal effect on biological tissues which in turn induce a range of cellular responses that promote tissue repair and regeneration. The thermal effects are commonly observed when high frequency and high intensity US waves are applied to the tissue that cause the temperature to rise above normal levels (40-45°C) for a prolonged period of time (longer than 5 minutes). These effects include an increase in tissue blood flow, an increase in the extensibility of collagen and the induction of a mild inflammatory response [9, 12]. While these effects have therapeutic benefit, prolonged heating has been shown to cause tissue damage and eventually destruction. Tissue heating is negligible when low-frequency, low-intensity US is administered.

The non-thermal effects of US namely cavitation and acoustic microstreaming are considered to have more therapeutic benefit than the thermal effects. Cavitation refers to the formation of gas filled air bubbles that expand and collapse in response to changes in tissue pressure caused by US waves [13]. Acoustic microstreaming is a phenomenon that occurs when energy

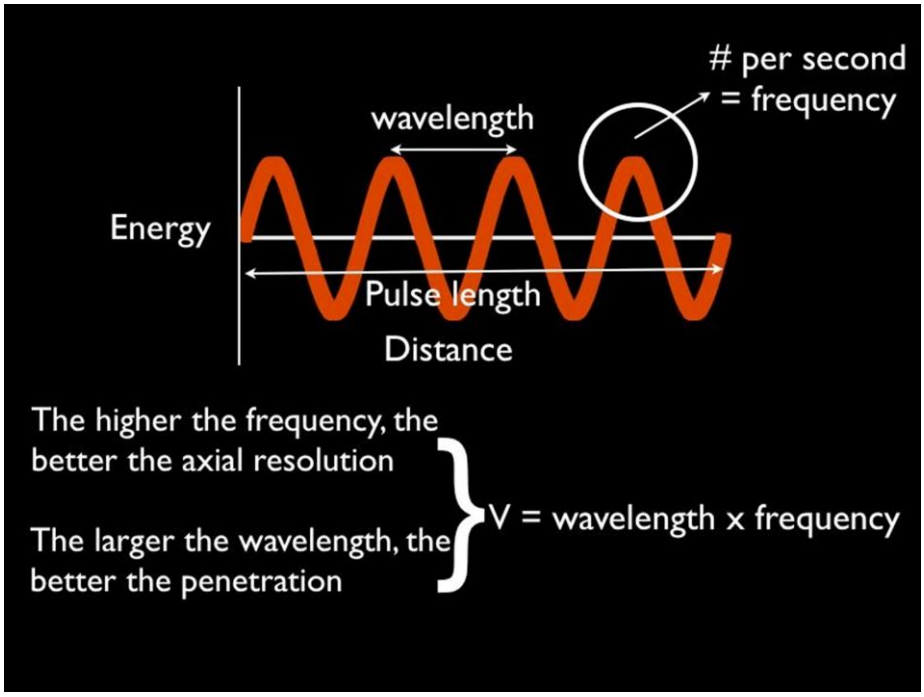

Figure 1-2: The properties of an US wave. The waves are a form of mechanical energy that have a number of key features. The frequency of the wave refers to the number of peaks per unit time while the wavelength is the distance between each peak. High frequency US are useful for superficial injuries but due to the attenuation effect on US waves it cannot be used to treat injuries that are much deeper. Therefore for treatment of bone injuries, low frequency and long wavelength US are used [32].

from the US waves are transferred to the tissue fluid causing it to flow in the direction that the waves are propagating (Figure 1-3) [13]. The pressure changes induced by these effects are thought to enhance protein synthesis, increase blood flow, activate fibroblasts and induce bone healing [9].

Doan et al. (1999) initially observed that LIUS was able to enhance the proliferation of human fibroblasts, osteoblasts and monocytes [14]. Since then several studies have been carried out to test the effects of US on the expansion of many different cell types such as rabbit intervertebral disc cells, chondrocytes (grown on 3D scaffolds) and human periodontal ligament cells [15-17]. However, other studies have shown that LIUS had little or no effect on cell proliferation. Ebisawa et al. (2004) observed that expansion of MSCs was not enhanced by LIPUS treatment [18]. The discrepancies in the findings in these studies can be attributed to differences in US protocols used, namely differences in the intensity of US (ranging from 30-200 mW/cm^2). Differences in the cell source, culture environment, presence of growth or differentiation factors and duration of the treatment may also have affected the outcome of these studies [19].

Recent studies have consistently shown that LIUS increases matrix production by many different cell types *in vitro* [16-18, 20]. This effect has been well documented in chondrocytes and osteoblasts [20]. LIPUS was also found to promote differentiation of chondrocytes, osteoblasts and MSCs by inducing the expression of lineage-specific genes that coordinate cellular maturation [21]. These findings indicate that US enhances cell proliferation, growth and differentiation.

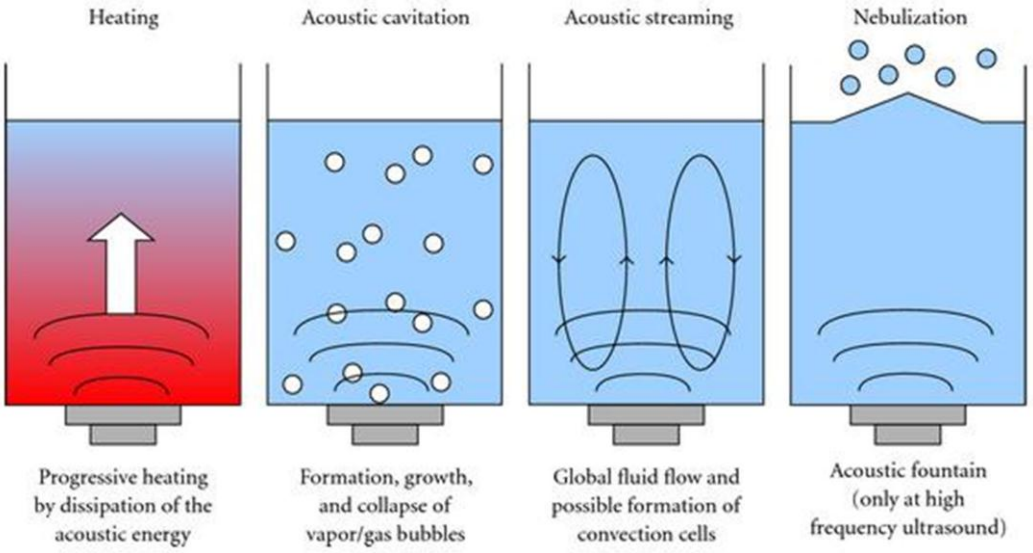

Figure 1-3: The biophysical effects of US. Generally US waves cause heating of biological tissues as the acoustic energy of the wave dissipates. This normally occurs as a result of prolonged exposure to US or when high frequency US is used. Cavitation and microstreaming are responsible for the therapeutic effects of LIUS. Microstreaming causes changes in flow of tissue fluid which can perturb the cell membrane and alter its permeability and the function of its components [13].

1.4. The mechanism of action of ultrasound:

Although the effects of US have been well documented for a range of cell types, the molecular mechanisms by which it alters cellular processes has not yet been elucidated. Several groups have attempted to determine the impact of LIUS at a molecular level with limited success. Tang et al. (2007) observed that stimulating osteoblasts and chondrocytes with LIPUS transiently increases the expression of specific integrins, namely $\alpha_5\beta_1$ [22, 23]. Integrins are heterodimeric transmembrane proteins that consist of an α and β subunit that provide a link between the extracellular matrix (ECM) and the intracellular cytoskeletal components and actin filaments. Integrins are thought to function by undergoing conformational changes which activate them and reveal their ligand binding site. This in turn enables the integrins to bind to cytoskeletal components and other signalling molecules to activate several intracellular signalling pathways [24]. These pathways are normally activated in response to mechanical stress thus enabling the cells to react to changes in their physical environment. Therefore integrins act as sensitive mechanoreceptors on the surface of cells.

US waves generate pressure which is transferred to adherent cells via interactions with the ECM. Lai et al. (2010) recently hypothesised that LIPUS may activate integrins by perturbing the cell membrane and mechanically inducing a conformational change in their structure in response to vibrations in the ECM. This theory is termed the "Frequency Resonance Hypothesis" [25, 26]. The increase in integrin expression observed in chondrocytes and osteoblasts after LIPUS treatment was shown to activate a number of downstream kinases including focal adhesion kinase (FAK), Phosphatidylinositol 3-kinases (PI3K) and Mitogen activate protein kinase (Figure 1-4).

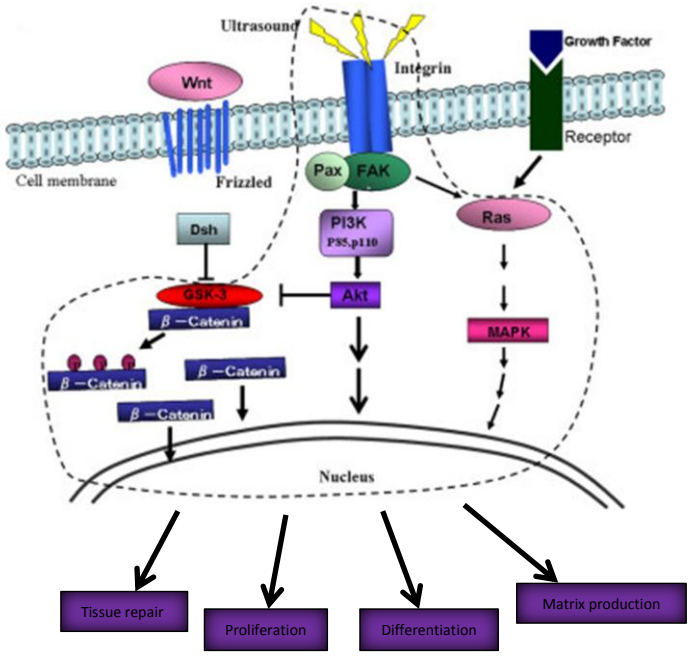

Figure 1-4: Intracellular signalling pathways activated by LIUS. Treating cells with LIUS induces conformational changes in the structure of several integrins which in turn causes these proteins to become activated. Integrins then activate a number of downstream signalling pathways namely the PI3K/AKT, Ras/MAPK and the canonical Wnt signalling pathways. Activation of these integrin-mediated signalling pathways induces the expression of genes that are responsible for regulating a wide range of biological processes such as tissue repair, cell proliferation and differentiation and the production of components of the extracellular matrix [27].

Integrin pathways have also been shown to enhance cell proliferation and differentiation [27]. For example Tang et al. (2006) found that inhibiting PI3K, FAK and integrin $\alpha_5\beta_1$ in osteoblasts antagonised the US-induced increase in cyclooxygenase 2 (COX-2) expression. In response to injury COX-2 normally enhances the production of prostaglandins which promote osteoblast proliferation and differentiation. These findings indicate that US promotes bone formation by activating the integrin/FAK/PI3K/AKT pathway to induce the expression of COX-2 [28]. Several distinct pathways that enhance proliferation and differentiation have been implicated in the response to US stimuli, however their precise role has not been elucidated.

Furthermore the actin cytoskeleton is a key regulator of cell migration, morphogenesis and differentiation. Activation of integrins by LIUS may induce changes in the actin cytoskeletal structure which activate several downstream signalling pathways [29, 30]. Given the differences in the way the studies are conducted such as differences in US intensities used, different treatment cycles or whether continuous or pulsed US is applied, it is not surprising that these studies have generated such diverse results. Therefore a more universal US protocol should be applied to study the effects that the mechanical stress is having on the cells. While a few studies have attempted to optimise the US treatment used, there remains to be a universally applicable US treatment regime. The lack of standardisation of treatment may hinder future research in this area as differences in the type of treatments used will affect the type of response generated.

1.5. Hypothesis:

Low intensity, low frequency ultrasound is capable of enhancing the proliferation, adherence and osteogenic differentiation potential of rat bone marrow derived MSCs (BMSCc).

1.6. Aims:

LIUS has the potential to stimulate repair and regeneration of bone tissue. It has recently been suggested that LIUS may activate BMSCs causing them to proliferate and differentiate into bone forming cells. However, the effects of LIUS on BMSCs have not yet been elucidated [8, 30]. Therefore the aim of this study was to determine the biophysical effects of LIUS on rat bone marrow derive MSCs. Generally LIPUS treatment uses high frequencies ranging from 1-3 MHz to promote tissue healing. However, in the current study low intensity (25mW/cm^2), low frequency US (45 kHz) was tested.

Low frequency US was used as it can penetrate deeper into tissues than higher frequency US which makes it more suitable for treating hard tissues such as bone. Also previous studies have shown that kHz frequency US promotes cell proliferation, migration and differentiation of osteoblasts to a similar or greater degree than high frequency US [33]. Furthermore, high frequency LIPUS treatment has a short interval where the tissue receives pulses at a kHz frequency and it has been suggested that these pulses may be responsible for the biological effects observed after treatment [34]. During the study only a single five minute dose of continuous US was applied to the cells in order to observe the immediate effects of US on cell proliferation, differentiation and morphology. Continuous US treatment was used in order to supply the cells with a greater dose of US.

To test the biophysical effects of US, colony-forming unit assays were performed to test whether US is able to enhance the adherence and proliferation of BMSCs. Cells were also

stained with Calcein AM in order to test whether low frequency US treatment creates pores within cells (sonication) which would enable calcium influx into the cells. Calcium would in turn cause exocytosis of vesicles containing growth factors to stimulate cell growth. The effect of low frequency US on the osteogenic differentiation potential of BMSCs was also tested to observe whether US can promote differentiation down the osteoblast lineage. This would confirm whether US is promoting bone healing by stimulating BMSCs to undergo differentiation down the osteoblast lineage. Lastly, to test whether low frequency US has the same effect on integrin signalling pathways as therapeutic LIUS, PCR was used to analyse the expression of integrins α_5 and β_1 which are normally upregulated after US treatment.

2. MATERIALS AND METHODS:

2.1. Isolation and culture of rat bone marrow-derived mesenchymal stem cells:

6 weeks old Wistar-Han rats (weighing 200-250 grams) were sacrificed by cervical dislocation and both femurs were removed. The adherent tissue was removed from the bones and the epiphyses were cut off. The BM was aspirated by inserting a fine needle into the diaphysis of the bone and flushing the cells out with 10 ml of culture media. The BM was centrifuged at 800 rpm for 5 minutes and then resuspended in fresh growth media consisting of Alpha-modified Eagle's medium (Alpha-MEM; Biosera) supplemented with 20% Foetal Bovine Serum (FBS; Sigma-Aldrich) and 1% Penicillin and Streptomycin. The cells were plated in 75cm^2 tissue culture flasks (Starstedt) and incubated at 37^{o}C and 5% CO_2. After 24 hours the media was changed to remove non-adherent blood cells and after a further 3 days the cells were washed repeatedly in PBS (to remove non-adherent cells) and fresh media was added. The cells were passaged when the flask became 70-80% confluent with Trypsin/EDTA (Invitrogen). After the first passage, the media was supplemented with 10% FBS for all subsequent cultures.

2.2. Ultrasound stimulation:

Cells were seeded onto a 6-well plate and cultured for 24 hours to enable the cells to adhere. The anti-reflective chamber (used to house the 6-well plate during US treatment) was sterilised using 70% industrial methylated spirit (IMS; VWR) and then filled with sterile deionised water. The chamber was then placed in the incubator for 24 hours prior to treatment. 24 hours before treatment, the US transducer (DuoSon) was also soaked in IMS. 30 minutes prior to treatment, the DuoSon machine, hotplate (used to maintain the temperature of the cells at 37^{o}C during treatment) and clamp stand were sterilised with IMS

and allowed to air-dry in the laminar flow hood. The media in the 6-well plates was then removed (to take off any non-adherent cells which could interfere with the US waves) and 9 ml of fresh culture media was added to each well. Immediately before treatment the transducer was rinsed with growth media. The 6-well plate was inserted into the anti-reflective chamber and placed on the hotplate. The transducer was placed in the clamp stand and lowered by ~2mm into each well. The cells were treated with US for 5 minutes at an intensity of 25 mW/cm^2. After treatment, the media was removed and 2 ml of media was added to each well.

2.3.1. Colony-forming unit (CFU) assay:

BMSCs were seeded at a density of 140 cells/ cm^2 and treated with or without US. The cells were cultured for 7 days and then stained with Methylene Blue dye (MB; Hopkin and Williams) to visualise the colonies. Initially the cells were fixed in neutral-buffered formalin for 30 minutes at room temperature. 0.1% MB dye was made up in 0.01 M of Borate buffer (0.1M Boric acid and 0.01M Sodium tetraborate pH 8.6; Sigma-Aldrich) and then added to the cells for 30 minutes. The residual dye was washed off with deionised water and photographs were taken of the wells (Nikon D40) and number of colonies were counted using ImageJ analysis. Neutral Red (NR diluted in Dimethyl sulfoxide [DMSO]; Sigma-Aldrich) was also used to stain colonies in CFU assays. 1ml of dye was added to the cells for 2 minutes and then removed. Residual dye was washed off with deionised water and photographs were then taken.

2.3.2. Semi-quantitative analysis of colonies using ImageJ:

Given that a colony is defined as a cluster of 50 or more cells, the number of colonies was estimated by setting the threshold colony size at 8000 μm^2. This value was chosen since the

average size of a BMSC is ~160μm^2 (40μm length and 4μm width) and 50 of them make up a colony. A cluster of pixels that exceeded this value was considered to be a colony (Figure 2-1). A heat map and a table (listing the number and sizes of the colonies) were generated. To calculate the number of cells in each well, the area of each colony (μm^2) was divided by the average size of a BMSC (160 μm^2). Then the number of cells in each colony were added together to give the total cell number.

2.4. Quantification of Methylene Blue dye:

Cells were seeded at a range of densities and stained with MB. The wells were rinsed thoroughly and an elution solution (0.5M concentrated Hydrochloric acid in 70% ethanol) was added for 5 minutes. The solution was collected and centrifuged at 12,000 rpm for 3 minutes to remove any cells. The dye was transferred to a 96-well plate and the absorbance was measured (630nm). A standard curve was generated (Figure 2-2). The curve was then used to determine the number of cells present after a CFU assay was performed on cells treated with or without US.

2.5. Osteogenic differentiation:

Cells were seeded at 140 cells/ cm^2 and treated with or without US. 24 hours later osteogenic differentiation media (consisting of Alpha-MEM high glucose supplemented with 10% FCS, 10nm Dexamethasone, 10mM β-Glycerophosphate and 50μg/ml Ascorbic Acid; Sigma-Aldrich) was sterile filtered and then added to the cultures. The media was changed every 48 hours for 2 weeks. The cells were then stained with Alkaline Phosphatase using the Alkaline Phosphatase, Leukocyte Kit 86-C (Sigma Aldrich GmbH) according to the manufacturer's protocol. NR was used to counterstain the cells.

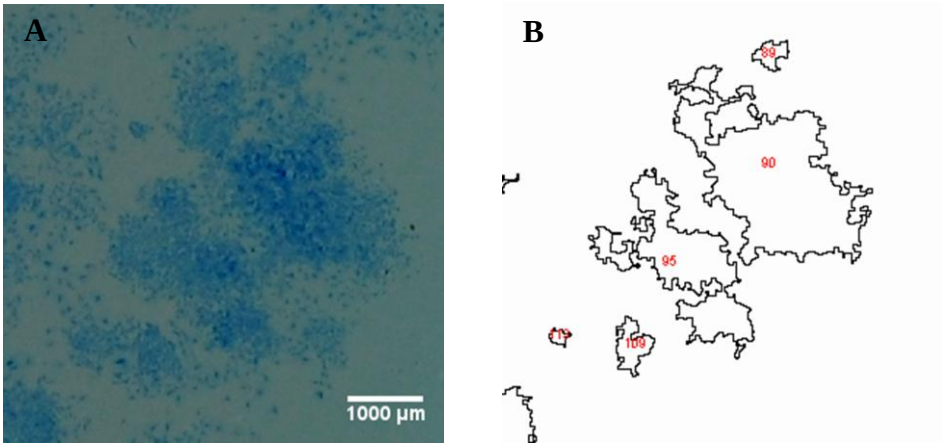

Figure 2-1: ImageJ analysis of colonies. An image of the MB stained colonies were taken (A) and a heat map (B) was generated based on the criteria for the size of a colony.

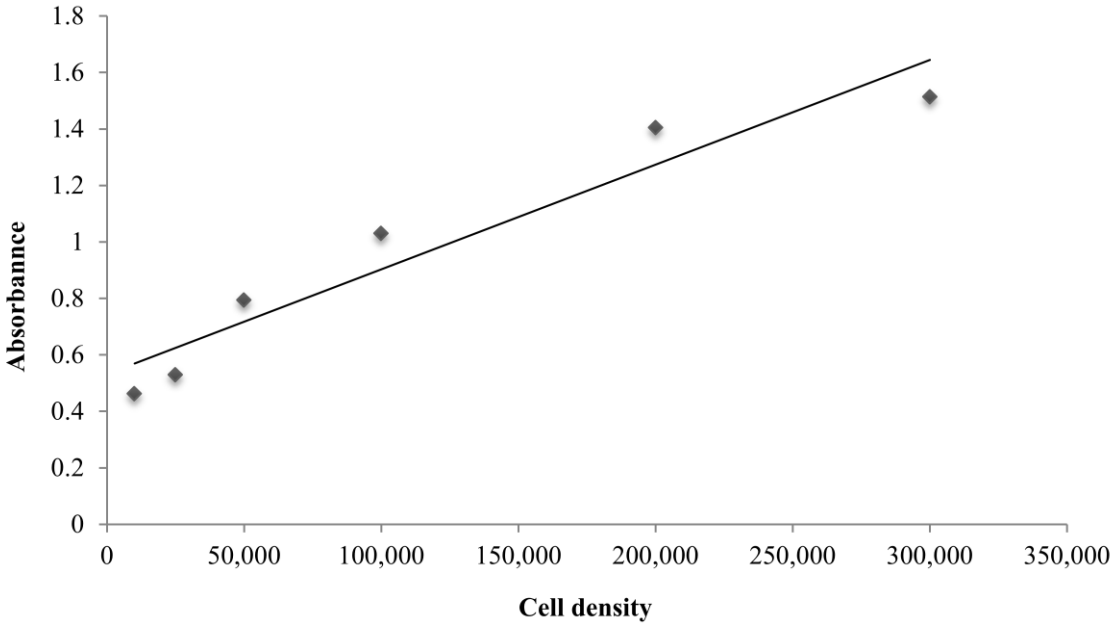

Figure 2-2: Standard curve for determining cell density. MB dye was eluted from wells containing cells at a range of cell densities. The absorbance was then measured for each density and a curve was generated. The equation for the straight line curve is y = 4E-06x + 0.5323. The equation was used to determine the number of cells present after a CFU assay was performed on cells either treated with or without US after eluting the dye and measuring its absorbance.

2.6. Calcein AM staining:

Cells were seeded at a density of 100,000 per well and incubated with a 1 mg/ml Calcein AM (in anhydrous DMSO; Biotium) for 30 minutes at 37^{o}C and 5% CO_2. Cells were washed with PBS to remove any residual stain and then treated with or without US (as described above). Samples of media from each well were transferred to a 96-well plate and the fluorescence emission was detected using the Twinkle microplate fluorometer (Berthold technologies).

2.7.1. RNA extraction, quantification and cDNA synthesis:

6 x 10^5 cells were treated with or without US and incubated for either 4 or 24 hours and subsequently harvested. The cells were trypsinised and pelleted. Total RNA was extracted using the RNeasy mini kit (Qiagen) according to the manufacturer's instructions. The concentration (ng/µl) and purity ($A_{260/280}$) of RNA was quantified using a Biophotometer (Eppendorf). cDNA was then synthesised by adding 2µg of RNA (12µl) to 2µl of oligo-dT primers and heating it to 80^{o}C for 10 minutes. 6µl of mastermix (containing 2µl 10x buffer RT, 2µl dNTPs, 1µl RNase inhibitor and 1µl Omniscript reverse transcriptase; Qiagen) was then added to each sample and incubated at 37^{o}C for 60 minutes and then at 95^{o}C for 5 minutes. The cDNA was concentrated using Microcon centrifugal filters (Millipore) according to the manufacturer's instructions.

2.7.2. Reverse-transcriptase PCR (RT-PCR):

50ng of cDNA from each sample was added to a PCR mastermix consisting of 12.5µl RED Taq (PCR ready mix; Sigma-Aldrich), 2µl of forward and reverse primer mix (Table 1) and 9.5µl of RNase free water. The PCR was carried out in a Mastercycler Gradient Thermal Cycler using the appropriate cycling conditions (95^{o}C for 30 seconds, 60^{o}C for 20 seconds and 72^{o}C for 20 seconds). The products were run on a 1.5% agarose, 1xTris-acetate EDTA

gel at 120V for 30 minutes. The gel was then transferred to a G:BOX (Syngene) imaging system in order to visualise the gel. ImageJ analysis was then used to quantify the density of the bands.

Gene	Forward primer	Reverse primer	Product size (bp)	Cycle number	Manufacturer
Gapdh	5’-GGCATTGCT CTCAATGACAA-3’	5’-TGTGAGGGA GATGCTCAGTG-3’	233	29	Invitrogen
Integrin α_5	5'-CCTAGGTCTG CTCATCTATGTCC-3'	5'-GGCTTGAGC TGAGCTTTTTC-3'	93	37	Invitrogen
Integrin β_1	5'-ATCATGCAG GTTGCAGTTTG-3’	5’-CGTGGAAAA CACCAGCAGT-3’	72	37	Invitrogen

Table 1: A list of rat primers used to carry out the RT-PCR.

3. RESULTS:

The aim of this study was to examine the short-term biophysical effects of low-intensity, low-frequency continuous US stimulation on the proliferation, differentiation and colony forming unit (CFU) ability of BMSCs. Furthermore, the expression of US-sensitive genes was also examined.

3.1. The effects of ultrasound on cell morphology:

Cell morphology is considered to be a good indicator for the cells responsiveness to mechanical stimuli such as US since cells often change shape and size when exposed to mechanical stress. In osteoblast cells LIPUS was found to increase cell size as well as alter the organisation of actin cytoskeleton [36, 37]. To assess whether US can alter BMSC morphology, cells were treated with or without US and photographs were taken 1, 2 and 7 days later. Figure 3-1 shows that 1 day after treatment, the US stimulated BMSCs exhibited a neuronal-like morphology. The cells displayed long projections and had become flattened and more spread out, whereas the non-stimulated cells displayed a fibroblast-like morphology more typical of BMSCs.

The non-stimulated cells maintained this structure during prolonged culture while the US stimulated cells were found to lose the neuronal-like morphology 2 days after treatment. The cells then adopted the typical fibroblast structure similar to the non-stimulated cells. However even up to 7 days after treatment the cells remained more flattened and spread out than non-stimulated cells (Figure 3-1). This indicates that low-frequency US is able to alter the morphology of BMSCs.

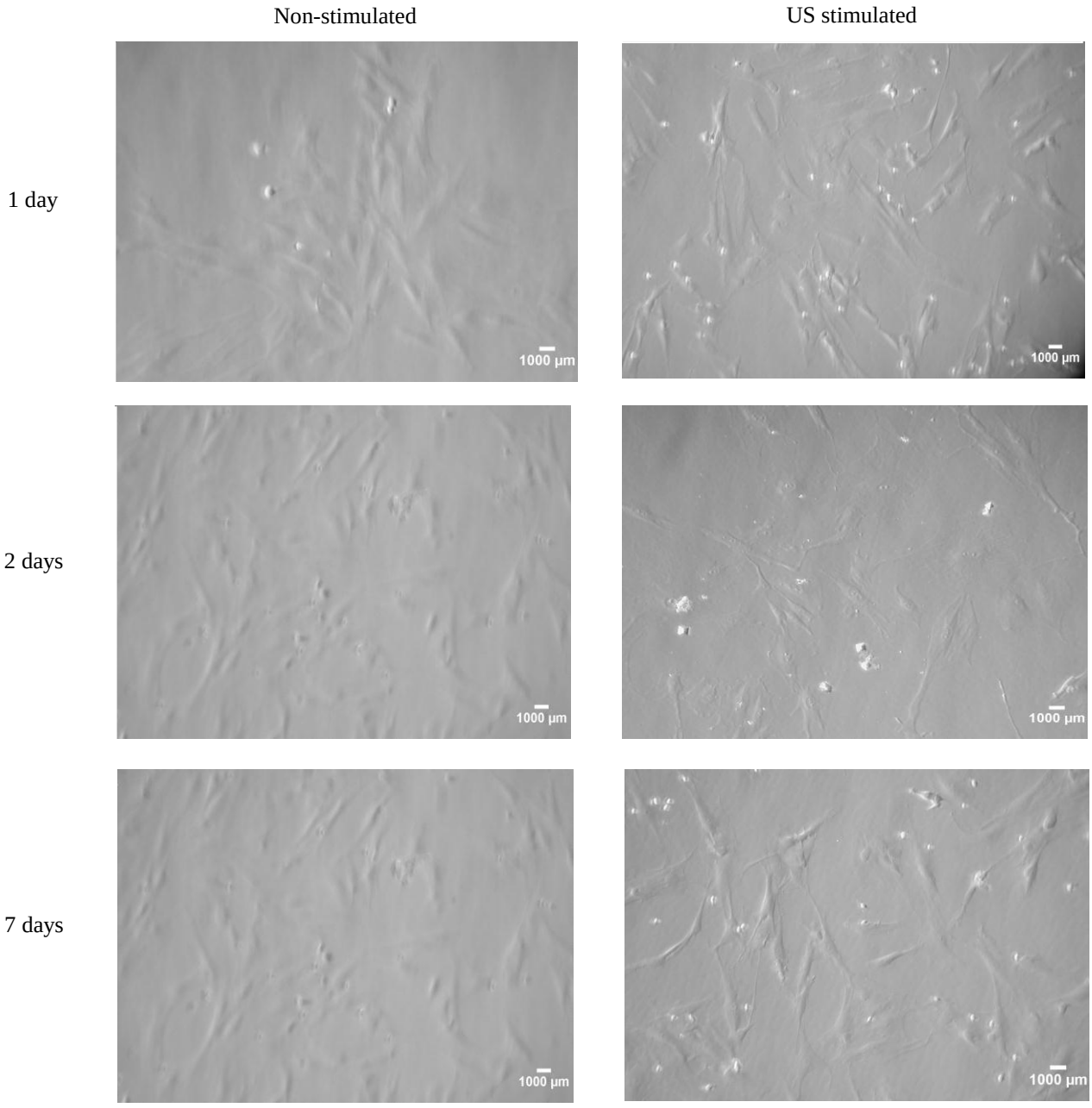

Figure 3-1: The effects of US on cell morphology, BMSCs were treated with or without US and photographs were taken after a number of days indicated to observe the changes in cell morphology induced by therapeutic low-frequency, low-intensity US treatment.

3.2. Optimum cell seeding density for colony forming unit assays:

Initially BMSCs were seeded at a range of densities and cultured for 7 days. A CFU assay was then performed, to determine at which seeding density a sufficient number of colonies are generated that don't overlap, to allow the colonies to be easily distinguished. The cells were stained with Methylene Blue (MB) and ImageJ was used to quantify the number of colonies. Figure 3-2 shows that the optimum seeding densities were 2,500 and 1,250 cells given that a significant number of colonies were identified and were easily distinguished by ImageJ. At higher cell densities while there were a greater number of colonies generated but were difficult to distinguish. At lower seeding densities, very few colonies were generated which would be insufficient for the analysis required.

The aim of this study was to test the effects of US on a pure population of primary BMSCs. However, it has previously been shown that primary BMSC cultures often contain a population of osteogenic progenitors that adhere to culture plastics. To identify the numbers of progenitors that were present at each seeding density Alkaline Phosphatase (ALP) staining was performed. ALP was selected as it is an early marker of bone mineralisation and is commonly used to identify osteogenic progenitors in culture. Cells were counterstained with Neutral Red (NR) and ImageJ analysis was performed. Figure 3-3 shows that a greater number of progenitors were identified when the seeding density was higher. The best seeding density was 1,250 cells since there were a sufficient number of colonies generated with very few ALP positive cells present. Based on this data, the optimum seeding density was 1,250 (130 cells/cm^2) cells and for all subsequent CFU assays cells were seeded at this density.

It was observed that there was a significant difference in the sensitivity of the MB and NR stains where greater numbers of colonies were identified after NR staining compared to MB

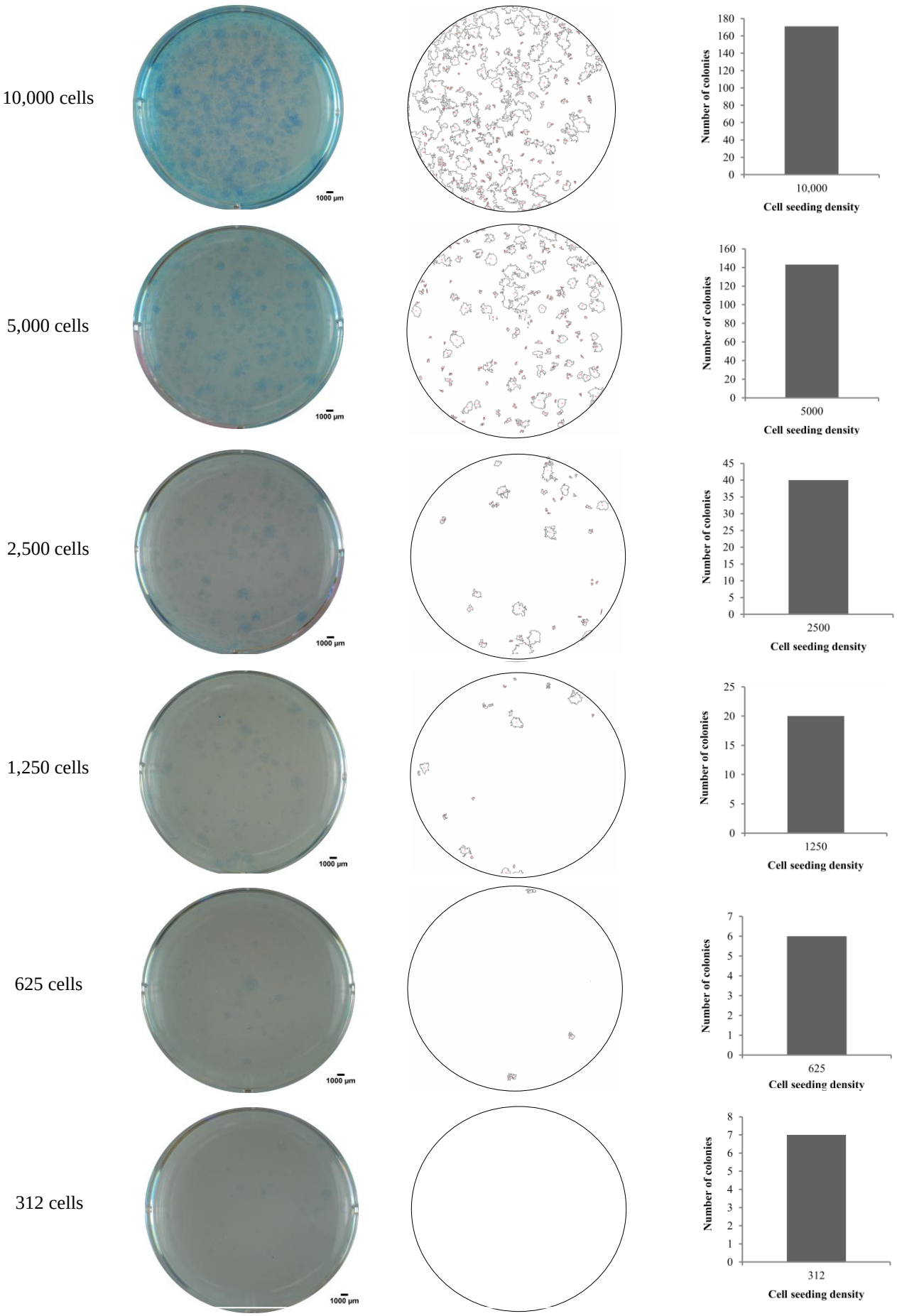

Figure 3-2: A CFU assay to determine the optimum cell seeding density. Colonies were stained with MB and images were taken of the wells (left). ImageJ was used to analyse the number of colonies in each well. A heat map (centre) and data regarding the number and sizes of the colonies was generated (right).

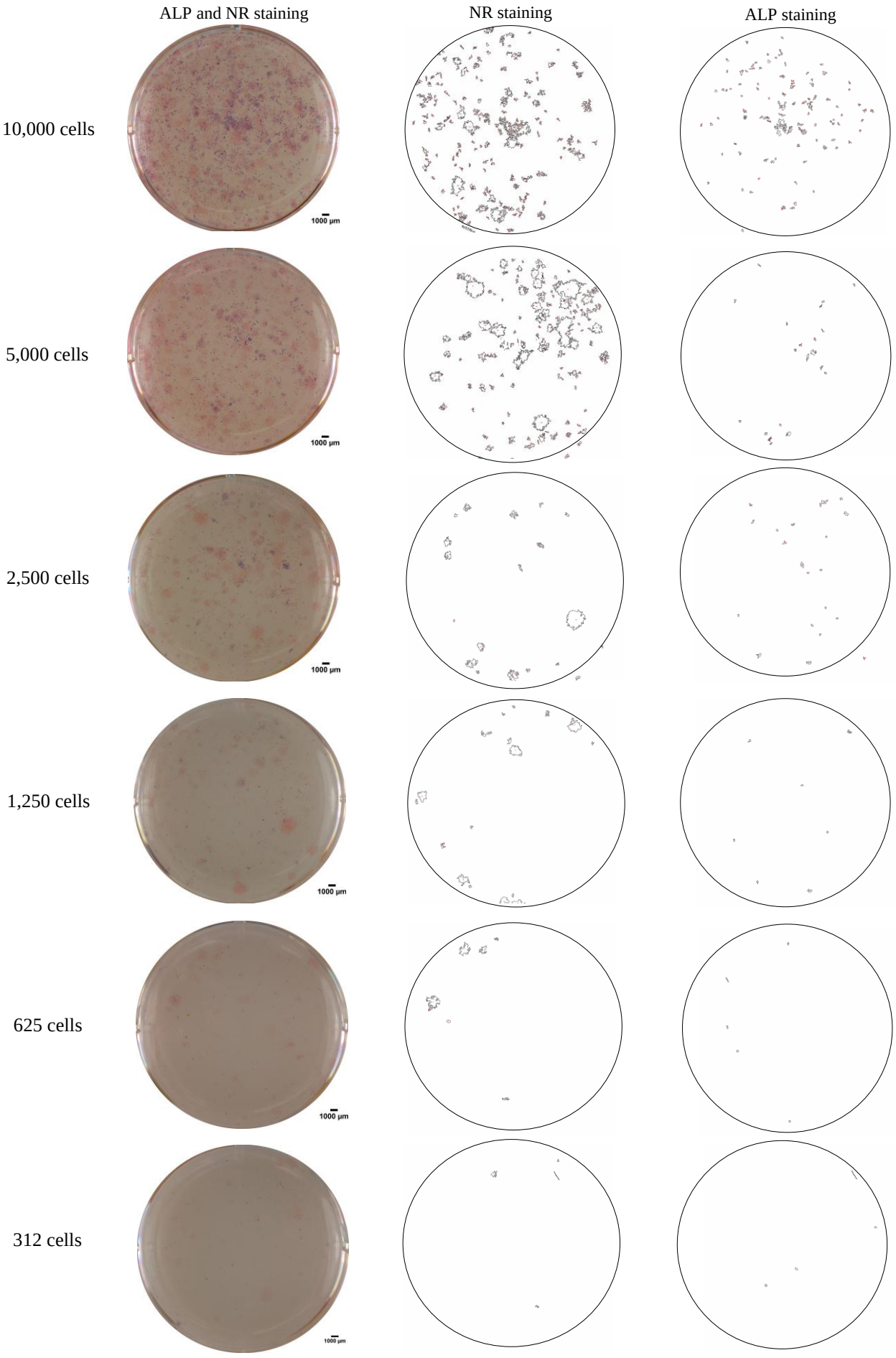
ALP and NR staining
NR staining
ALP staining
10,000 cells
5,000 cells
2,500 cells
1,250 cells
625 cells
312 cells
1000 µm

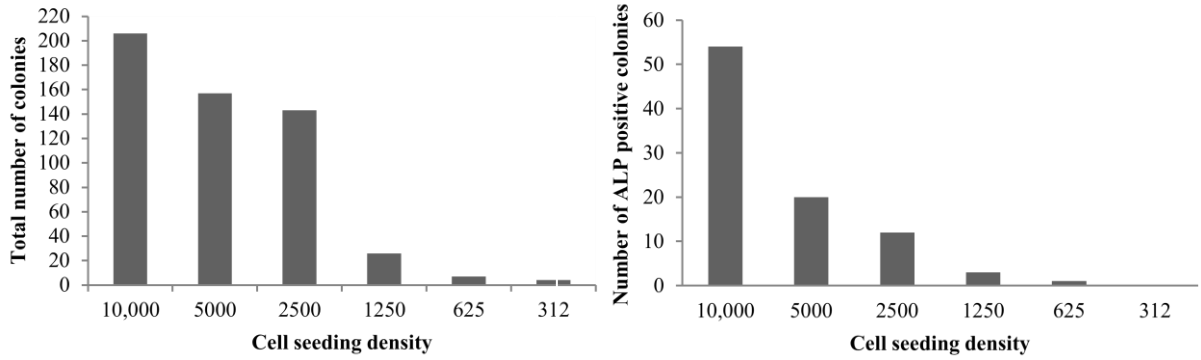

Figure 3-3: A CFU assay to determine the number of ALP positive colonies present at different seeding densities. Cells were stained with ALP and NR (left). ImageJ analysis was used to determine the number of colonies. Heat maps were generated for NR (centre) to determine the total number of colonies and ALP (right) to determine the number of osteogenic progenitors in the population. The number of colonies are shown graphically.

(Figures 3-2 and 3-3). This is probably because NR stains cells more strongly and evenly than MB making it easier to detect. Based on this observation NR was identified as a more suitable dye for subsequent CFU assays.

3.3. Colony forming unit ability of cells after ultrasound treatment:

BMSCs were seeded at 130cells/cm^2 and stimulated with or without US. The cells were cultured for 7 days (as described in the Materials and Methods) and then stained with MB or NR. ImageJ was subsequently used to analyse the number and size of colonies present, to assess the effects of US treatment on colony formation. Figure 3-4A shows that US treatment did not increase the number of colonies generated compared to non-stimulated cells when both dyes were used. However, the NR dye stained a larger number of smaller colonies which were not detected by the MB dye.

As well as colony number it was also found that the size distribution of the colonies did not vary between the US stimulated and non-stimulated cells when stained with both MB and NR (Figure 3-4B and C). This is where the majority of the colonies (70-80%) were found to be between 0-50,000 μm^2 indicating that most colonies were relatively small. Only a small proportion of colonies exceeded this size when treated with or without US which indicates that US treatment had no effect on the number or size of the colonies generated. Therefore, low-frequency, low-intensity US does not enhance the colony forming unit ability or increase the proliferation rate of BMSCs.

3.4. Assessing the reliability of ImageJ analysis of colony number:

In order to assess the validity of the data obtained by ImageJ analysis of colony number and size, BMSCs were again stimulated with or without US and a CFU assay was performed. The dye was then eluted and the number of cells in each well was quantified. The data generated

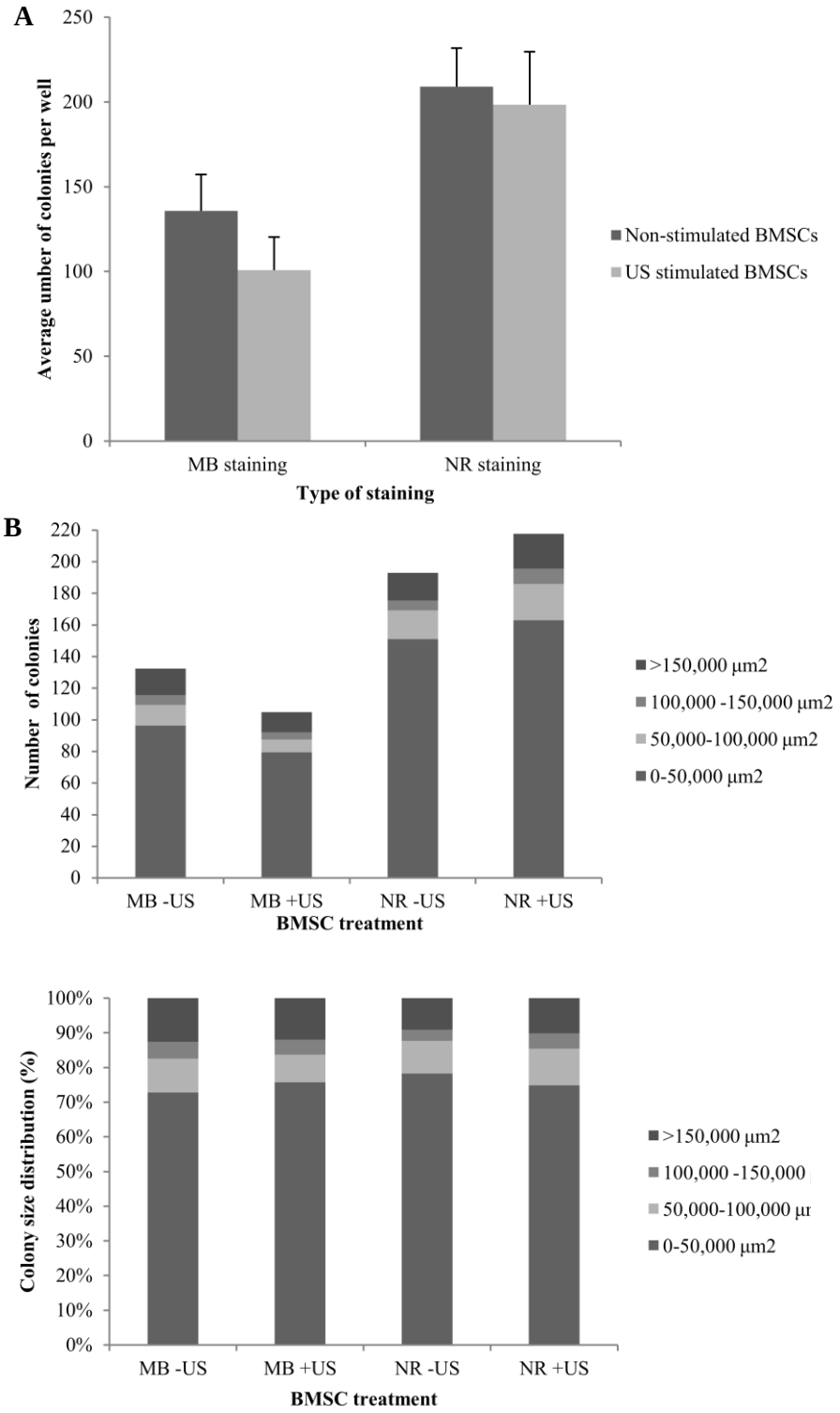

Figure 3-4: The effects of low-frequency, low-intensity US on the ability of BMSCs to generate colonies. Cells were treated with or without US and a CFU assay was performed. The colonies were stained with either MB or NR and ImageJ analysis was performed.(A) The number of colonies present after the CFU assay using the different stains. (B) The number of colonies that are a particular size. (C) The percentage distribution of the colony sizes. For the MB staining experiment 21 technical repeats were performed using three biological samples. For the NR staining, 12 technical repeats were performed using two biological samples.

by ImageJ was also used to calculate the number of cells present in each well based on colony size (as described in the Materials and Methods). Figure 3-5 shows that the cell numbers determined by dye elution and ImageJ analysis are relatively consistent. The table shows that the total number of cells in each well was similar when both techniques were used. This confirms that the data generated by ImageJ regarding the number and sizes of colonies in the CFU assays is fairly accurate and is suitable for quantifying colony number.

3.5. The physical effects of ultrasound:

It has previously been shown that US is able to enhance the initial adherence of BMSCs to tissue culture plastic [8]. To test whether low-frequency, low-intensity US is able to induce this effect, BMSCs were placed in a 6 well-plate and immediately stimulated with US. A CFU assay was then performed and it was found that there were significantly fewer colonies generated when non-adherent BMSCs were stimulated with US compared to stimulated and non-stimulated adherent cells (Figure 3-6A).

It is known that US waves are able to travel through a range of materials namely glass and plastic [35] and it has therefore been speculated that US waves may be able to pass through tissue culture plastics. To test this, adherent cells were cultured in plastic 6 well-plates and three wells were stimulated with US and the others were not stimulated. A CFU assay was carried out and the number of colonies in the non-stimulated wells was examined. Figure 3-6A shows that there was no significant difference between the number of colonies generated by US stimulated and non-stimulated wells (Figure 3-6A).

During the CFU assays carried out on adherent cells it was observed that colonies generated in wells exposed to US tended to cluster together in a specific region of the well. This created a crescent shaped area where very few colonies were present (Figure 3-6B). Comparatively,

Sample 1				Sample 2			
Eluted dye	CFU assay	Eluted dye	CFU assay	Eluted dye	CFU assay	Eluted dye	CFU assay
Non-stimulated	**Non-stimulated**	**US stimulated**	**US stimulated**	**Non-stimulated**	**Non-stimulated**	**US stimulated**	**US stimulated**
56175	82252	112925	116259	99925	67259	86425	114420
87925	87246	75925	144137	50425	47523	92425	80223
83425	79412	43925	78180	26675	58002	70425	101164
41175	37433	67675	83365	31425	35912	97512	110108
59675	75949	118463	131657	59175	44263	84925	88453
86675	75949	68675	960412	20925	62176	62675	86675

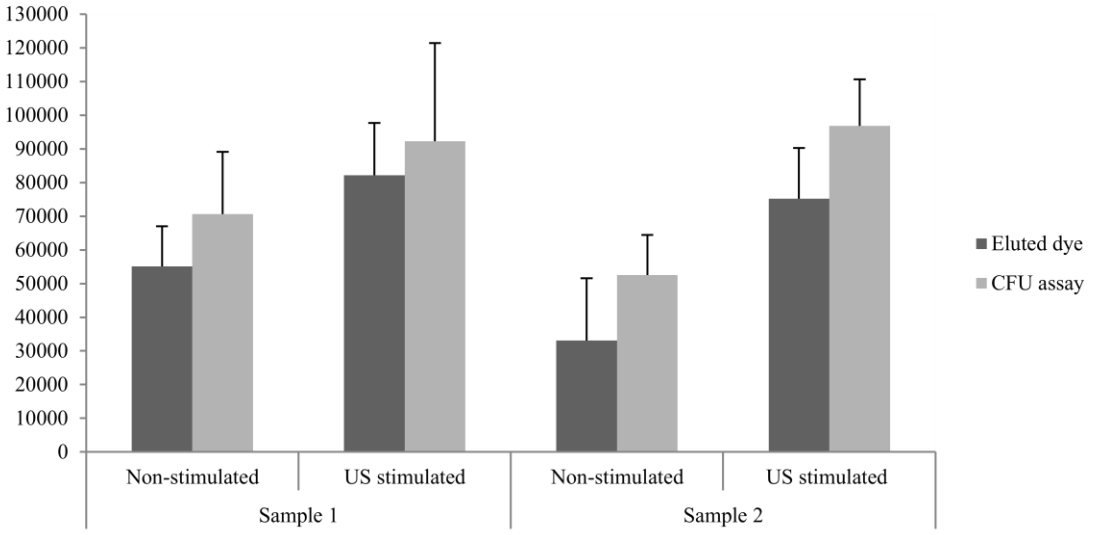

Figure 3-5: Determining the number of cells present in each well. Cells were treated with or without US and stained with MB and the number of cells was analysed by ImageJ and then the dye was eluted and quantified. The number of cells determined by both techniques was then compared. For each treatment group 12 technical repeats were performed using two biological samples.

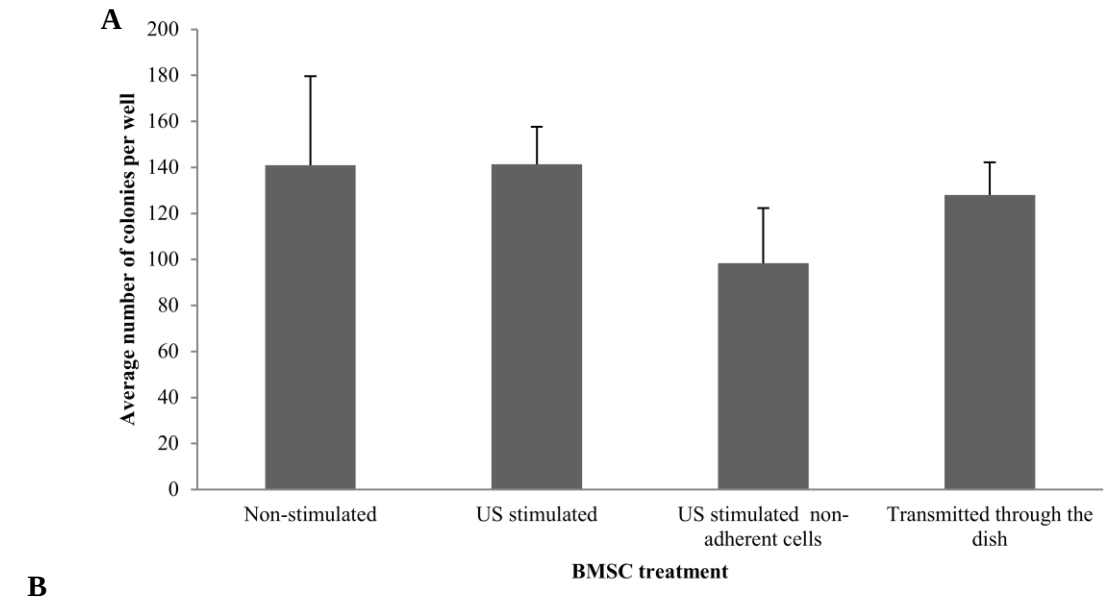

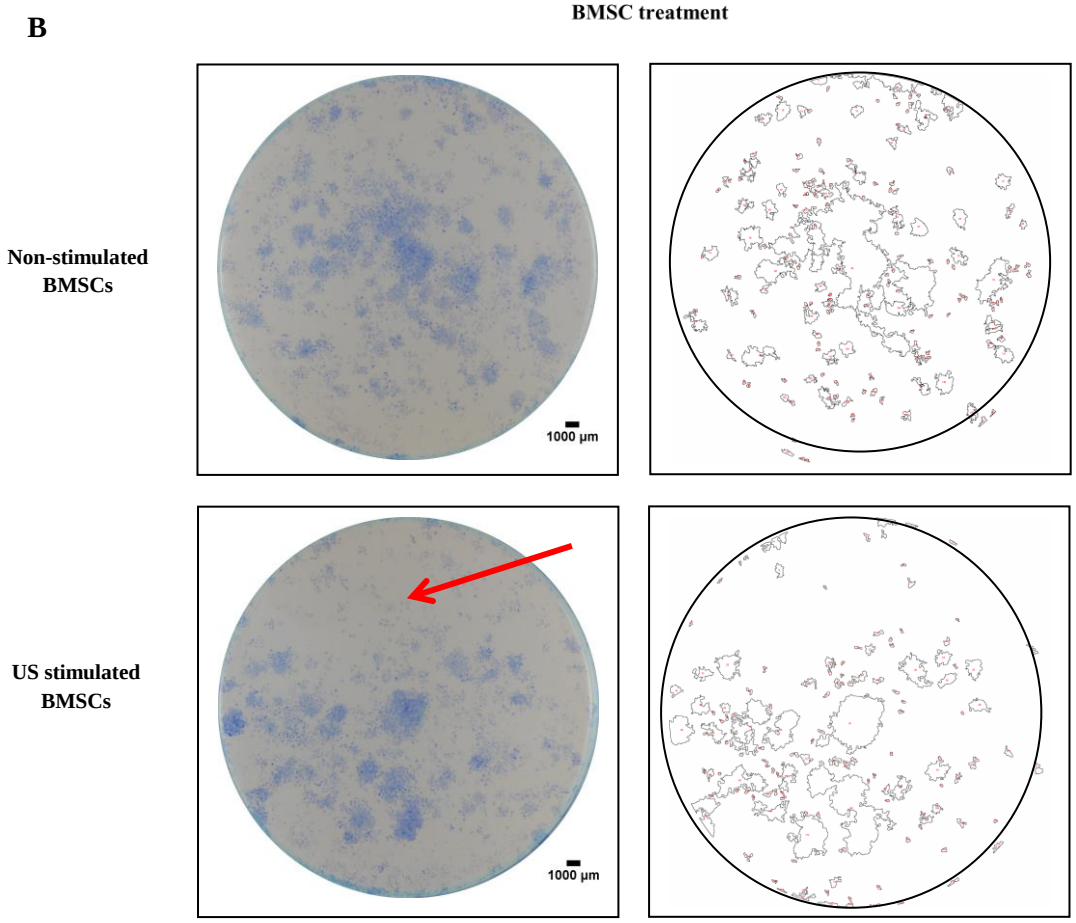

Figure 3-6: Determining the effects of US on the adherence of BMSCs and whether US waves can transmit through the tissue culture dish and effect non-stimulated wells. (A) The number of colonies generated after a CFU assay on adherent BMSCs treated with or without US, non-adherent BMSCs stimulated with US and BMSCs in the same dish as those treated with US. (B) A representative image of MB stained wells treated with or without US and respective heat maps. The red arrow indicates a region where there are very few colonies. In this experiment, 12 technical repeats were performed using 2 biological samples.

the colonies in non-treated wells were more dispersed and did not exhibit this clustering effect. This suggests that US may be dislodging the adherent BMSCs from the base of the wells and causing them to migrate to a specific region and re-adhere to generate colonies. This phenomenon was observed during every CFU assay performed during the study however the size and location of the crescent shaped region varied significantly between assays.

3.6. Low-intensity, low-frequency ultrasound induces sonoporation of bone marrow-derived mesenchymal stem cells:

A common use of US in biology is for the disruption or deactivation of biological materials. Sonoporation occurs when US waves disrupt the cell membrane triggering the release of cellular contents. To test whether low-intensity, low-frequency US can briefly disrupt the membrane of adherent BMSCs, 100,000 cells were treated with Calcein Acetoxymethyl (AM). Calcein AM is a hydrophobic dye that is taken up by intact live cells. Within the cell it is hydrolysed by esterases to produce a strongly fluorescent, hydrophilic compound which is retained in the cytosol [38]. After incubation with Calcein AM, the cells were treated with or without US for 5 minutes. The media was then removed and the fluorescence was quantified to determine the level of efflux of Calcein from the cells.

Figure 3-7 shows that the media removed from non-stimulated cells had low levels of fluorescence emission indicating that very little Calcein had escaped from the cells. Conversely, the media taken from wells treated with US had significantly higher fluorescence reading (Figure 3-7) which shows that cells treated with US expelled a greater amount of Calcein AM dye than non-treated cells. This suggests that low-intensity, low-frequency US is able to create pores within the membranes of BMSCs that enable Calcein AM to escape into the media.

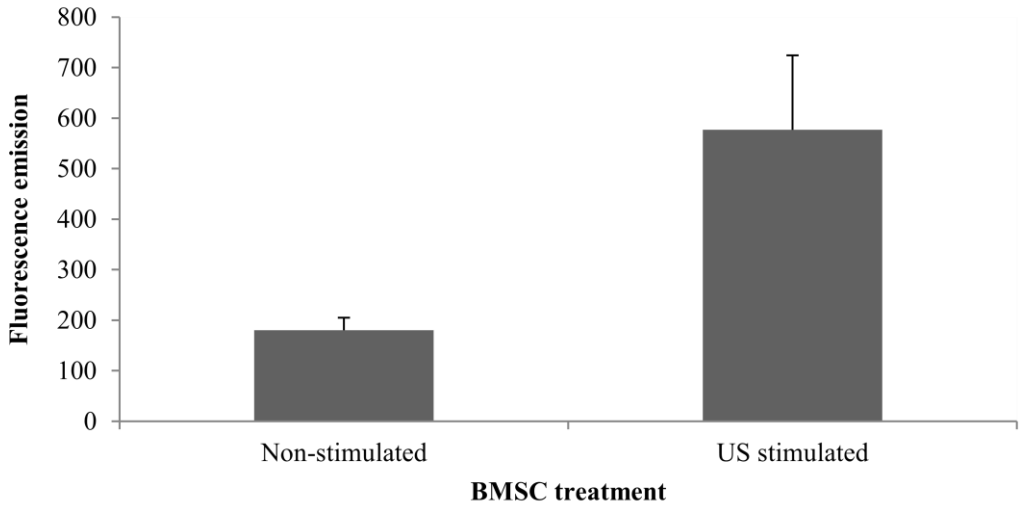

Figure 3-7: Calcein AM staining of BMSCs stimulated with or without US. The fluorescence emission shows how much Calcein AM leaked out of the cells after 5 minutes of treatment with or without US. For this experiment 6 technical repeats were performed using 1 biological sample.

3.7. The effects of ultrasound on cell adhesion:

While measuring levels of Calcein efflux from US stimulated BMSCs, it was observed that a large number of cells had detached from the bottom of the wells. To test whether US was responsible for the cell detachment, cells were seeded at a range of densities (Figure 3-8) and treated with or without US. The media was collected and the number of cells in the media was counted using a Neubauer Haemocytometer for each cell density. Figure 3-8 shows that a greater number of cells detached from wells stimulated with US than non-stimulated wells at every seeding density. Furthermore the number of detached cells increased when the cells were seeded at a higher density. When 50 and100, 000 cells were seeded, approximately 7-8% of the cells had detached from the bottom of the well after 5 minutes of US treatment. At a seeding density of 300,000 cells, the number significantly increased compared to non-stimulated cells. In the case of non-stimulated cells, it was found that at all seeding densities very few cells detached from the base of the wells after 5 minutes. This data suggests that low-intensity, low-frequency US waves are able to disrupt the attachment of the cells from the base of the wells causing them to be dislodged.

3.8. The effect of ultrasound on the osteogenic differentiation potential of bone marrow-derived mesenchymal stem cells:

BMSCs are capable of differentiating into osteoblasts under appropriate culture conditions [3]. To test whether low-frequency, low-intensity US is able to enhance the osteogenic differentiation potential of BMSCs, cells were treated with or without US and cultured in standard growth or osteogenic differentiation media for 2 weeks. The cells were then stained with ALP. BMSCs cultured in normal growth media generated very few ALP positive colonies (Figure 3-9A). Only approximately 5-20% of colonies in the wells were

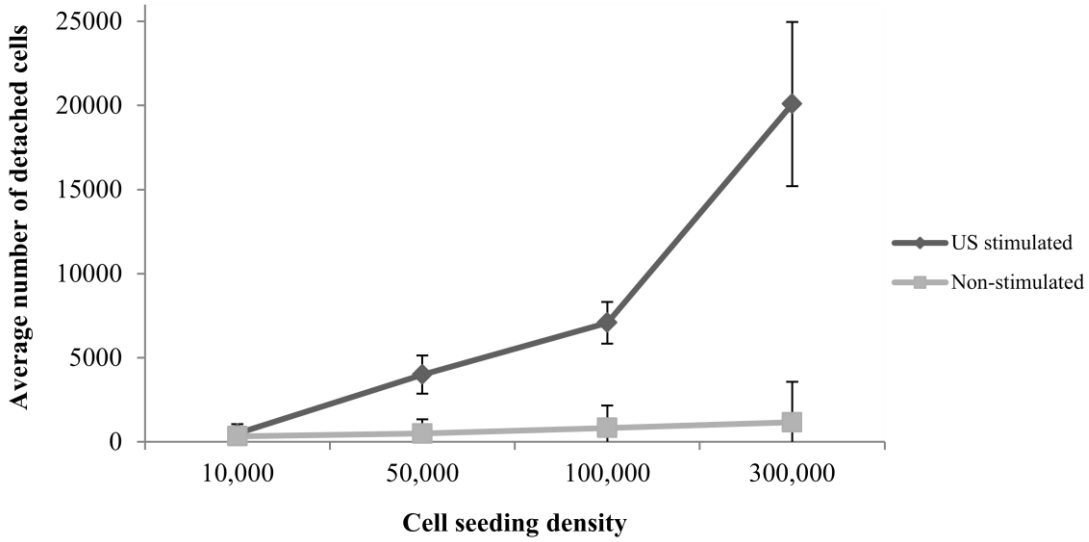

Figure 3-8: The effects of US on the detachment of BMSCs from the culture dish. In this experiment 12 technical repeats were performed using 2 biological samples.

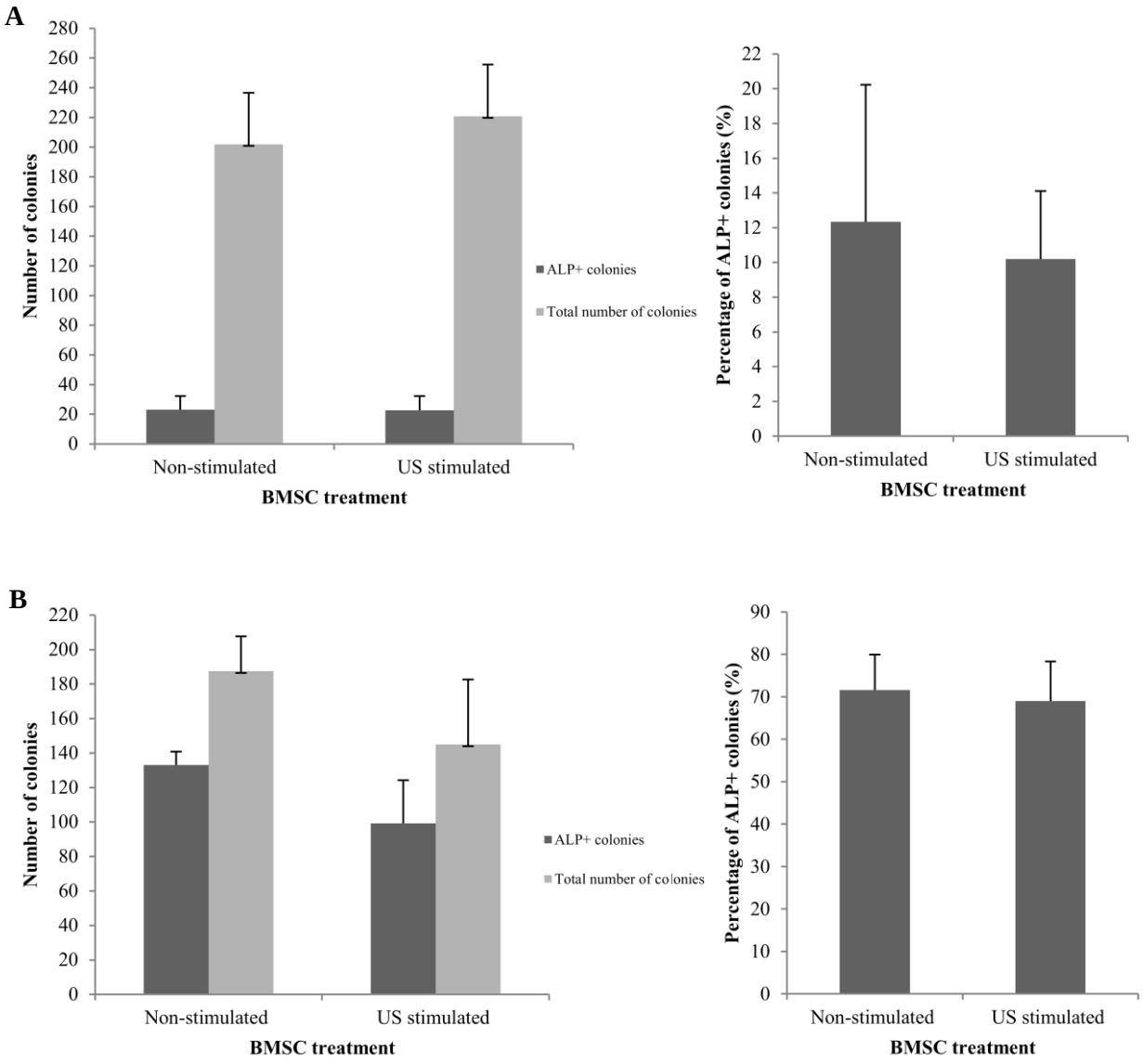

Figure 3-9: The effects of US on the osteogenic differentiation potential of BMSCs. (A) The number and percentage of ALP positive colonies after 2 weeks of culture in standard growth media. (B) The number and percentage of ALP positive colonies after 2 weeks of culture in osteogenic differentiation media.

ALP positive while the remaining colonies remained undifferentiated. Furthermore there appeared to be no significant difference in the number of positive colonies generated in the US-stimulated and non-stimulated wells. This suggests that US itself is not osteogenic and is unable to force the cells down the osteogenic lineage.

Figure 3-9B shows that BMSCs cultured in osteogenic differentiation media generated a significantly greater number of ALP positive colonies. This is where 60-80% of colonies in the wells underwent osteogenic differentiation after 2 weeks of culture in differentiating media. However, there was no difference in the number of ALP positive colonies present in the US-stimulated and non-stimulated wells. These findings show that low-intensity, low-frequency US is unable to enhance the differentiation potential of BMSCs even in osteogenic-specific culture conditions.

3.9. The activation of mechanotransduction pathways in bone marrow-derived mesenchymal stem cells by low-intensity, low-frequency ultrasound:

Previous studies have shown that LIPUS increases the expression of genes in mechanotransduction pathways, namely integrins [28]. To assess whether BMSCs upregulate integrin expression after US stimulation, the expression of integrins α_5 and β_1 were analysed before and after US treatment. Figure 3-10A shows that 4 hours after treatment the expression of integrin β_1 was slightly elevated compared to non-stimulated cells. However 24 hours after treatment the expression declined while it became slightly elevated in non-stimulated cells. Similarly Figure 3-10B shows that integrin α_5 expression was marginally higher in US treated cells compared to non-treated BMSCs 4 hours after treatment. The expression then declined 24 hours after treatment while the levels in non-treated cells remained largely unchanged. Therefore, in this study low-frequency US treatment did not significantly alter the expression

A

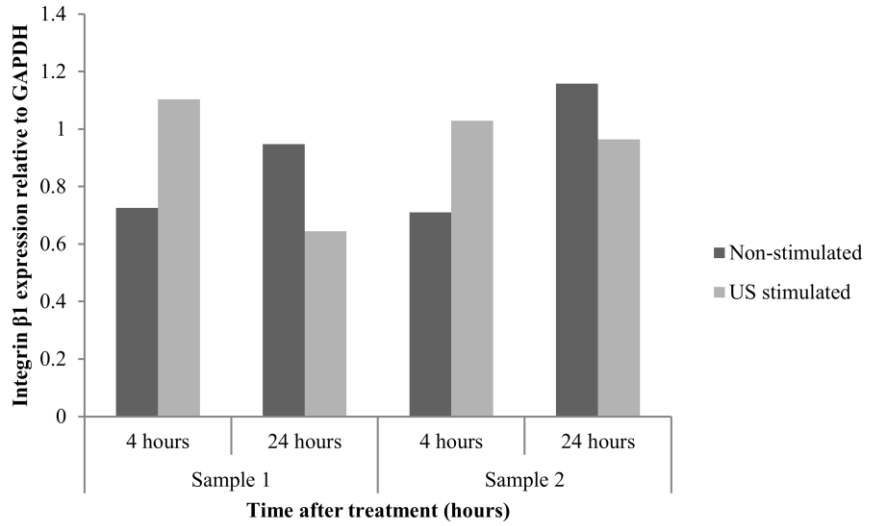

B

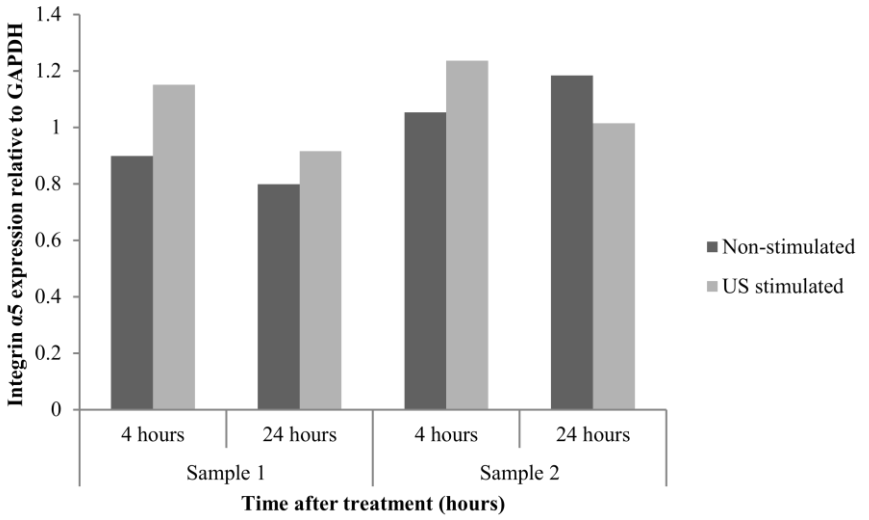

Figure 3-10: The effects of low-frequency, low-intensity US on the expression of its responsive genes. (A) The expression of integrin β_1 in US stimulated and non-stimulated cells 4 hours and 24 hours after treatment relative to GAPDH. (B) The expression of integrin α_5 in US stimulated and non-stimulated cells 4 hours and 24 hours after treatment relative to GAPDH. In this experiment reverse-transcriptase PCR was performed and then the bands were quantified using ImageJ analysis.

of mechanosensitive genes in the same way as high-frequency US waves, as reported elsewhere [28, 29].

4. DISCUSSION:

Bone marrow-derived mesenchymal stem cells (BMSCs) are considered to be a desirable source for therapy since the cells can be obtained from various sources and display multipotent differentiation potential. However, isolating sufficient numbers of MSCs for therapeutic purposes has proven to be difficult. In this study, it was postulated that LIUS waves may be inducing the proliferation and differentiation of BMSCs down an osteogenic lineage. In order to test whether US induces these effects on BMSCs, cells were stimulated with low-frequency, low-intensity US and the proliferation, differentiation and colony forming unit (CFU) ability of the cells was determined. The data obtained from this study indicate that low-frequency, low-intensity US did not significantly enhance the proliferation or differentiation potential of BMSCs compared to non-stimulated cells.

It was observed that low-frequency US waves did not enhance the ability of BMSCs to form colonies where it was shown that there was no significant difference in the number or size of colonies generated by stimulated and non-stimulated cells. However, it was found that in some experiments US stimulated cells generated a greater number of colonies (Figure 3-5) compared to non-stimulated cells while in other experiments the treated cells generated fewer colonies than the control population (Figure 3-4). This demonstrates that the effect of US on BMSCs is highly variable between experiments and may be a reflection of differences in experimental conditions. A study conducted by Schmitz et al. (2011) revealed that small variations in the parameters can have a significant effect on the outcome of the experiment. For example minor changes in volume of growth media can have a massive impact on the pressure and intensity of the US waves at the cell layer. This could affect the way the cells respond to the treatment significantly [40]. This may be the cause of the variations observed between experiments.

In this study, the effects of low-frequency, low-intensity US on the adherence of BMSCs was also tested. It was observed that significantly fewer colonies were generated when non-adherent BMSCs were stimulated with US compared to adherent cells. This may be due to the fact that the US transducer was placed in the well in order to stimulate the cells. Given that the cells were suspended in a large volume of growth media it is possible that the transducer picked up a number of BMSCs when it was removed from the well. This would have reduced the number of cells capable of generating colonies therefore making it difficult to assess the effects of US treatment on cell adherence.

Furthermore, it was found that the US waves could not affect the CF ability of non-stimulated cells placed within adjacent wells of the same dish (Figure 3-6A). This would suggest that the US waves did not travel through the plate and stimulate cells that were not directly exposed to the transducer. However, it was shown previously that US treatment had no significant effect on the CFU ability of BMSCs (Figure 3-4), therefore a CFU assay is not a suitable experiment to test whether the US waves are able to travel through the plate. It would be more appropriate to test another factor that is known to be altered in response to low-frequency, low-intensity US stimulation. It is important to confirm whether US waves can travel through tissue culture plastics because in this study each well was stimulated with US for 5 minutes. However, if the US waves are capable of travelling through the plate, each well would have been treated continuously for 30 minutes rather than a single 5 minutes pulse of US treatment.

While low-frequency, low-intensity US was unable to increase the CF ability of BMSCs, the waves did induce physical changes in the cells. It was observed that even at a low frequency (in the kHz range) US waves are still capable of causing sonophoresis of the BMSCs. This was confirmed by determining the efflux of Calcein AM, a dye that is normally retained in the

cytosol of the cells. It was shown that there was greater efflux in treated cells compared to control cells (Figure 3-7).

Although US stimulation did not significantly affect the proliferation and CF ability of BMSCs, this does not necessarily mean that US is unable to promote cell proliferation and colony formation. It was observed that after US treatment, a small population of cells detached from the base of the well and became resuspended in the media. Given that the media was changed after US treatment, it is conceivable that a small proportion of BMSCs were lost. This would reduce the number of cells available to generate colonies. Therefore, the amount of colonies observed may not be a true reflection on the number that would have been generated.

This finding was further confirmed by the observation that US stimulated cells often cluster in regions of the well, leaving other areas with scarcely any cells (Figure 3-6B). This finding shows that the cells are dislodged from the well and travel along the well and adhere to a different region. The direction of cell migration appeared to be non-random and it was probably influenced by the angle of the transducer in the well. The transducer was slightly tilted within the wells such that it was closer to the cell layer in a certain region of the well and further away from cells in other regions. This could have caused cells closest to the transducer to dislodge and migrate towards a region further away from the transducer. This phenomenon was only observed in US treated wells while untreated BMSCs showed a more random distribution throughout the well.

The detachment of BMSCs from the tissue culture surface is not a phenomenon that is observed when high frequency US is used. This is likely to be a consequence of using low frequency US waves. This is because at lower frequencies, the wavelength is longer which

increases the depth of penetration of the waves by the cells. This non-thermal effect would explain why there appears to be no significant change in the CF ability of the BMSCs.

Low-frequency, low-intensity US treatment was found to transiently alter the structure of the cells. It was observed that immediately after US stimulation, the cells would round up. After 24 hours the BMSCs adopted a more neuronal morphology where the cells became flattened with small projections (Figure 3-1). This suggests that US is affecting the cytoskeleton of the cell causing the changes in morphology observed. Acoustic energy generated by US waves are thought to activate integrin-mediated mechanotrasnduction pathways when the waves reach the cell membrane to alter the cytoskeleton and influence cellular metabolism and gene expression [39]. Previous studies showed that integrin expression increases when cells (namely osteoblasts) are stimulated with US [28]. Even though low-frequency, low-intensity US was found to alter the cell morphology this did not correspond to a significant change in the expression of integrins α_5 and β_1 which are key components of the mechanotransduction pathway (Figure 3-10). It is possible that other pathways may be responsible for the changes in cell structure observed. It is also equally possible that the expression of these genes may have increased immediately after US treatment and then rapidly declined. The consequent changes in cell structure may then occur much later. To confirm this, cells should be harvested immediately after US treatment to test these effects.

It was also observed that US did not affect the osteogenic differentiation potential of BMSCs even when the cells were cultured in osteogenic specific conditioned media. In normal growth media very few US stimulated colonies were found to express the early marker of bone mineralisation Alkaline Phosphatase (ALP) after two weeks of culture. A greater proportion of colonies cultured in osteogenic differentiation media were found to differentiate compared to colonies cultured in normal culture medium (Figure 3-9). However, there was no difference

in the number of differentiated colonies generated by US stimulated and non-stimulated cells. It is important to note that ALP is not an osteogenic specific marker and is only used as an indicator of early differentiation. Other markers such as Alizrin Red staining should be employed to definitively analyse the osteogenic differentiation status of BMSCs.

These findings are interesting because it was thought that US treatment may promote fracture healing by inducing proliferation and differentiation of BMSCs down the osteogenic lineages. However, based on the data obtained from this study it appears as though US alone is unable to promote the differentiation of BMSCs. Even when cells are placed in the appropriate culture environment, it was still unable to promote cellular differentiation. Therefore it appears as though low-frequency, low-intensity US does not affect the differentiation potential of BMSCs.

In conclusion, this study suggests that low-frequency, low-intensity US does not enhance the proliferation, differentiation or CF ability of BMSCs. However several external factors that influence the behaviour of the US at the cell layer are likely to be responsible for the observations made. The changes in cell morphology observed in response to US treatment indicate that the waves are producing a biophysical effect on the cells. The magnitude of the response and the physiological changes it induces on the cells remains to be elucidated.

4.1. Future work:

Based on the findings in this study, the US setup should be adjusted to reduce the variability between experiments. Firstly, given that continuous US waves are applied to the cells it would be more appropriate to culture the cells in larger individual dishes and have the transducer constantly in motion. This would prevent standing waves from forming and reduce the heating of the plate which would limit the thermal effects of US.

A comparison should also be made between the biophysical effects of low-frequency, low-intensity US, LIPUS and continuous LIUS. It would reveal which type of stimulation is more potent and produces the greatest effect on the BMSCs. For therapeutic purposes it would be more useful to utilise the treatment type that has the greatest impact on the proliferation and differentiation of BMSCs. It is not sufficient to compare the results from this study with other studies that have used LIPUS and LIUS treatment as the treatment parameters used in other studies are different to those used in this study.

To further assess the proliferation of BMSCs, more sensitive cell viability and proliferation assays should be performed. Also in the CFU assays NR should be used for colony counting as it is a more sensitive and strong dye than MB which has been shown to easily leech out of cells during the wash steps of the staining process. Also the staining is much more uneven than the NR dye making it difficult to detect and quantify. Gene expression analysis should also be conducted on cells immediately after US stimulation, 1 hour, 4 hours and 24 hours after treatment. This is to determine which genes are mechanosensitive and can be considered US responsive genes. Then the pathways activated by US can be accurately determined.

To observe the changes in the cytoskeleton that are associated with US simulation, confocal microscopy could be used. Dynamic changes in the cell membrane and the actin filaments should be monitored immediately after treatment and again several hours later. This is to determine how the direct effect of US stimulation on the cell membrane results in changes in the actin cytoskeleton. This would provide insight into how the cell physically responds to US and then how these changes alter gene expression and cellular metabolism.

BIBLIOGRAPHY:

(1) Pal R, Hanwate M, Jan M, Totey S (2009). Phenotypic and functional comparison of optimum culture conditions for upscaling of bone marrow-derived mesenchymal stem cells. Journal of Tissue Engineering and Regenerative Medicine; 3: p163-174.

(2) Sotiropoulou PA, Perez SA, Salagianni M, Baxevanis CN, Papamichail M (2006). Characterisation of the optimal culture conditions for clinical scale production of human mesenchymal stem cells. Stem Cells; 24: p462-471.

(3) Shi Y, Hu G, Su J, Li W, Chen Q, Shou P (2010). Mesenchymal stem cells: a new strategy for immunosuppression and tissue repair. Cell Research; 20: p510-518.

(4) Bonab MM, Alimoghaddam K, Talebian F, Ghaffari SH, Ghavamzadeh A, Nikbin B (2006). Aging of mesenchymal stem cell in vitro. *BMC Cell Biology;* **7**(14).

(5) Bianchi G, Banfi A, Mastrogiacomo M, Notaro R, Luzatto L, Cancedda R,Quarto R (2003). *Ex vivo* enrichment of mesenchymal cell progenitors by fibroblast growth factors. Experimental Cell Research; 287(1): p98-105.

(6) Matsubara T, Tsutsumi S, Pan H, Hiraoka H, Oda R, Kato Y (2004). A new technique to expand human mesenchymal stem cells using basement membrane extracellular matrix. Biochem Biophys Res; 313(3): p503-8.

(7) Boudreau NJ, Jones PL (1999). Extracellular matrix and integrin signalling: the shape of things to come. Biochem. Journal; 339: p481-488.

(8) Choi WH, Choi BH, Min BH, Park SR (2011). Low-intensity ultrasound increased colony forming unit-fibroblasts of mesenchymal stem cells during primary culture. Tissue Engineering; 17(5): p517-526.

(9) Speed CA (2001). Therapeutic ultrasound in soft tissue lesions. Rheuamtology; 40: p1331-1336.

(10) Yang RS, Lin WL, Chen YZ, Tang CH, Lu BY, Fu WM (2005). Regulation by ultrasound treatment on the integrin expression and differentiation of osteoblasts. Bone; 36: p276-283.

(11) Demmink JH, Helders PJM, Hobæk H, Enwemeka C (2003). The variation of heating depth with therapeutic ultrasound frequency in physiotherapy. Ultrasound in Medicine and Biology; Volume 29 (1): p113-118.

(12) O'Brien Jr. WD (2007). Ultrasound-biophysics mechanisms. Progress in Biophysics and Molecular Biology; 93: p212-255.

(13) Legay M, Gondrexon N, Person SL, Boldo P, Bontemps A (2011). Enhancement of Heat Transfer by Ultrasound: Review and Recent Advances. International Journal of Chemical Engineering; 2011: p1-17.

(14) Doan N, Reher P, Meghji S, Harris M (1999). *In vitro* effects of therapeutic ultrasound on cell proliferation, protein synthesis and cytokine production by human fibroblasts, osteoblasts and monocytes. Journal of Oral and Maxillofacial Surgery; 57(4): p409-419.

(15) Iwashina T, Mochida J, Miyazaki T, Watanabe T, Ando K, Sakai D (2006). Low-intensity pulsed ultrasound stimulates cell proliferation and proteoglycan production in rabbit intervertebral disc cells cultured in alginate. Biomaterals; 27(3); p354-361.

(16) Kobayashi Y, Sakai D, Iwashina T, Iwabuchi S, Mochida J (2009). Low-intensity pulsed ultrasound stimulates cell proliferation, proteoglycan synthesis and

expression of growth factor-related genes in human nucleus pulposus cell line. European Cells and Materials; 30(17); p15-22.

(17) Inubushi T, Tanaka E, Rego EB, Ohta A, Okada H, Tanne K (2008). Effects of ultrasound on the proliferation and differentiation of cementoblast lineage cells. Journal of Periodontology; 79(10): p1984-1990.

(18) Ebisawa K, Hata K, Okada K, Kimata K, Torii S, Watanabe H (2004). Ultrasound enhances transforming growth factor β-mediated chondrocyte differentiation of human mesenchymal stem cells. Tissue Engineering; 10(5-6): p921-929.

(19) Cui JH, Park K, Park SR, Min BH (2006). Effects of low-intensity ultrasound on chondrogenic differentiation of mesenchymal stem cells embedded in polyglycolic acid: An *in vivo* study. Tissue Engineering; 12(1): p75-82.

(20) Wu CC, Lewallen DG, Bolander ME, Bronk ME, Kinnick R, Greenlead JF (1996). Exposure to low-intensity ultrasound stimulates aggrecan gene expression by cultured chondrocytes. Transactions-Orthopaedic Research Society; 21: p622.

(21) Suzuki A, Takayama T, Suzuki N, Kojima T, Ota N, Ito K (2009). Daily low intensity pulsed ultrasound stimulates production of bone morphogenetic protein in ROS 17/2.8 cells. Journal of Oral Science; 51(1): p29-36.

(22) Tang CH, Lu DY, Tan TW, Fu WM, Yang RS (2007). Ultrasound Induces Hypoxia-inducible Factor-1 Activation and Inducible Nitric-oxide Synthase Expression through the Integrin/Integrin-linked Kinase/Akt/Mammalian Target of Rapamycin Pathway in Osteoblasts. The Journal of Biological Chemistry; 282: p25406-25415.

(23) Choi BH, Choi MH, Kwak MG, Min BH, Woo ZH, Park SR (2007). Mechanotransduction pathways of low intensity ultrasound in C-28/12 human chondrocyte cell line. Proc Inst Mech Eng H; 221(H): p527-535.

(24) Luo BH, Springer TA (2006). Integrin structures and conformational signalling. Curr Opin Cell Biol; 18(5): p579–586.

(25) Lai CH, Chen SC, Tsai YH, Zuo CS, Chang WH, Lai WF et al. (2010). Effects of low-intensity pulsed ultrasound, dexamethasone/TGF-beta1 and/or BMP-2 on the transcriptional expression of genes in human mesenchymal stem cells: chondrogenic vs. osteogenic differentiation. Ultrasound Med Biol; 36(6):p1022-33.

(26) Johns LD (2002). Nonthermal Effects of Therapeutic Ultrasound: The Frequency Resonance Hypothesis. Journal of Athletic Training; 37(3): p293-299.

(27) Takeuchi R, Ryo A, Yamazaki Y, Kumagai K, Aoki I, Saito T (2008). Low-intensity pulsed ultrasound activates the phosphatidylinositol 3 kinase/Akt pathway and stimulates the growth of chondrocytes in three-dimensional cultures: a basic science study. Arthritis Res Ther; 10(4): R77.

(28) Tang CH, Yang RS, Huang TH, Lu DY, Chuang WJ, Huang TF, Fu WM (2006). Ultrasound stimulates cyclooxygenase-2 expression and increases bone formation through integrin, focal adhesion kinase, phosphatidylinositol 3-kinase, and Akt pathway in osteoblasts. Mol Pharmacol; 69(6): p2047-57.

(29) Yang RS, Lin WL, Chen YZ, Tang CH, Lu BY, Fu WM (2005). Regulation by ultrasound treatment on the integrin expression and differentiation of osteoblasts. Bone; 36: p276-283.

(30) Angle SR, Sena K, Summer DR, Virdi AS (2011). Osteogenic differentiation of rat bone marrow stromal cells by various intensities of low-intensity pulsed ultrasound. Ultrasonics; 51: p281-288.

(31) Chen FH, Tuan RS (2008). Mesenchymal stem cells in arthritic diseases. Arthritis Research & Therapy; 10(5): p223-235.

(32) http://med.dartmouth-hitchcock.org/ultrasound_guided_anesthesia/essential_clinical_themes.html

(33) Reher P, Doan N, Bradnock B, Meghji S, Harris M (1998). Therapeutic ultrasound for osteoradionecrosis: an *in vitro* comparison between 1 MHz and 45 KHz machines. Eur Jour Canc; 34: p1962-1968.

(34) Man J, Shelton RM, Cooper PR, Scheven B (2012). Low-intensity, low-frequency ultrasound promotes proliferation and differentiation of odontoblast-like cells. Journal of Endodontics. (Article is under review).

(35) Hendee WR, Ritenour ER (2002). Medical Imaging Physics. New York: Wiley-Liss Inc. p302-352.

(36) McCormick SM, Saini V, Yazicioglu Y, Demou ZN, Royston TJ (2006). Interdependence of Pulsed Ultrasound and Shear Stress Effects on Cell Morphology and Gene Expression. Ann Biomed Eng; 34(3): p436-445.

(37) Hauser J, Hauser M, Muhr G, Esenwein S (2008). Ultrasound-induced modifications of cytoskeletal components in osteoblast-like SAOS-2 cells. Journal of Orthopaedic Research; 27(3): p286-294.

(38) Bratosin D, Mitrofan L, Palii C, Estaquier J, Montreuil J (2005). Novel fluorescence assay using calcein-AM for the determination of human erythrocyte viability and aging. Cytometry A; 66(1): p78-84.

(39) Grossi A, Yadav K, Lawson MA (2007). Mechanical Stimulation Increases Proliferation, Differentiation and Protein Expression in Culture: Stimulation Effects Are Substrate Dependent. J Biomech; 40(15):3354-3362.

(40) Hensel K, Mienkina MP, Schmitz G (2011). Analysis of ultrasound fields in cell culture wells for *in vitro* ultrasound therapy experiments. Ultrasound in Medicine and Biology. (Preprint).

THE DYNAMIC CHANGES IN HISTONE MODIFICATIONS ON THE HOX GENES THAT ACCOMPANY EMBRYONIC STEM CELL DIFFERENTIATION

By

Hafsa Munir

ABSTRACT:

Embryonic stem cells (ESCs) are a pluripotent cell population that are able to self-renew and differentiate into cell types of all three germ layers. ESCs are able to differentiate by maintaining developmental genes in a transcriptionally poised state. The Hox genes are developmental regulators which are arranged in clusters. During differentiation, the genes are sequentially expressed according to their position in the cluster. To determine whether changes in histone modifications on Hoxb genes during differentiation reflect changes in their expression, ESCs were differentiated and quantitative PCR was used to determine the patterning of Hoxb1, 5 and 9 expression. Native Chromatin Immunoprecipitation (NChIP) was performed to determine the enrichment of histone modifications.

The data showed that changes in histone modifications on Hoxb1 and 5 correlated with the temporal and spatial patterning of expression. Hoxb9 expression did not correlate with its position in the cluster and the levels of histone modifications did not reflect the patterning of expression observed. Also the fold enrichment of marks on the Hoxb genes did not correspond with changes in levels on Hoxa genes. This shows that changes in histone modifications on Hoxb genes reflect their transcriptional status, however but were not predictive of gene expression.

Table of Contents

Table of Figures

List of Tables

1. INTRODUCTION:

1.1.Features of embryonic stem cells:

Embryonic stem cells (ESCs) are pluripotent cells derived from the inner cell mass of pre-implantation embryos [1]. These cells are able to self-renew indefinitely and differentiate into cell types of all three germ layers (endoderm, mesoderm and ectoderm) [2]. A number of cell types have been generated by differentiating ESCs *in vitro* such as neuronal, pancreatic, and haematopoietic cells (Figure 1-1) [3]. Due to these features ESCs provide an attractive target for cell replacement therapy, although there are immunological and ethical issues which limit their therapeutic potential. ESCs provide an invaluable tool for studying the mechanisms involved with maintaining pluripotency and driving differentiation [4]. Murine ESCs in particular provide a good model for analysing the changes in gene expression during differentiation as the conditions required for lineage-commitment have been well defined [5].

In order for ESCs to maintain the potential to differentiate, lineage-restricted genes are kept in a poised state. In response to external stimuli, these genes become activated causing cells to differentiate [6]. This pluripotent state is maintained by a network of transcription factors that repress the expression of lineage-specific genes including Oct4, Sox2 and Nanog [7]. The importance of these factors for maintaining the pluripotency of ESCs has been demonstrated by the requirement of only a few (Oct-4, Sox2, Klf4 and c-Myc) to reprogram somatic cells into induced pluripotent stem cells (iPSCs) which exhibit characteristic features of ESCs [8]. This technology offers the potential for generating patient-specific stem cells that overcome issues associated with ESC-therapy [9].

In culture, murine ESCs are kept in an undifferentiated state by the presence of Leukaemia inhibitory factor (LIF). This cytokine activates the JAK-STAT3 pathway in ESCs, to maintain

Figure 1-1: Embryonic stem cells derivation and differentiation

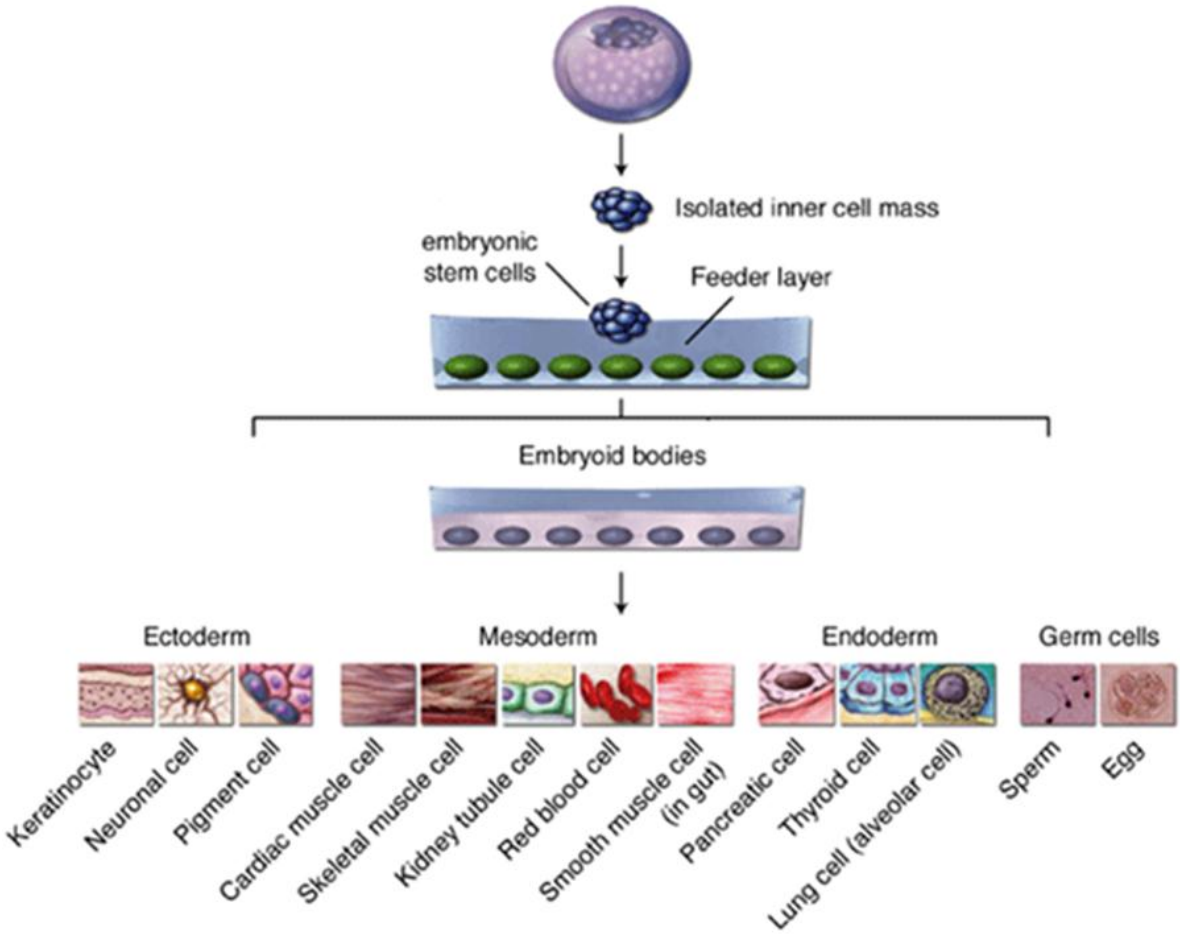

Figure 1-1: Embryonic stem cells are isolated from the inner cell mass of blastocyst stage embryos at the preimplantation stage [1]. The cells can then be grown *in vitro* either on feeder cells or on gelatinised flasks in the presence of Leukaemia Inhibitory Factor. The cells are capable of self-renewing indefinitely and can differentiate into cell types of all three germ layers. A wide range of cell types have been generated from embryonic stem cells (as shown) *in vitro* by placing the cells in the appropriate culture conditions. Adapted from Hyslop et al. (2005) [29].

their pluripotency and high proliferation rate [10]. However, the exact mechanism by which LIF prevents terminal differentiation of ESCs is currently unknown. Therefore, maintaining ESCs in an undifferentiated state requires tightly controlled patterns of pluripotent gene expression and repression of lineage-specific genes.

1.2.The homeobox (Hox) genes:

The Hox genes are a family of developmental genes that are transcriptionally poised in ESCs. These genes were initially identified in *Drosophila*, as mutations in these genes resulted in the positioning of different segments of the organism to be altered [11] suggesting that the transcription factors encoded by Hox genes dictate the anterior-posterior axis of vertebrates. In mice, there are 39 Hox genes which are distributed between four clusters (Hoxa to Hoxd) located on different chromosomes (Figure 1-2) [12]. Hox genes in each cluster are arranged in the order in which they are expressed along the anterior-posterior axis. Furthermore, the genes show temporal expression whereby genes at the 3' (anterior) end of the cluster are expressed during early development whilst 5' (posterior) genes are expressed much later (Figure 1-2) [13]. As well as the spatial and temporal nature of Hox gene expression, paralogous genes between clusters exhibit similar expression patterns [14, 15]. This illustrates the importance of patterning of Hox gene expression during embryonic development. The tightly controlled pattern of Hox gene expression provides an ideal model for studying the mechanisms that regulate expression of transcriptionally poised genes in ESCs [6].

The combination of Hox gene expression within a segment determines its morphological identity. Therefore, to prevent inappropriate expression of Hox genes, transcription must be tightly regulated. The presence of retinoic acid response elements (RAREs) on several of the Hox genes (Hoxa1, a4 and Hoxb1, b4) regulates their temporal and spatial activation [16].

Figure 1-2: Arrangement of Hox genes in the four clusters and the patterning of expression across the developing embryo

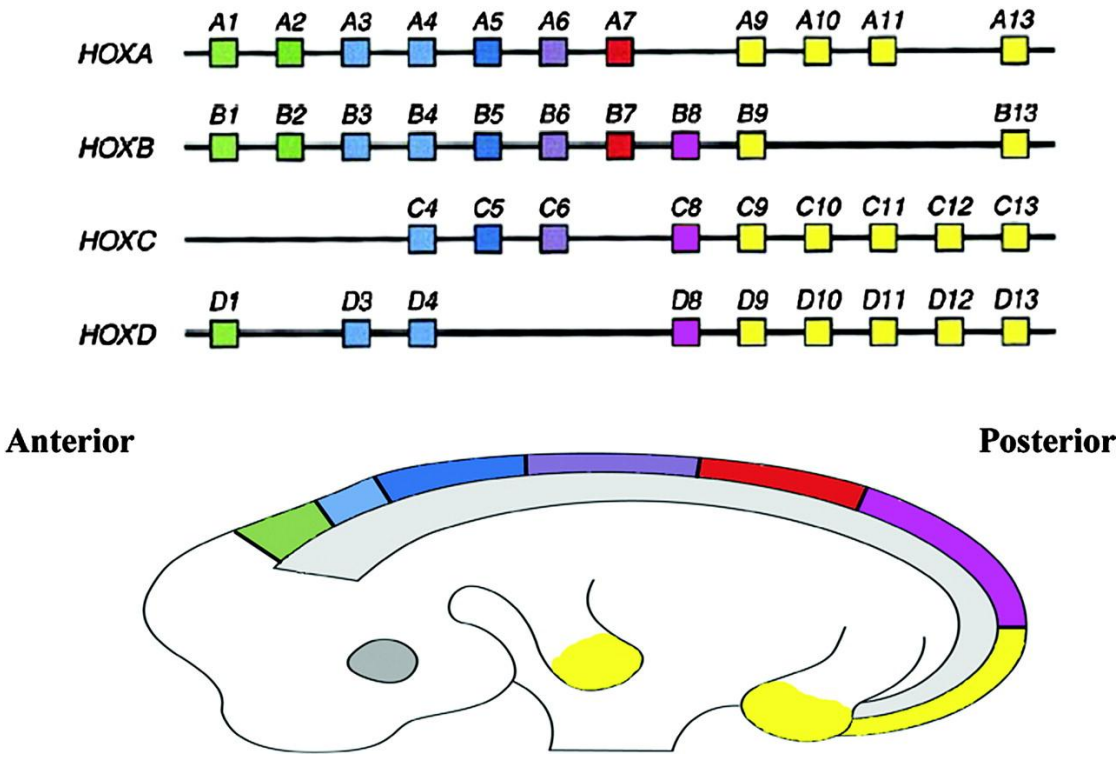

Figure 1-2: The Hox genes in the mouse are distributed between four clusters that are located on four different chromosomes. The genes are arranged in the order in which the genes are expressed during development. This is where genes at the 3' end of the cluster are expressed early on during differentiation in the more anterior end of the organism. Genes at the 5' end of the cluster are expressed in the later stages of development in the more posterior regions of the organism. Therefore, the genes in each cluster are arranged according to their temporal and spatial activation during development [15].

This is where genes at the 3' end of the cluster (Hoxb1 and Hoxb2) can be activated by the addition of exogenous RA whilst genes at the 5' end do not respond in the same way [17]. In culture, addition of RA to ESCs is able to induce the sequential activation of the Hox genes in an anterior-posterior manner that is dictated by the spatial arrangement of the genes in the cluster [18]. The mechanism by which RA regulates the temporal activation of Hox genes is unclear. However, it is apparent that a complex system must control the RA-induced patterning of gene expression.

1.3.The role of chromatin in transcriptional regulation:

It is widely accepted that transcription is regulated by the structural organisation of the proteins that package the DNA into the nucleus, termed chromatin. Chromatin structure is able to influence gene expression by altering the accessibility of the DNA to transcriptional regulators [19]. Chromatin comprises of repeating structural units, the nucleosome, that are comprised of histone proteins which DNA wraps around (Figure 1-3A). Nucleosomes form large complex structures which then limit the accessibility of the DNA (Figure 1-3B) [20]. The accessibility of the DNA can be altered by the presence of chromatin remodelling proteins which open the chromatin and allow transcriptional regulators and transcriptional machinery to bind to the DNA [19]. However, this alone does not explain how transcriptional regulators are only able to bind to specific genes and how these interactions are regulated.

1.4.Modifications of histone tails:

It is now recognised that post-translational modification of the histone tails plays an important role in regulating transcription. Histone tails are unstructured and can be modified by the addition of specific chemical moieties at specific residues e.g. lysine. These moieties such as

Figure 1-3: DNA packaging onto chromatin

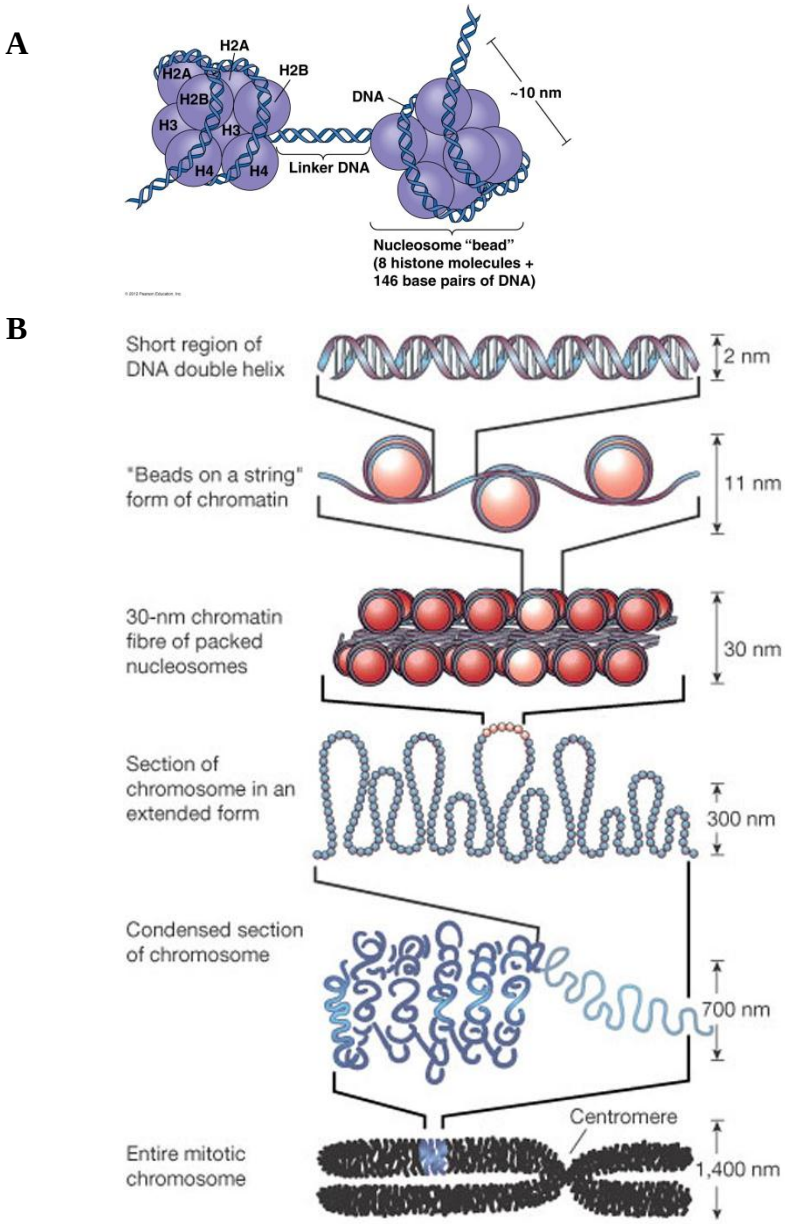

Figure 1-3: (A) The structure of the nucleosome. The nucleosome consists of histone proteins which bind together to form an octameric protein core around which the DNA is wound. This nucleosome is formed by the heterodimerisation of two histone H3 and H4 molecules to form a tetramer. The tetramer binds to two histone H2A and H2B dimers to form the compact octamer. The histone proteins that make up the complex are basic which enables them to tightly bind to the negatively charged phosphate backbone of the DNA. 146bp (base pairs) of DNA are able to wrap around each nucleosome in a 1.8 left handed superhelical turns. Every nucleosome is separated by a region of linker DNA which can vary in length from a few nucleotides to 80bp. [20, 30]. (B) The compaction of DNA by chromatin. The nucleosomes form a "bead on string" like structure. The chromatin is then able to fold into more highly condensed 30nm fibre structures which then interact with scaffolding proteins in the nucleus to form the compacted 700nm solenoids. These solenoids are then folded into chromosomes [20, 31].

acetyl, methyl, phosphate and ubiquitin groups are deposited and removed by a variety of specific enzymes (Figure 1-4) [21, 22].

Given the number of histone marks and array of modifying enzymes it is apparent that these modifications are highly dynamic. It has been suggested that histone modifications can affect the transcription of the gene by changing the shape of the histone tail in a way that promotes or reduces interactions with transcriptional regulators or components of the pre-initiation complex [23]. Although the exact nature of this regulation is not completely understood, it is thought to be due to modifications altering the charge on the nucleosome which affects the association of DNA with the histones [24]. However, it is now recognised that different combinations of histone modifications create alternate chromatin states which reflect the transcriptional status of the gene [24]. The activity of the histone modifying enzymes is highly dependent on the presence of specific intracellular and extracellular cofactors. The enzymes probably localise to particular region of the genome at specific times in response to appropriate environmental cues. Consequently, the chromatin state and target gene expression reflects the metabolic state of the cell [25].

1.5.Distribution of the histone marks:

Whether histone modifications play a role in regulating transcription is unclear however if this is the case then their distribution would vary depending on the transcriptional state of the gene. Studies revealed that specific histone modifications are associated with transcriptionally active or silenced genes [26]. For example, H3K4me3 and H3K9ac marks are highly enriched on transcriptionally active genes while H3K9me2 and H3K27me3 are associated with silent genes (Figure 1-5) [26]. As well as selective enrichment on particular genes, the distribution of histone modifications across individual genes varies depending on whether it is involved

Figure 1-4: Post translational modifications on N-terminal core histone tails

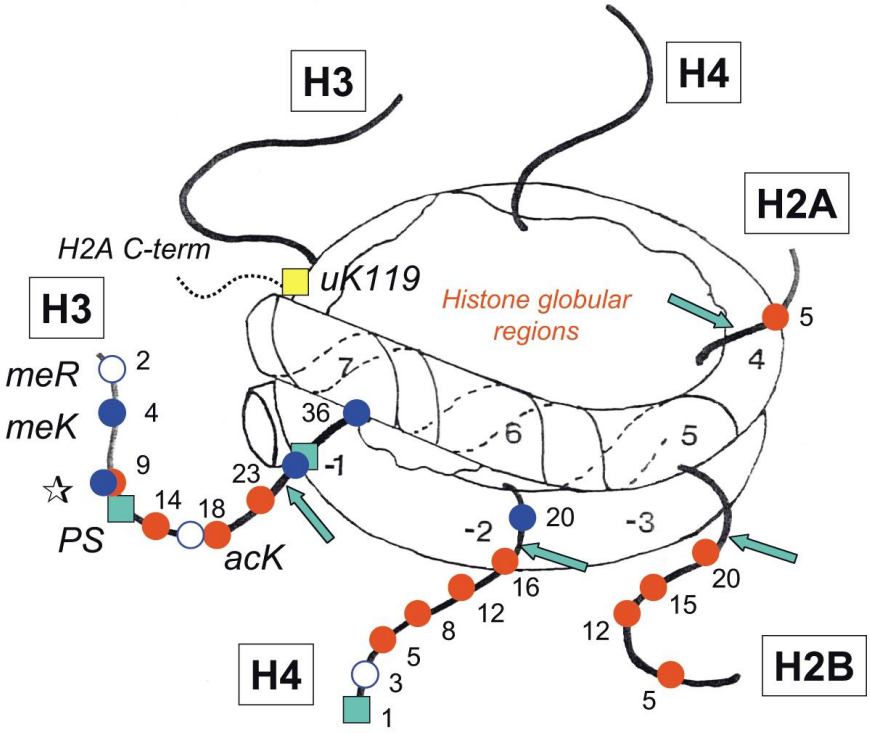

Figure 1-4: Histone tails can be modified by depositing several different types of chemical moieties onto them including acetyl, methyl, phosphate and ubiquitin groups. Acetylation and deacetylation of histone tail residues are performed by histone acetyl transferases and histone deacteylases respectively. These proteins show varying specificity depending on the lysine residue the mark is placed on [22]. Methyltransferases on the other hand are much more specific and exhibit residue specific activity. Further complexity is also introduced by the fact that lysine residues can be mono-, di- and tri-methylated [23]. Several kinases and phosphatases as well as enzymes involved with ubiquitination have also been identified. However, histone acetylation and methylation have been more widely studied as these marks are considered to have a more important role in regulating gene expression [22, 32].

Figure 1-5: Distribution of the histone modifications across a typical gene

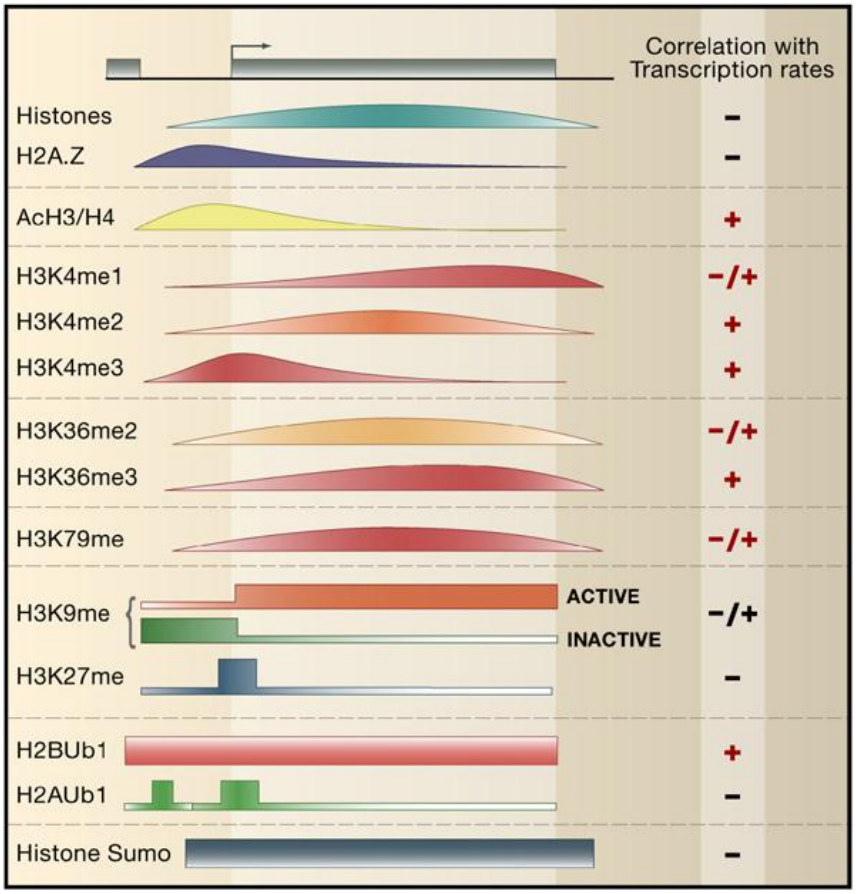

Figure 1-5: The distribution of different histone marks on a gene relative to the promoter, intergenic regions and the open reading frame. The curves show the pattern of enrichment of each mark on the gene as determined by genome-wide analysis [33]. Different marks correlate with different transcription rates of genes for example H3K4me3 levels are higher on transcriptionally active genes while H3K27me3 is enriched on silenced genes.

with coordinating transcriptional initiation or elongation (Figure 1-5). For example, marks involved in initiating transcription are located at the promoter of genes while those that coordinate the elongation stage are located within the body of the gene [27]. This illustrates the complexity of the systems involved in coordinating gene expression.

1.6.The epigenetic state of embryonic stem cells:

Studies have shown that ESCs possess more loosely packed euchromatin that is enriched with active histone modifications. During differentiation, cells accumulate highly compact heterochromatin domains that are transcriptionally inactive correlating with activation of developmentally controlled programmes of gene activation and silencing [28]. For this to occur the genes must be poised for activation while ESCs are in a pluripotent state. Bernstein et al. (2006) identified a distinctive chromatin signature on developmental genes in ESCs. On these genes, H3K27me3 was found to be enriched across the gene while H3K4me3 levels were high at the promoter [6]. Therefore, these active and repressed marks were colocalised on these developmental genes. This was termed a "bivalent chromatin" mark and genes possessing this mark had low expression levels in ESCs. Upon differentiation the genes retained either the active (H3K4me3) or repressive (H3K27me3) mark which correlated with the transcriptional status of the gene [6]. Consequently, it was suggested that these marks maintain genes in a transcriptionally silent state whilst keeping them poised for activation once differentiation is induced. The existence of bivalent marks may explain how Hox genes are poised in ESCs and expressed once differentiation is induced.

1.7. Hypothesis:

The changes in enrichment of histone modifications on Hoxb genes during ESC differentiation reflect the transcriptional state of the genes.

Aims:

The aim of this study was to determine the changes in histone modifications on the Hoxb genes that accompany differentiation. To achieve this, ESC differentiation and Hox gene expression was stimulated by adding RA. Native chromatin immunoprecipitation was then used to determine the relative enrichment of different histone marks on Hoxb1, 5 and 9 genes and pluripotent genes Pou5f1 and Nanog. Gene expression was also determined by quantitative PCR to observe how variations in histone modifications correlate with changes in gene expression during differentiation.

2. MATERIALS AND METHODS:

2.1. Cell culture:

The CCE/R male mouse embryonic stem cell line was cultured as a monolayer in Dulbecco's Modified Eagles Medium (DMEM; Gibco) supplemented with 20% Foetal Bovine Serum (FBS; Gibco), 10% sterile water, 1% L-Glutamine (Gibco), 1% Penicillin and Streptomycin (Gibco), 1% non-essential amino acids (Gibco), 0.25% of 50mM 2-Mercaptoethanol (Gibco) and Leukaemia Inhibitory Factor (LIF/ESGRO; Millipore). The CCE/Rs were cultured on T75cm^2 flasks coated with 0.1% Gelatin and incubated at 37^{o}C, 5% CO_2. Cells were harvested by incubating with Trypsin/EDTA (Gibco) and centrifuging at 1,500 rpm for 5 minutes. Samples were washed in ice cold Phosphate Buffered Saline/5mM Na Butyrate three times and stored at -80^{o}C.

Differentiation was induced by replating CCE/Rs onto non-adherent plastic 10cm dishes and culturing them in the absence of LIF. 48 hours later the media was supplemented with 1μM retinoic acid (RA). Images were captured on different days of differentiation using a Canon Digital EOS 400D. Embryoid bodies were harvested on day 2, 3 and 5 and washed in ice cold PBS/Na Butyrate and stored at -80^{o}C.

2.2.1. Extraction of chromatin from undifferentiated and differentiated CCE/Rs:

Samples were thawed and cells were resuspended in 1xTBS buffer (a list of reagents for all NChIP buffers shown in Table 1) to a concentration of 2x10^{7}cells/ml. An equal volume of 1% TWEEN-40/1xTBS and 10μl of PMSF was added. The cells were homogenised using a Dounce all-glass homogeniser and an 'A' pestle and viewed under the microscope to ensure that high yields of nuclei were obtained (70-80%). The samples were centrifuged at 2,000 rpm for 10 minutes at 4^{o}C. The nuclei pellet was then washed in 5% sucrose/1xTBS solution and

Table 1: Components of the NChIP buffers

Solution	Constituents
TBS buffer	15mM NaCl
	10mM Tris-HCl (pH7.4)
	3mM NaCl
	2mM MgCl2
	5mM Na Butyrate
Digestion buffer	0.32M Sucrose
	50mM Tris-HCl (pH 7.4)
	4mM MgCl2
	1mM CaCl2
	0.1mM Phenylmethanesulfonylfluoride (PMSF)
	5mM Na Butyrate
Lysis buffer	1mM Tris-HCl (pH 7.4)
	0.2mM Na2EDTA
	0.2mM PMSF
	5mM Na Butyrate
Incubation buffer	75mM NaCl
	20mM Tris-HCl (pH 7.4)
	5mM Na2EDTA
	0.1mM PMSF
	5mM Na Butyrate
Buffer A	50mM Tris-HCl (pH7.4)
	10mM Na2EDTA
	5mM Na Butyrate
	50mM NaCl
Buffer B	50mM Tris-HCl (pH7.4)
	10mM Na2EDTA
	5mM Na Butyrate
	100mM NaCl
Buffer C	50mM Tris-HCl (pH7.4)
	10mM Na2EDTA
	5mM Na Butyrate
	150mM NaCl
TE buffer	10mM Tris-HCl (pH7.4)
	1mM Na2EDTA (pH8)

centrifuged at 3,000rpm for 10 minutes. The pellet was resuspended in digestion buffer and the concentration of chromatin was determined by measuring the $A_{260/280}$. The sample was centrifuged at 2,000rpm for 10 minutes and resuspended in digestion buffer at a concentration of 0.5mg/ml.

50U micrococcal nuclease (Sigma) was then added to 1ml aliquots of the chromatin solution and incubated in a water bath at 37^{o}C for 5 minutes to digest the chromatin. The reaction was stopped by adding 0.5M Na_2EDTA and placing samples on ice for 5 minutes. Samples were centrifuged at 13,000rpm for 2 minutes and the supernatant (S1) was stored at 4^{o}C. The pellet was resuspended in 1ml lysis buffer and then dialysed overnight against 2L of lysis buffer at 4^{o}C. Samples were centrifuged at 2,000rpm for 10 minutes and supernatant (S2) was removed and stored at 4^{o}C. The pellet (P) was resuspended in 200µl Lysis Buffer.

2.2.2. Analysis of the chromatin:

The concentration of chromatin in each fraction was determined by measuring the $A_{260/280}$ and the fractions were loaded onto a 1.2% agarose gel and run at 60V for 3 hours. The gel was stained with ethidium bromide and viewed under a UV illuminator. S1 and S2 fractions were pooled together and the concentration of the chromatin was measured ($A_{260/280}$).

2.2.3. Native Chromatin Immnoprecipitation (NChIP):

50-100µg of chromatin was added to siliconised eppendorfs with antibodies raised against different histone modifications (Table 2). The final volume was made up to 800µl with Incubation buffer and samples were incubated overnight on a slow stirrer at 4^{o}C. 200µl of 50% w/v protein A sepharose was then added and incubated for 3 hours at room temperature on a fast turntable. The samples were centrifuged at 13,000rpm for 10 minutes and the supernatant was removed and stored at 4^{o}C (Unbound).

Table 2: Antibodies used in the NChIP procedure

Antibody	Raised against	Dilution for 50-100µg of chromatin	Supplier
R612	H3K4me3	50µl	In-house
07-449	H3K27me3	10µl	In-house
R607	H3K9ac	50µl	Millipore
R639	H3K9me2	50µl	In-house
Preimmune	Mouse IgG	10µl	Millipore

At this point, only siliconised Pasteur pipettes and 15ml falcon tubes were used to prevent loss of chromatin material. The pellet was resuspended in 1ml Buffer A (Table 1) and layered onto 9ml of the same buffer. The samples were centrifuged at 2,000 rpm for 10 minutes. The pellets were then washed sequentially in 10ml Buffers B and C and then resuspended in 1ml Buffer C. The samples were centrifuged at 13,000rpm for 10 minutes and placed in 1% SDS/Incubation buffer and incubated for 15 minutes on a fast turntable. The samples were centrifuged and the supernatant was removed and stored (Bound 1). The pellet was washed in 1% SDS/Incubation buffer and then centrifuged. The supernatant was removed and mixed with Bound 1. 400µl of Incubation buffer was added to the bound fraction to reduce the concentration of SDS. Bound and unbound DNA was purified using a PCR purification kit (Qiagen) according to the manufacturer's instructions.

2.2.4. Quantification of DNA concentration by Picogreen staining:

2µl of each bound and unbound sample was added to 48µl of buffer TE (Table 1) and placed in a 96-well plate. Picogreen (Thermo Scientific) was diluted 1:200 in TE buffer and 50µl was placed in each well and fluorescence emission was detected by a plate reader. The percentage pull down was calculated using the calculation:

(Concentration of DNA from bound sample/Concentration of DNA from unbound sample)x100.

2.3. RNA extraction, quantification and cDNA synthesis:

Total RNA was extracted using the RNeasy mini kit (Qiagen) according to the manufacturer's instructions. The concentration and purity ($A_{260/280}$) of RNA was quantified using a nanodrop. cDNA was then synthesised using the Superscript III kit (Invitrogen) according to the manufacturers protocol.

2.4. Quantitative PCR (qPCR):

For NChIP analysis, the unbound samples were diluted down to the corresponding bound samples based on the values obtained from the picogreen staining. A 2xdilution was then performed for all samples. 2µl of cDNA was added to a PCR mastermix consisting of 0.5µM forward and reverse primers (ChIP primers shown in Table 3), 5µl SYBR green mix (Bioline) and 2µl distilled water. The quantitative PCR (qCR) was performed using the following cycling conditions:

- 95^{o}C for 15 minutes
- 94^{o}C for 15 seconds
- 60^{o}C for 30 seconds

40 cycles

- 72^{o}C for 30 seconds
- Dissociation stage (95^{o}C for 15 seconds, 60^{o}C for 15 seconds and 95^{o}C for 15 seconds)

For the expression analysis, cDNA from each sample was diluted to 5µg/µl and qPCR was carried out as described above (expression primers; Table 4).

Table 3: NChIP primers used in qPCR

Gene	Forward primer	Reverse primer	Annealing temperature
Hoxb1.1	AGCCCTACAGCCTTGGGGTGG	TTCAACCCAGCTGCCCCTCAC	60
Hoxb1.2	TCCTAGGGGATCGCTGGCGG	GCCGTTTGGGGGAGACACCC	60
Hoxb1.3	CCGCAGCCCCCATACGGAAC	CGGGGAGTGAGAGTGCTGGGT	60
Hoxb5.1	AGAGGGGATAGCCGCACCCT	CTGGCTCTGTGCAACCGCCA	60
Hoxb5.2	TGGCCGCATACATAGCAAAACGA	GGAGGGCTTGATTTGTGGATCGTGG	60
Hoxb5.3	GCCCTGCACTAACGGCGACA	TCCTCGGGCTCAGAGGACGC	60
Hoxb9.1	CTCGCCCGATTGATTTATGT	CACCCCCTGCTCAACTTCT	60
Hoxb9.2	TCCGAAAGCCCTCTGCAC	GACATTCTCAGACATTATCCGCG	60
Hoxb9.3	CCTCCAGCCAAGTTTCCTTC	GCAGGTAGGGGTGGTAGACA	60
Hoxa1	GCGCGTCACCTACACTGAG	CGTGACTCTACCAGCCAATG	60
Hoxa5	GATCGGCAGCTGACGGCCTC	CGCTTCCGACCTCGGGCTTC	60
Hoxa9	AGCTGCGCGATCCCTTTCGA	GTGTCCGCCCGGCAGAACAA	60
Pou5f1/1	GCATGTTTTAGGCTCTCCA	GCCTTCATTTTCAACCTTC	60
Pou5f1/2	CCTGGCTTCAGACTTCG	AGATCCCCAATACCTCTGA	60
Nanog/1	GCAGCCGTGGTTAAAAGATG	AGGGAGGCAAAGCTTAGGG	60
Nanog/2	ATCCACTGAGCCATCTCACC	CTGGTCTGCAGAGCTAGTTCAA	60
GAPDH1	CACCATCCGGGTTCCTATAA	ATTTTCACCTGGCACTGCAC	60
GAPDH2	CGTCCCGTAGACAAAATGGT	TGACCTTGAGGTCTCCTTGG	60

Table 4: Primers used for expression analysis in qPCR

Gene	Forward primer	Reverse primer	Annealing temperature (°C)
Gapdh	CGGCCGCATCTTCTTGTGCA	AGTGGGGTCTCGCTCCTGGA	60
Pou5f1	GAGGAGTCCCAGGACATGAA	AGATGGTGGTCTGGCTGAAC	60
Nanog	CTCATCAATGCCTGCAGTTTTTCA	CTCCTCAGGGCCCTTGTCAGC	60
Klf4	CCAGACCAGATGCAGTCACAA	TGGCATGAGCTCTTGATAATGG	60
Sox2	GCGGCAACCAGAAGAACAG	GTTGTGGCATCTTGGGGTTCT	60
Hoxb1	CCATATCCTCCGCCGCAG	CGGACTGGTCAGAGGCATC	60
Hoxb5	CCTCTGAGCCCGAGGAAG	CCAGGGTCTGGTAGCGAGTA	60
Hoxb9	CAGGGAGGCTGTCCTGTCTAATC	CTTCTCTAGCTCCAGCGTCTGG	60

3. RESULTS:

Differentiation of ESCs is concomitant with a reduction in the expression of pluripotent genes (Pou5f1 and Nanog) and the induction of the Hox genes. The Hoxb cluster contains 10 genes that are arranged according to their order of expression during differentiation. It is thought that dynamic changes in histone modifications on these genes during differentiation are linked to variations in transcription. To assess this, ESCs were differentiated and enrichment of histone modifications on Hoxb1, 5 and 9 were analysed to determine whether variations correlate with changes in expression of these genes.

Male mouse CCE/R cells were differentiated by being replated onto non-adherent dishes and cultured without leukaemia inhibitory factor (LIF; Figure 3-1). Loss of this pluripotency signalling molecule is associated with reduction in the expression of pluripotent genes (Nanog and Pou5f1). Retinoic acid (RA) was added 48 hours later to stimulate the sequential expression of Hoxb genes during differentiation (Figure 3-1) [17]. CCE/Rs were differentiated for 5 days and samples were harvested on day 2 (after addition of RA), day 3 and day 5 (continued culture in RA) and compared to undifferentiated ESCs (day 0). Pluripotent gene expression (Pou5f1, Sox2, Nanog and Klf4) was analysed by quantitative real-time PCR (qPCR), as these genes are downregulated when ESC differentiation is induced. Hoxb1, 5 and 9 expression was also analysed to observe changes in expression of genes from different regions of the cluster during differentiation. Native Chromatin immunoprecipitation (NChIP) analysis was performed to characterise the changes in levels of H3K4me3, H3K27me3, H3K9ac and H3K9me2 on Hoxb1, 5 and 9 and the pluripotent genes Pou5f1 and Nanog during differentiation (Figure 3-1).

Figure 3-1: Outline of the experiment

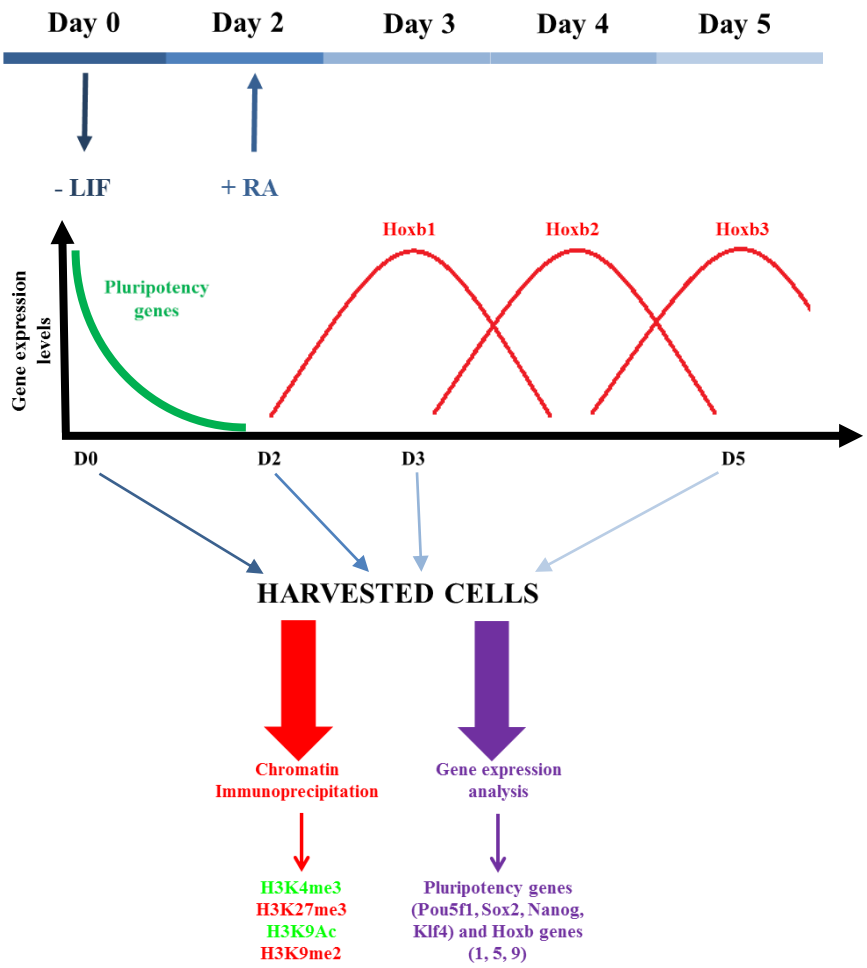

Figure 3-1: In this experiment Hoxb gene expression was stimulated in the CCE/Rs by detaching the cells from the flask and culturing them on non-adherent dishes in the absence of leukaemia inhibitory factor (LIF) at day 0, to allow embryoid bodies to form. At day 2, retinoic acid (RA) was added to temporally activate the Hox genes during differentiation. The cells were differentiated for 5 days and were harvested on days 0, 2, 3 and 5. The expression of pluripotent genes (Pou5f1, Sox2, Nanog and Klf4) were analysed by qPCR to confirm that the cells had undergone differentiation as these genes are known to be significantly downregulated upon differentiation. The expression of Hoxb1, 5 and 9 were also analysed to show the temporal activation of the Hoxb genes during differentiation. This is where Hoxb1 (the first gene in the cluster) should be expressed at the early stages of differentiation while Hoxb9 and 13 (last two genes in the cluster) should be expressed at a much later stage. Native chromatin immunoprecipitation (NChIP) was also performed, to observe the changes in the levels of histone modifications (H3K4me3, H3K27me3, H3K9ac and H3K9me2) on the pluripotent genes (Pou5f1 and Nanog) and Hoxb1, 5 and 9 genes that arise during CCE/R differentiation.

3.1. Differentiation induced changes in embryonic stem cell morphology:

CCE/Rs were differentiated and images were taken on each day that samples were harvested. Undifferentiated CCE/R grew in colonies where the cells layered on top of each other making it difficult to distinguish individual cells (Figure 3-2). Within colonies, cells displayed cytosolic processes surrounding a rounded nucleus. Upon replating, the cells aggregated together forming large, non-adherent embryoid bodies. As differentiation progressed the size of the bodies increased considerably concomitant with an increase in death. By day 5 the bodies formed an outer layer surrounding the darker mass inside the body (Figure 3-2) marking the formation of the three germ layers [5].

3.2. Changes in gene expression associated with differentiation:

To confirm that the cells had undergone differentiation, pluripotent gene expression (Pou5f1, Sox2, Klf4 and Nanog) was analysed on days 0, 2, 3 and 5. As expected, the expression declined progressively during differentiation (Figure 3-3). Pou5f1, Nanog and Klf4 expression was highest in the undifferentiated cells and then declined considerably after LIF removal. By day 3 the levels were significantly reduced and continued to decline until day 5 of differentiation. Conversely, Sox2 expression remained unchanged at day 2 and then steadily declined at day 3 and 5 (Figure 3-3). This indicates that the pluripotency of CCE/Rs was significantly reduced by day 5 and the cells had begun differentiating.

To determine whether RA stimulated the Hoxb cluster during differentiation, Hoxb1, 5 and 9 expression was analysed. Given that the RAREs are located upstream of the Hoxb1 gene, its expression should be induced before all other genes in the cluster. Figure 3-4 shows that Hoxb1 expression increased by 6-fold 24 hours after RA was added to the media (day 3). The expression then declined by day 5 to the same levels as undifferentiated cells. After adding

Figure 3-2: Changes in the cell morphology during differentiation

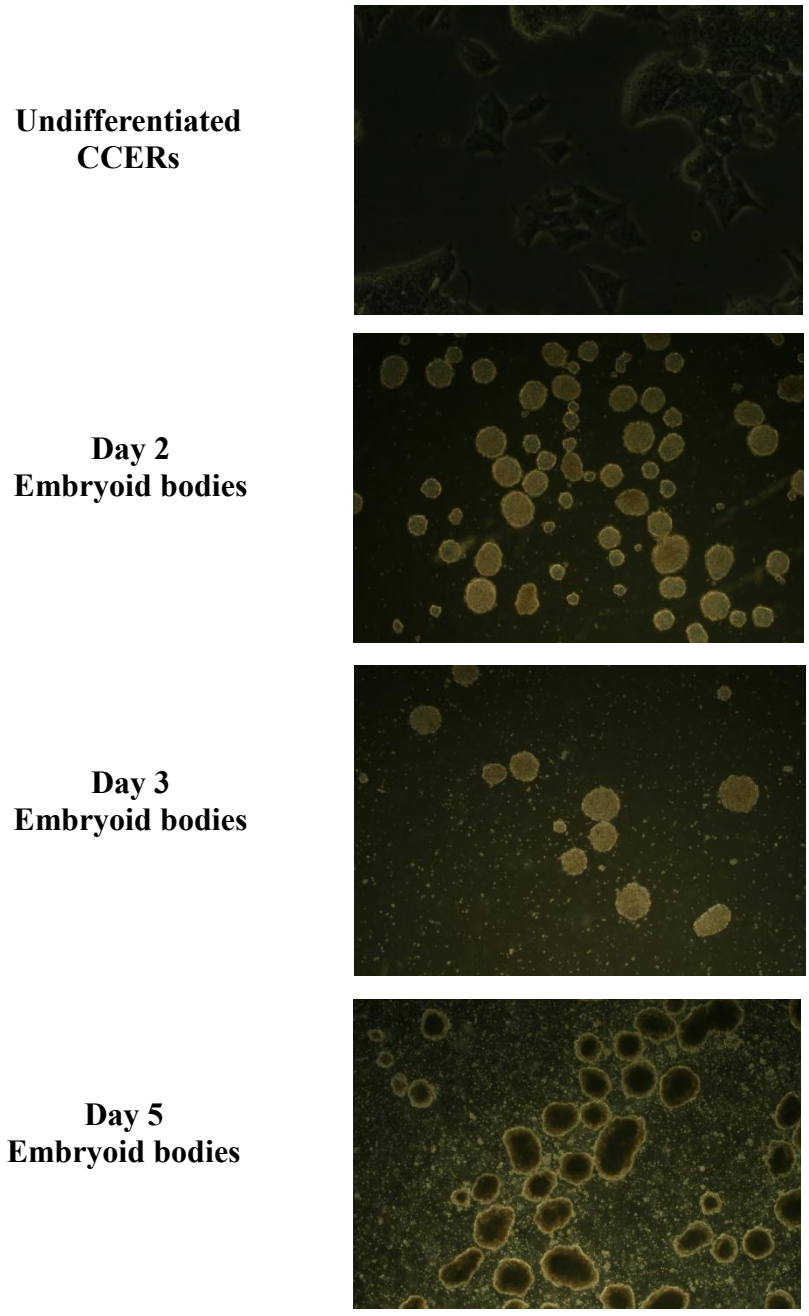

Figure 3-2: Light microscope images were taken of the CCE/Rs on different days of differentiation. The image of the undifferentiated CCE/Rs (day 0) were taken at 40x magnification while images of the embryoid bodies (day2-5) were taken at 2.5x magnification.

Figure 3-3: Quantifying changes in pluripotent gene expression during differentiation

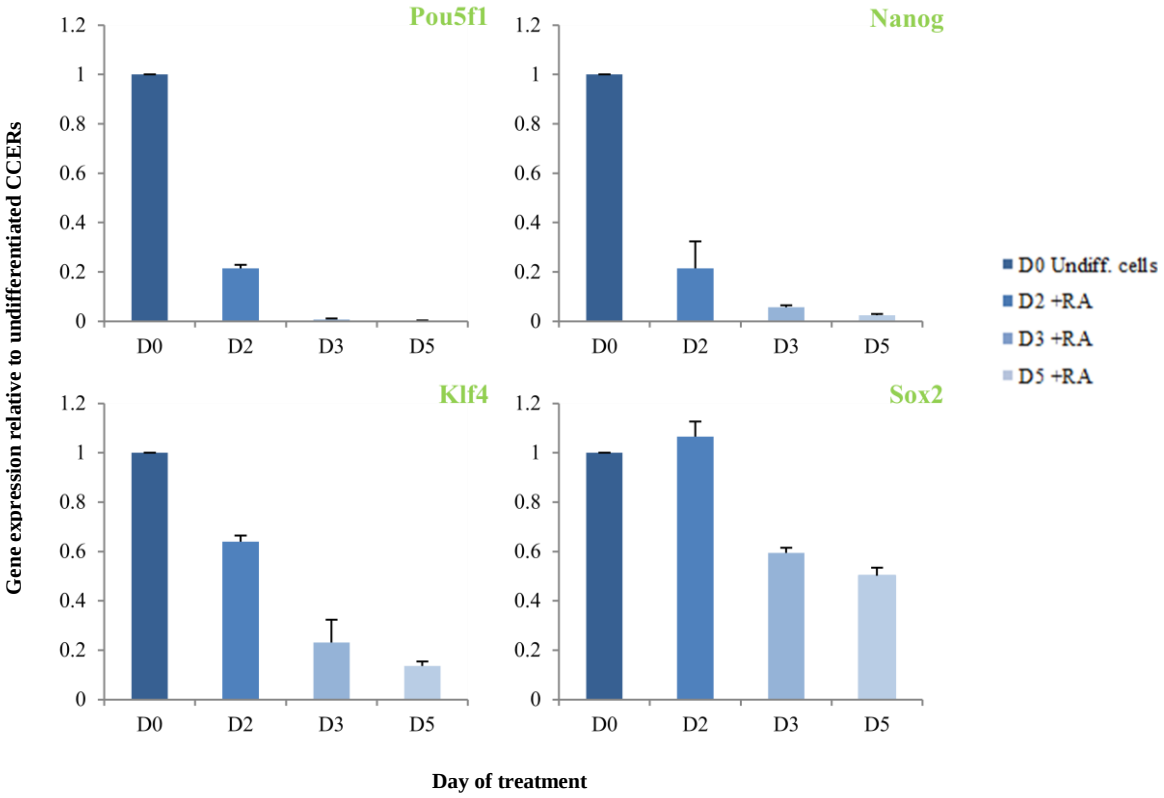

Figure 3-3: qPCR analysis was used to determine the changes in relative mRNA expression levels of pluripotent genes (Pou5f1, Sox2, Nanog and Klf4) during differentiation of CCE/Rs for 5 days. Pluripotent gene expression was calculated relative to the levels at Day 0. The data shows the mean ± standard error of the mean (SEM) of three technical PCR replicates from a single experiment.

Figure 3-4: Quantifying changes in Hoxb gene expression during ESC differentiation

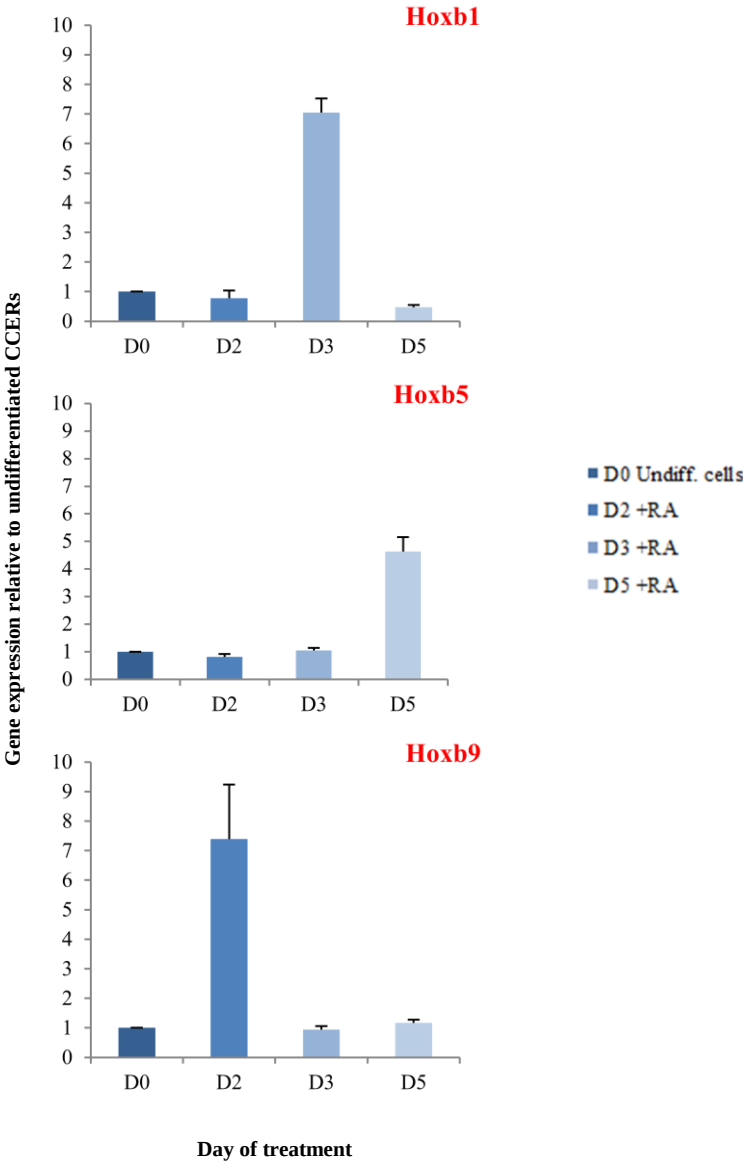

Figure 3-4: qPCR analysis was used to determine the changes in relative mRNA expression levels of the Hoxb1, 5 and 9 genes during differentiation of CCE/Rs for 5 days. Hoxb gene expression was calculated relative to the levels at Day 0. The data shows the mean ± SEM of three technical PCR replicates from a single experiment.

RA, Hoxb5 expression was maintained at the same levels as observed in the undifferentiated cells. At day 5 there was a 4-fold increase in the expression indicating that the gene was expressed at a later stage of differentiation (Figure 3-4). This temporal activation of Hoxb1 and Hoxb5 correlates with the position of the genes within the cluster.

In contrast, the expression of Hoxb9 was not found to correlate with its position in the cluster. Expression was significantly upregulated at day 2 by approximately 8-fold and then declined by day 3 to similar levels as undifferentiated cells (Figure 3-4). The levels then increased marginally by day 5 suggesting that levels may have again increased later on during differentiation (~ day 6 or 7) which would potentially correlate with the position of the genes position in the cluster. However, this was not tested.

3.3.1. Analysis of the native chromatin immunoprecipitation procedure:

The changes in histone modifications that accompany ESC differentiation were analysed by NChIP (Figure 3-5). In brief, the NChIP procedure involved homogenising the cells to release the nuclei. Chromatin was extracted by micrococcal nuclease digestion and solubilised chromatin was isolated (S1). The pellet was dialysed overnight with lysis buffer and solubilised chromatin was collected (S2). The pellet (P) was resuspended in lysis buffer and the three fractions were resolved on an agarose gel to assess the quality of the extracted chromatin. Figure 3-6A shows the quality of the chromatin from day 0 sample. Distinct bands of chromatin into mono-, di-, tri- and tetra-nucleosomes were observed in the S1 fraction indicating that the chromatin had been properly digested. In contrast, the S2 fraction comprises of the larger chromatin fragments obtained after micrococcal nuclease digestion. It is possible that the sample was not digested for a sufficient amount of time and consequently

Figure 3-5: NChIP procedure

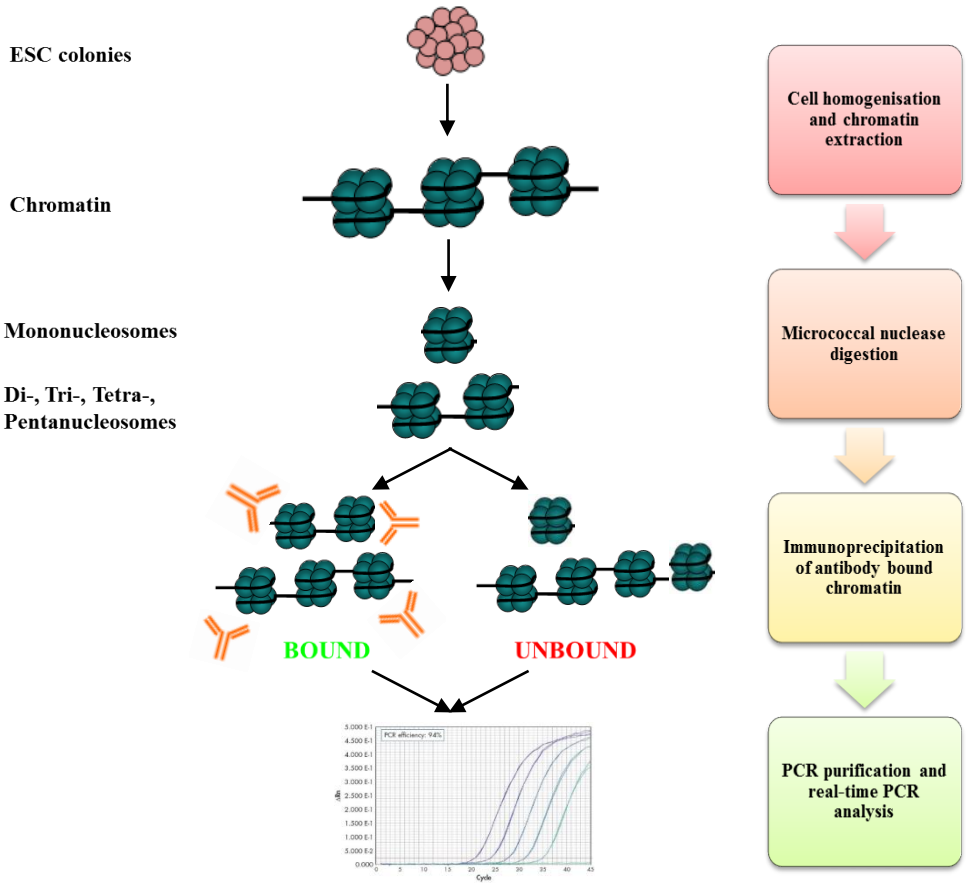

Figure 3-5: Cells at each day of differentiation were homogenised and chromatin was extracted. The chromatin was subsequently digested with micrococcal nuclease into mono-, di, tri-, tetra- and oligonucleosomes. The chromatin was immunoprecipitated with antibodies raised against different histone modifications. The antibody bound chromatin was then immunoprecipitated on protein A Sepharose beads and separated from the unbound fraction. The DNA was then purified and the fold enrichment of the histone modifications at different regions of the genes was analysed by qPCR.

Figure 3-6: NChIP analysis

A

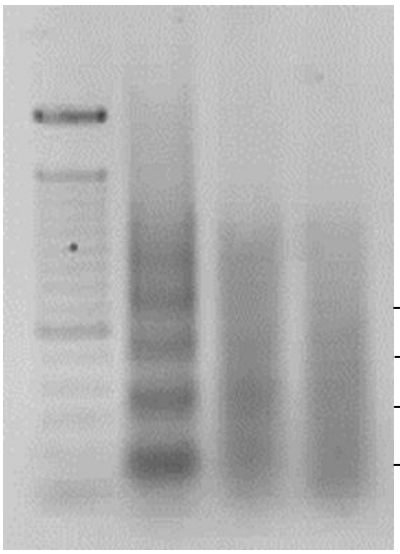

B

Percentage bound (%)	Antibody				
Day of treatment	H3K4me3	H3K27me3	H3K9Ac	H3K9me2	Preimmune
Undifferentiated CCERs	1.064 +/-0.591	7.4005 +/- 1.6105	1.941	2.823	0.7025 +/- 0.1025
D2 CCERs (+RA)	1.16 +/- 0.157	5.649 +/- 2.279	2.3295 +/- 0.979	4.4135 +/- 3.505	0.5675 +/- 0.284
D3 CCERs (+RA)	1.278 +/- 0.095	5.6195 +/- 0.597	2.655 +/-0.514	1.673 +/- 0.986	0.2325 +/- 0.029
D5 CCERs (+RA)	11.074 +/- 10.706	33.345 +/- 27.945	1.5585 +/- 0.879	4.561 +/- 2.719	3.549 +/- 3.185

Figure 3-6: Analysis of the chromatin extracted from CCE/Rs. (A) shows the chromatin from undifferentiated CCE/Rs resolved on a 1.2% agarose gel. The S1 fraction shows the chromatin isolated after micrococcal nuclease digestion. The S2 fraction corresponds to the soluble chromatin taken after overnight dialysis with lysis buffer. The P fraction shows remaining insoluble molecules that could not be digested. The size of the bands was determined using a 100 base pair ladder as a marker. (B) shows the percentage pull down of H3K4me3, H3K27me3, H3K9Ac and H3K9me2 bound DNA on each day of differentiation. The percentage pull down of the Preimmune was also calculated, to serve as a negative control. The pull down would be low because the anti-serum is not raised against any chromatin proteins and therefore DNA should not pulled down. The data shows the mean ± SEM from two NChIP experiments.

distinct bands were not observed (Figure 3-6A). The P fraction appeared as smear on the gel as this contained the high molecular weight insoluble material.

To ensure that the input sample for the immunoprecipitation was representative of the starting material, the solubilised chromatin fractions (S1 and S2) were combined. Chromatin was incubated with antibodies raised against specific histone modifications. The bound chromatin was immunoprecipitated onto beads and the unbound chromatin was collected. The bound chromatin was eluted from the beads and DNA was purified. Equal concentrations of bound and unbound DNA were analysed by qPCR to determine the fold enrichment of the histone modifications on each gene (Figure 3-5).

Chromatin from each sample was incubated with antibodies raised against the H3K4me3, H3K27me3, H3K9ac and H3K9me2 histone modifications. Two active and two repressive marks were selected to determine whether changes in the levels of these modifications correlate with each other during differentiation. Furthermore, these marks were analysed to assess whether changes in the enrichment of each mark correlates with the changes in expression of target genes. A pre-immune no antibody control was also performed for each sample to control for non-specific background signal. Picogreen fluorescence staining was used to determine the concentration of bound and unbound DNA from each sample (Figure 3-5). The percentage bound compared to unbound DNA was then calculated to show the efficiency of the pull down (Figure 3-6B).

The antibody pull down varied depending on the antibody used with the typical pull down varying from 1-33% (Figure 3-6B). The pull down for H3K4me3 and H3K9ac ranged from 1-2% while H3K9me2 had a 2-4% pull down efficiency. The H3K27me3 had the highest pull down efficiency between 5 and 33% which varied depending on the sample tested. As

expected, the pre-immune had a comparatively lower pull down efficiency which ranged between 0.2-3% depending on the sample.

3.3.2. Calculating the fold enrichment of the histone modifications on target genes:

To determine the fold enrichment of the marks, equal concentrations of bound and unbound DNA were analysed by qPCR (Figure 3-7). The delta threshold cycle (ΔC_T) mathematical model was then used to calculate the enrichment of the marks. The C_T value indicates the cycle number at which the fluorescent signal generated by the reaction crosses the threshold and this reflects on the amount of DNA present in the sample. The ΔC_T was given by calculating the difference between the C_T values in the bound and unbound samples. The fold enrichment of each modification was then calculated by applying the formula $\mathbf{2^{(-\Delta C_T)}}$. In order to determine the fold enrichment of a mark on a particular gene, a range of primers corresponding to different regions (promoter region and downstream of the promoter) of individual genes were analysed. This was carried out to determine whether enrichment at specific regions of the gene correlate better with changes in gene expression than others.

3.4. Quantifying changes in the levels of histone modifications on pluripotent genes during differentiation:

Initially, the fold enrichment of H3K4me3 and H3K27me3 on the pluripotent genes Pou5f1 and Nanog were determined (Figure 3-8). The data indicates that in undifferentiated cells there were high levels of H3K4me3 at the Pou5f1 promoter and downstream. However, by day 2 the levels declined by approximately 15-fold at both sites and continued to decline at the promoter on day 3. The levels subsequently rose considerably by day 5 of differentiation at both regions. In contrast, H3K27me3 levels were lowest in the undifferentiated cells and increased marginally by day 2. At both sites, the levels were maintained through day 3 and

Figure 3-7: Quantitative PCR amplification plot

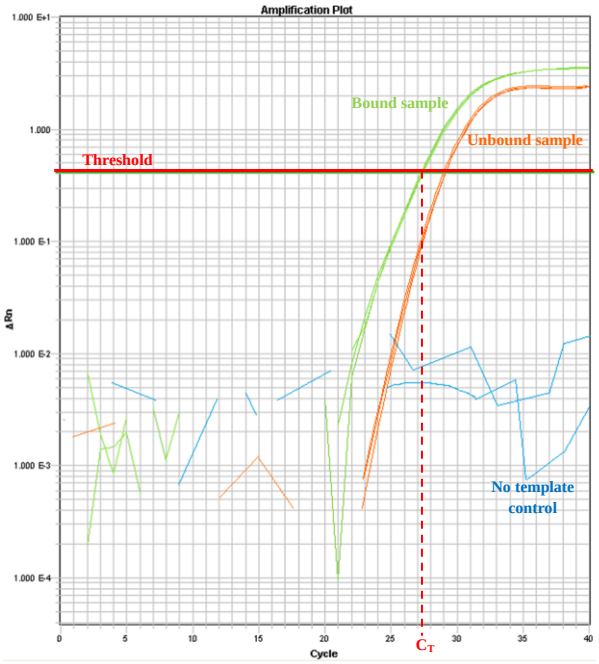

Figure 3-7: qPCR analysis was used to determine the fold enrichment of bound DNA relative to unbound DNA from the NChIP experiments. To quantify the increase in levels of amplicon during the PCR reaction, SYBR green reporter dye was used. The dye binds to nucleic acid in double-stranded DNA and emits a fluorescent signal which is then detected by the machine. Therefore, when the amplification of the product increased, there was a proportional increase in the fluorescence intensity. The ROX^{TM} passive reference dye was used to normalise the reporter dye signal. This was to correct for any changes in volumes or pipetting errors between samples. To normalise the reporter signal, the fluorescence intensity of the reporter dye was divided by the intensity of the passive dye to give the normalised reporter value (Rn). The ΔRn was then determined by calculating the difference between the Rn value from a sample and the Rn value at the baseline.

The bound and the unbound samples show that the PCR reaction begins with an exponential increase in the levels of amplicon which correlates with an exponential increase in the fluorescence emission. Then the reaction reaches a plateau as a result of depletion of reagents required to generate more product. The fluorescence emission from the no template control was significantly below the threshold as no DNA was present, therefore PCR product could not be generated. The C_T value refers to the cycle at which the fluorescence reaches the pre-set threshold level. The threshold was fixed at a point in the exponential phase of the reaction. Samples containing larger amounts of target DNA reached the threshold at an earlier cycle (bound sample) while samples containing less targeted DNA had a higher C_T value (unbound sample). Each PCR reaction was performed in triplicate and the mean C_T value was calculated (as long as the C_T values obtained from the replicates were within half a cycle of each other). Based on the C_T values obtained from the bound and unbound samples, the fold enrichment was determined by calculating the difference between the C_T values of the bound and unbound samples and then applying the formula $\mathbf{2^{-\Delta C_T}}$ to determine the level of enrichment of these modifications.

Figure 3-8: Changes in H3K4me3 and H3K27me3 levels on pluripotent genes during CCE/R differentiation

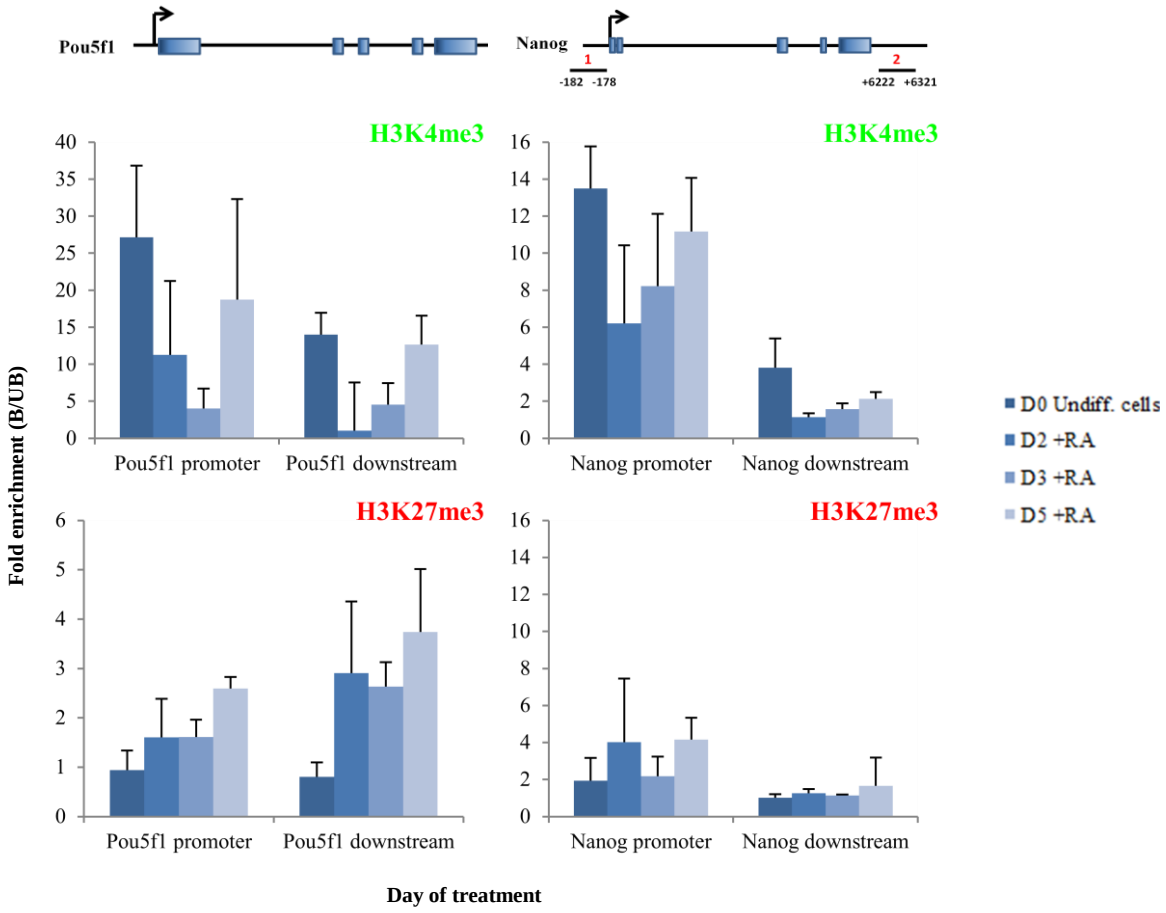

Figure 3-8: Native chromatin immunoprecipitation (NChIP) was used to characterise the changes in histone modifications on the Pou5f1 and Nanog genes that accompany CCE/R differentiation. The levels of H3K4me3 and H3K27me3 (antagonistic marks) at the promoter and downstream of the promoter were analysed. The location of the primers used for the qPCR analysis on the Nanog gene is shown on the map of the gene (above the graph). The fold enrichment of the histone modifications was calculated from the antibody-bound and unbound DNA by qPCR analysis. The data shows the mean ± SEM of three technical repeats using two biological samples.

then rose again moderately by day 5. Importantly, the levels of H3K27me3 on the Pou5f1 gene were much lower than the levels of H3K4me3 and the changes in enrichment were not as significant (Figure 3-8). The data shows that the levels of the active mark were highest in undifferentiated cells while the levels of the repressive mark were lowest. As differentiation proceeded, the levels of active mark declined and the levels of repressive mark were slightly elevated. This correlates with the reduction in the expression of this gene observed during differentiation (Figure 3-3). While the levels of H3K4me3 were high at day 5, this was accompanied by an increase in H3K27me3 levels which may explain why gene expression did not increase.

Similarly, at the Nanog gene (promoter and downstream) H3K4me3 enrichment was higher in undifferentiated CCE/Rs and declined by day 2 (Figure 3-8). However, the decline was significant at the promoter than downstream. At the promoter, the levels then increased marginally by days 3 and rose to a similar level as the undifferentiated cells by day 5. Downstream of the promoter, the levels remained largely unchanged after differentiation. To counteract the high levels of the active modification, there was an increase in H3K27me3 levels during differentiation. At the promoter there were low levels of this mark in undifferentiated cells and then at day 2 the levels increased which correlated with the reduction in Nanog expression observed at day 2 and 3 (Figure 3-3). Interestingly, H3K27me3 enrichment increased at day 5, when the levels of H3K4me3 became elevated which may have counteracted the effect of the increase in H3K4me3 levels. A similar pattern was observed downstream of the promoter, although the changes were not as marked (Figure 3-8).

The levels of H3K9 acetylation and dimethylation on the Pou5f1 and Nanog genes were also determined. There appeared to be no significant change in the levels of H3K9ac and

H3K9me2 at the promoter of Pou5f1 (Figure 3-9). Small changes in enrichment were observed for both marks downstream of the promoter although they were largely negligible. This suggests that these marks do not coordinate the transcription of Pou5f1 during differentiation. At the Nanog promoter, enrichment of H3K9ac was low in undifferentiated CCE/Rs and then increased at day 2. The levels then steadily declined until day 5 of differentiation. These dynamic changes in H3K9ac levels were not accompanied by significant alterations in H3K9me2 levels during differentiation. Downstream of the promoter, H3K9ac levels steadily remained low after differentiation was induced and then increased by ~2-fold at day 5. Simultaneously changes in H3K9me2 enrichment were negligible during differentiation. Therefore, changes in H3K9ac enrichment did not correlate with changes in H3K9me2 levels suggesting that these marks did not influence each other. Furthermore, given that the level of the active mark appears to increase during differentiation, changes in enrichment does not correspond to changes in the expression of the Nanog gene (Figure 3-3).

3.5.1. Quantifying changes in the enrichment of H3K4me3 and H3K27me3 on the Hoxb genes during differentiation:

The fold enrichment of H3K4me3 and H3K27me3 on the Hoxb1, 5 and 9 genes during differentiation was also analysed (Figure 3-10). The data indicates that at the promoter of the Hoxb1 gene (Hoxb1.1) there were low levels of the active H3K4me3 in undifferentiated cells and at day 2. The levels then peaked at day 3 and declined again at day 5. This correlates with the increase in Hoxb1 expression observed at day 3 of differentiation (Figure 3-4) but was not accompanied by a significant change in H3K27me3 levels. This is where the levels were highest in the undifferentiated cells and then marginally decreased after differentiation was

Figure 3-9: Changes in H3K9 acetylation and dimethylation on pluripotent genes during CCE/R differentiation

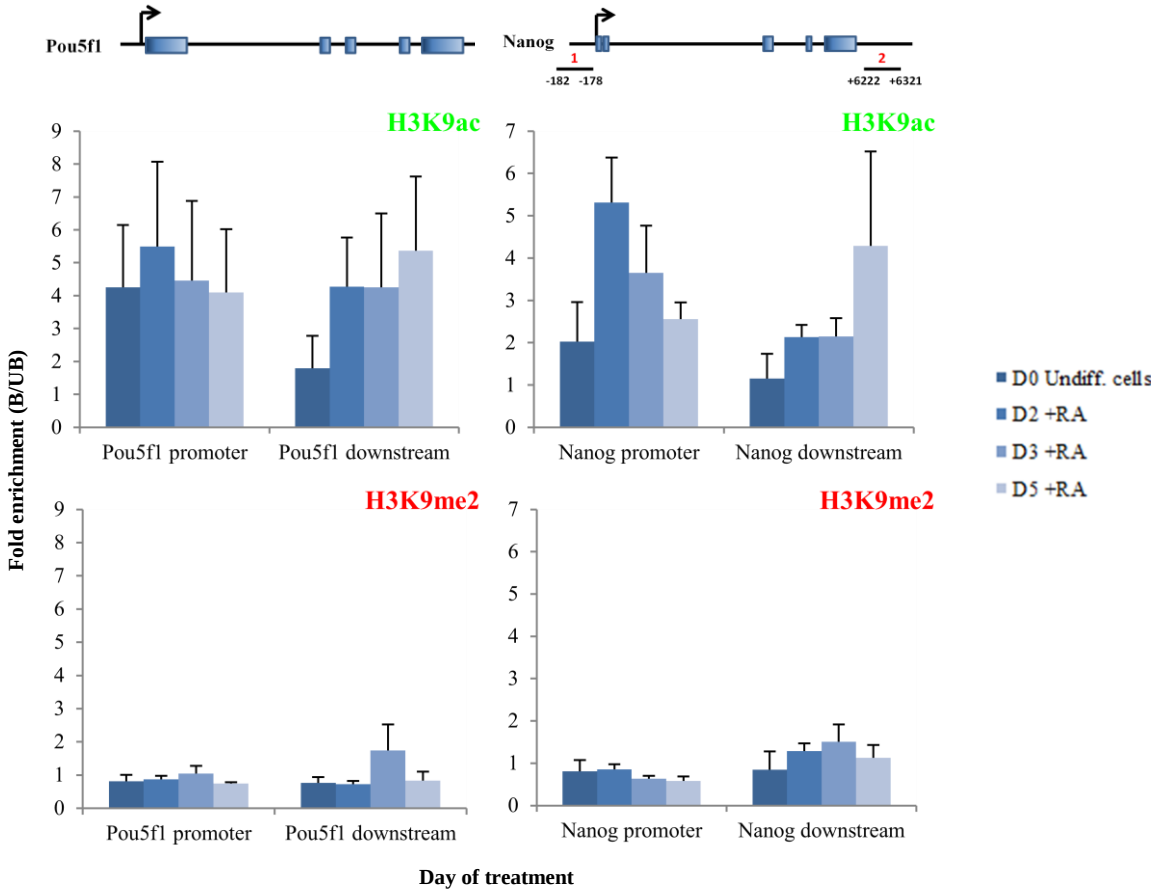

Figure 3-9: NChIP was used to characterise the changes in histone modifications on the Pou5f1 and Nanog genes that accompany CCE/R differentiation. The levels of H3K9Ac and H3K9me2 at the promoter downstream of the promoter were analysed. The fold enrichment of the histone modifications was calculated from the antibody-bound and unbound DNA by qPCR analysis. The data shows the mean ± SEM of two technical repeats using a single biological sample.

Figure 3-10: Changes in H3K4me3 and H3K27me3 levels on Hoxb genes during CCE/R differentiation

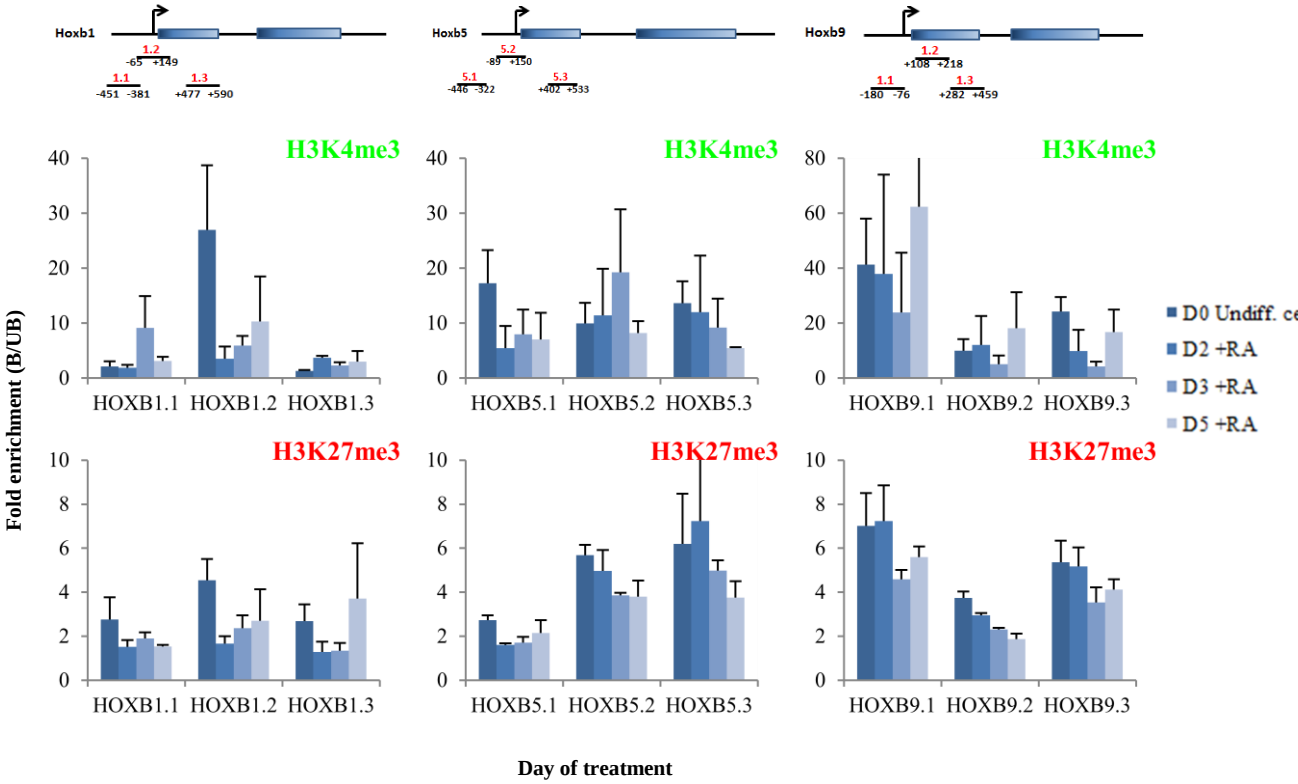

Figure 3-10: NChIP was used to characterise the changes in histone modifications on the Hoxb1, 5 and 9 genes that accompany CCE/R differentiation. The levels of H3K4me3 and H3K27me3 at three different regions of the gene (at the promoter, around the transcriptional start site and further downstream) were analysed. The fold enrichment of the histone modifications was calculated from the antibody-bound and unbound DNA by qPCR analysis. The data shows the mean ± SEM of three technical repeats using two biological samples.

induced (not to the same scale). The levels were then maintained as gene expression was induced.

Further down the gene (Hoxb1.2) the levels of H3K4me3 were found to be highest in undifferentiated cells. The levels of H3K27me3 were also higher at day 0 (not to the same scale). This suggests that the repressive mark was counteracting the effects of the active mark on the gene since there is a low level of Hoxb1 expression in undifferentiated cells. The levels of H3K4me3 and H3K27me3 then decreased by day 2 and then steadily increased as the expression of the gene increased (Figure 3-4). Downstream of the promoter (Hoxb1.3) there was no significant change in H3K4me3 levels during differentiation. There was however a decrease in the enrichment of H3K27me3 at day 2 and 3 when the expression of Hoxb1 increased. The levels then rose considerably by day 5 as gene expression declined. This data suggests that changes in enrichment of these marks across the gene correlate with changes in gene expression observed during differentiation.

The patterning of enrichment on the Hoxb5 gene was similar to the Hoxb1 gene (Figure 3-10) where the levels of H3K4me3 were highest in the undifferentiated cells at the Hoxb5.1 region of the gene. This was accompanied by higher H3K27me3 levels, which correlates with the low levels of Hoxb5 expression observed in undifferentiated cells. At day 2 the enrichment of both marks decreased and then steadied by day 5 although were lower than in undifferentiated cells. At Hoxb5.2, the levels of H3K4me3 steadily increased until it peaked at day 3 and then declined by day 5 while H3K27me3 levels were largely unchanged. At Hoxb5.3, both marks were higher in undifferentiated cells and then steadily declined as differentiation progressed (Figure 3-10). The decline in the enrichment of H3K4me3 by day 5 at all three regions of the gene does not correlate with the increase in the expression of Hoxb5 observed (Figure 3-4).

This suggests that there is no link between the enrichment of these marks and Hoxb5 expression.

Figure 3-10 reveals that across the Hoxb9 gene, the enrichment of H3K4me3 was high in the undifferentiated ESCs and then decreased by day 3. The levels then increased by day 5 to similar or greater levels as undifferentiated cells. The levels of H3K27me3 were also highest in undifferentiated cells and remained high at day 2 across the gene (not to the same scale). However, this does not correlate with the increase in Hoxb9 expression observed at day 2 (Figure3-4). H3K27me3 levels then gradually decreased until day 5 as the levels of H3K4me3 increased at which point Hoxb9 expression began to increase (Figure 3-4). The data suggests that there is no real link between the changes in Hoxb9 expression observed and the patterning of these histone modifications.

3.5.2. Quantifying changes in the enrichment of H3K9ac and H3K9me2 on the Hoxb genes during CCE/R differentiation:

The fold enrichment of H3K9ac and H3K9me2 was also analysed at the different regions of the Hoxb gene (Figure 3-11). The data shows that as differentiation progressed, the levels of the active acetyl mark at the Hoxb1 gene promoter steadily increased and peaked at day 5 (Hoxb1.1 and 1.2) while the levels remained largely unchanged downstream (Hoxb1.3). The levels of H3K9me2 across the Hoxb1 gene were significantly lower and remained largely unchanged during differentiation. Given that the levels did not change significantly at day 3 when Hoxb1 expression increases, it can be deduced that the enrichment of these marks does not reflect changes in transcription during CCE/R differentiation.

Analysis of the H3K9ac mark on the Hoxb5 gene revealed that the levels of this active mark were lowest in undifferentiated cells and significantly increased as differentiation progressed

Figure 3-11: Changes in H39ac and H3K9me2 levels on Hoxb genes during CCE/R differentiation

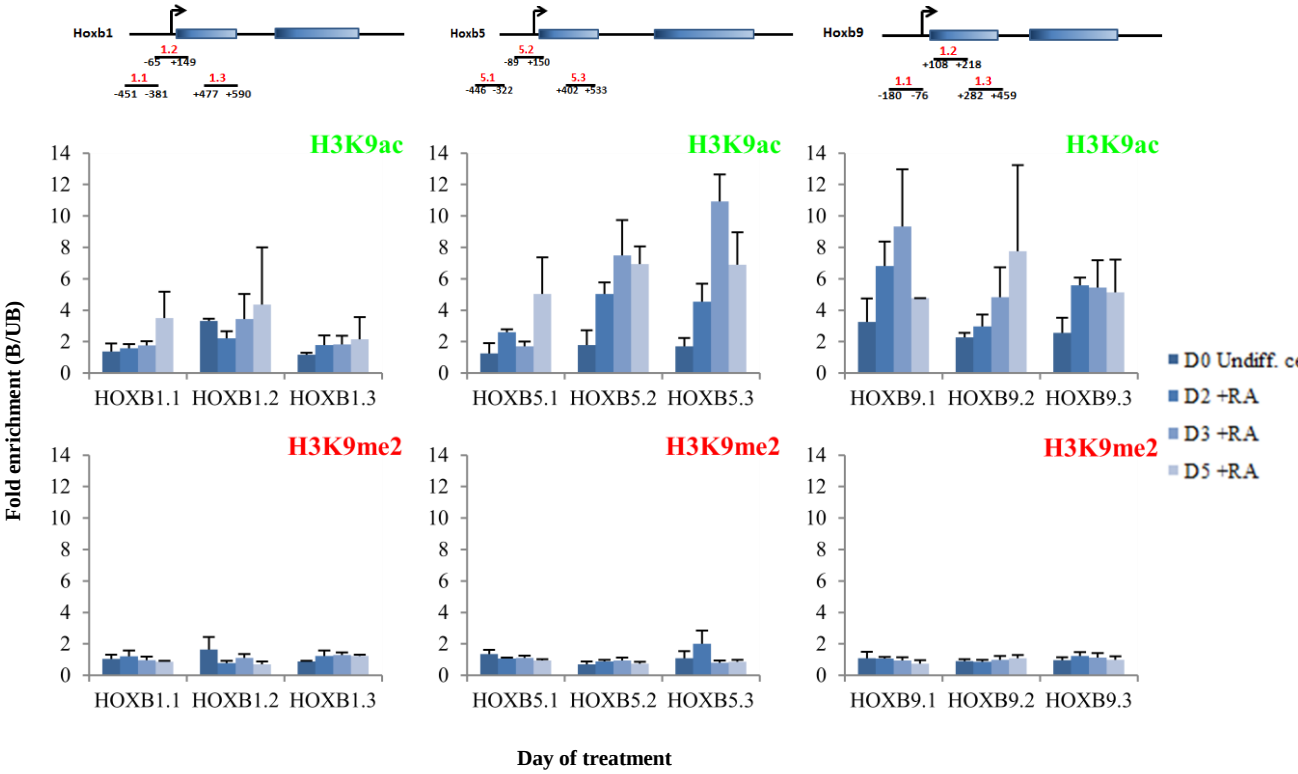

Figure 3-11: NChIP was used to characterise the changes in histone modifications on the Hoxb1, 5 and 9 genes that accompany CCE/R differentiation. The levels of H3K9Ac and H3K9me2 at three different regions of the gene (at the promoter, around the transcriptional start site and further downstream) were analysed. The fold enrichment of the histone modifications was calculated from the antibody-bound and unbound DNA by qPCR analysis. The data shows the mean ± SEM of two technical repeats using a single biological sample.

(Figure 3-11). The highest enrichment was observed at either day 3 or 5 of treatment which correlates with the increase in Hoxb5 expression observed. H3K9me2 enrichment remained largely unchanged across the gene, during differentiation. Analysis of the Hoxb5 gene indicates that H3K9ac may be more important mark for influencing gene expression as its levels seemed to increase as differentiation progressed while H3K4me3 levels remained largely unchanged. Likewise the enrichment of the repressive marks (H3K27me3 and H3K9me2) did not appear to change considerably during differentiation indicating that they did not influence transcription.

At Hoxb9, H3K9ac levels were lower in undifferentiated cells and gradually increased during differentiation (Figure 3-11). Across the gene, the enrichment appeared to be highest at day 3 and day 5 correlating with the timing of Hoxb9 expression (Figure 3-4). The change in H3K9ac across the gene was not accompanied by significant changes in the levels of H3K9me2. This suggests that the levels of active marks on the Hoxb9 gene are higher at the later stage of differentiation (day 5) when the gene is likely to be expressed. However, this does not coincide with significant reductions in the levels of repressive histone marks. Collectively, the data suggests that an increase in the levels of active marks (H3K4me3 and H3K9ac) at day 3 and 5 correlated with the slight increase in the expression of the gene observed at this stage of differentiation. However, the increase in expression observed at day 2 did not correspond with changes in histone modifications.

3.6. Patterning of histone modifications across the Hoxa1, 5 and 9 genes:

To determine whether the patterning of modifications on the Hoxb genes correlate with changes at the Hoxa cluster, the enrichment of these marks were analysed on Hoxa1, 5 and 9 (Figure 3-12). On Hoxa1 and 9, H3K4me3 levels were highest in undifferentiated cells and

Figure 3-12: Changes in levels of histone modifications on Hoxa genes during CCE/R differentiation

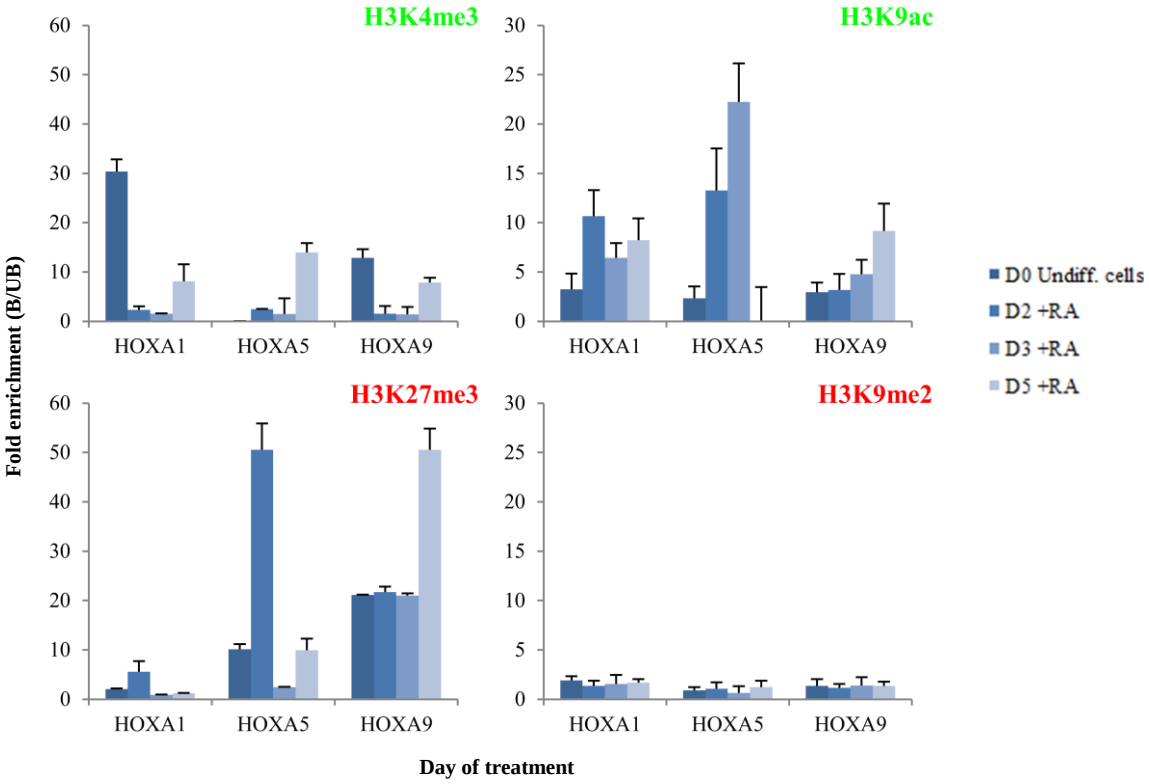

Figure 3-12: NChIP was used to determine whether the changes in histone modifications on the Hoxb1, 5 and 9 genes during differentiation correlate with changes in the levels on the corresponding Hoxa genes. The levels of H3K4me3, H3K27me3, H3K9Ac and H3K9me2 were analysed. The fold enrichment of the histone modifications was calculated from the antibody-bound and unbound DNA by qPCR analysis. The data for the H3K4me3 and H3K27me3 shows the mean ± standard error of the mean (SEM) of three technical repeats performed using two biological samples. The data for H3K9Ac and H3K9me2 shows the mean ± SEM of two technical repeats using a single biological sample.

then rapidly declined upon differentiation but then rose rapidly at day 5. At Hoxa1, this did not correspond with changes in H3K27me3 levels whereas on Hoxa9 the levels of H3K27me3 increased significantly at day 5. The levels of H3K4me3 on the Hoxa5 gene were found to increase at day 2 and then decline by day 3 (Figure 3-12). A similar pattern was also observed with H3K27me3 levels at day 2 and 3. H3K27me3 levels then increased at day 5 as H3K4me3 levels increased. The enrichment of these marks on the Hoxa genes during differentiation does not appear to correlate with changes in the Hoxb cluster.

Enrichment of H3K9ac and H3K9me2 on the Hoxa genes were also analysed (Figure 3-12). On the Hoxa1 gene, H3K9ac levels were lowest in the undifferentiated cells and then became elevated by day 2. The levels dropped slightly at day 3 and were maintained until day 5. Changes in the enrichment of H3K9me2 were negligible during differentiation. However, it was observed that the levels were highest in the undifferentiated cells when H3K9ac levels were low and then decreased slightly by day 2 as H3K9ac enrichment increased. The levels then gradually increased again by day 5 which shows that as the levels of the active mark increased, the levels of the repressive mark declined and vice versa. This pattern of enrichment was not observed at any region of the Hoxb1 gene (Figure 3-11).

At the Hoxa5 gene, H3K9ac levels increased as differentiation progressed with the highest levels being achieved at day 3 of differentiation. Analysis of H3K9me2 enrichment revealed that the levels were high until day 2 and then dropped as H3K9ac levels were elevated on day 3. The levels then rose at day 5 while H3K9ac enrichment declined considerably. At the Hoxa9 gene, H3K9ac levels were found to gradually increase as differentiation progressed while the levels of H3K9me2 remained largely unchanged. This pattern of enrichment on Hoxa9 was similar to that on the Hoxb9 gene where the levels of the active gene increased as differentiation progressed while the levels of the repressive mark was largely unchanged.

Collectively, the data suggests that the changes in the pattern of enrichment for all four histone modifications on the Hoxa1, 5 and 9 genes did not correlate with changes in the patterning on the corresponding Hoxb genes. This suggests that while genes in both clusters show similar patterns of expression, the enrichment of specific histone modifications vary.

3.7. The effect of cell differentiation on the histone marks present on the housekeeping gene GAPDH:

Analysis of Gapdh expression revealed that the levels were largely maintained during differentiation with the highest levels observed in the undifferentiated cells (Figure 3-13A). The levels then slightly decreased at day 2 and 3 and then rose again by day 5. Although the changes in expression were negligible which is expected given that it is a housekeeping gene. The enrichment of histone modifications on the Gapdh gene were also analysed (Figure 3-13B) and the data indicates that at the promoter (GAPDH1) changes in H3K4me3, H3K27me3 and H3K9ac levels were negligible (not to the same scale) and the fold enrichment was low. Conversely, H3K9me2 enrichment marginally increased as differentiation progressed. Surprisingly, downstream of the promoter (GAPDH2) the levels of H3K4me3 began to decline as differentiation was induced while the levels of H3K27me3 sharply increased at day 5. This was unexpected given that the levels of H3K9ac appear to increase as differentiation progressed and this was accompanied by a progressive decline in H3K9me2 levels. This data correlates with the expression data shown in Figure 3-13A since the levels of active mark are considerably higher on the gene at each stage of differentiation while the levels of repressive mark were much lower. The lack of changes in the enrichment of these histone modifications at GAPDH1 during differentiation correlates with the maintenance of Gapdh expression during differentiation. However, at GAPDH2 the levels

Figure 3-13: Changes in expression and levels of histone modifications on Gapdh during CCE/R differentiation

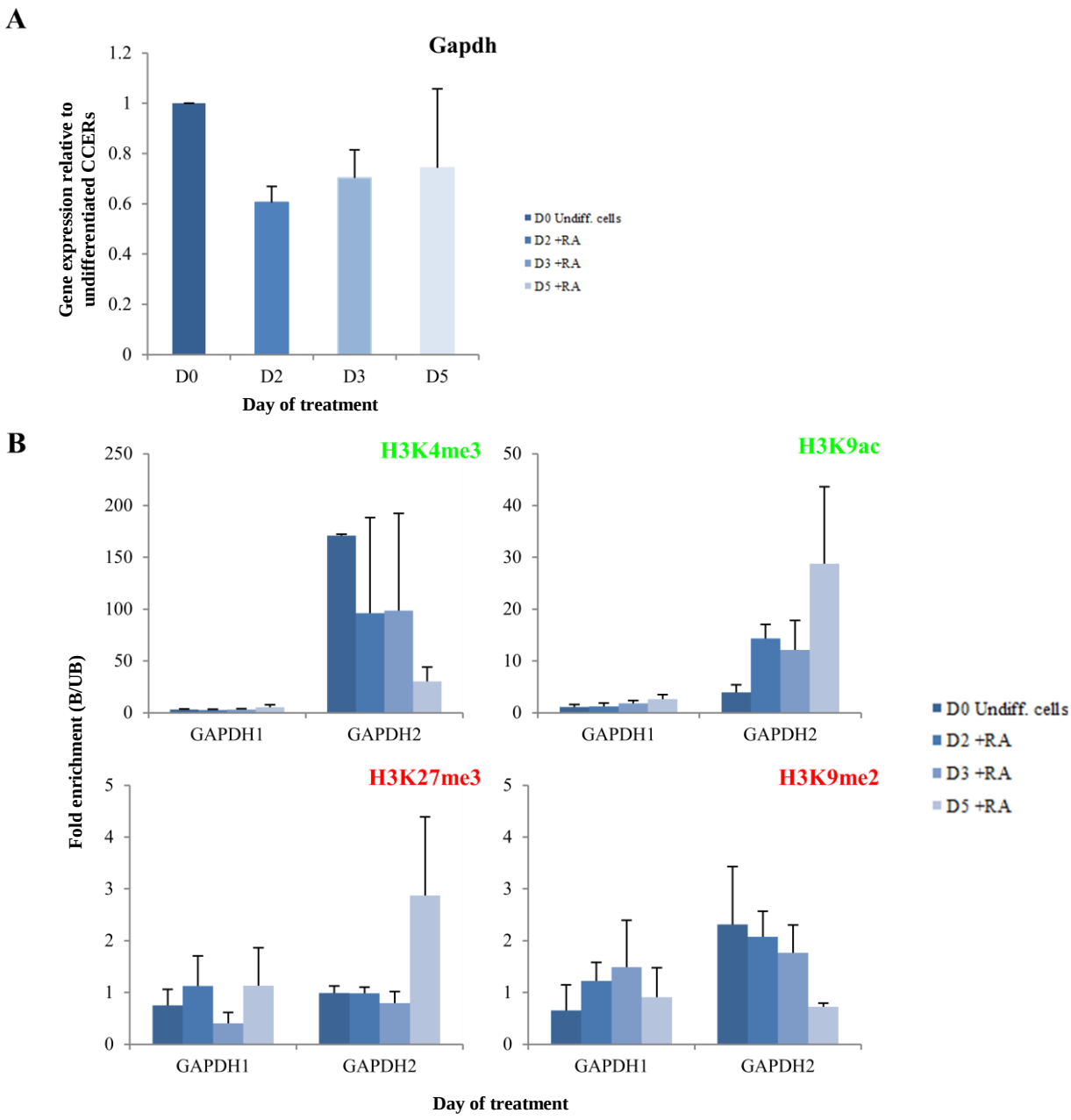

Figure 3-13: qPCR and NChIP analyses were used to determine the changes in expression of Gapdh and whether that correlates with changes in the level of histone modifications during CCE/R differentiation. (A) shows the expression of Gapdh for each sample during differentiation. (B) shows the levels of H3K4me3, H3K27me3, H3K9Ac and H3K9me2 present at two distinct regions of the gene. The fold enrichment of the histone modifications was calculated from the antibody-bound and unbound DNA by qPCR analysis. The data for the H3K4me3 and H3K27me3 shows the mean ± standard error of the mean (SEM) of three technical repeats performed using two biological samples. The data for H3K9Ac and H3K9me2 shows the mean ± SEM of two technical repeats performed using a single biological sample. For the expression analysis, the data shows the mean ± standard error of the mean (SEM) of three technical PCR replicates from a single experiment.

varied significantly. Therefore, normalisation of the data to Gapdh was not performed as the epigenetic state of the gene was not maintained during differentiation.

4. DISCUSSION:

Combinations of histone modifications are thought to influence the transcription of target genes by recruiting a range of transcriptional regulators. Therefore, enrichment of histone marks can be used to predict target gene expression. In this study the changes in enrichment of histone modifications on the transcriptionally poised Hoxb genes during ESC differentiation was analysed. H3K4me3, H3K27me3, K3K9Ac and H3K9me2 enrichment was assessed to determine whether combinations of these marks reflect the patterns of gene expression observed.

Analysis of pluripotent gene expression revealed that as expected expression of these genes significantly decreased as differentiation was induced. The decline in expression of Pou5f1 and Nanog was accompanied by a progressive decrease in the levels of active H3K4me3 and an increase in repressive H3K27me3 during differentiation (Figure 3-8). This enrichment pattern was not observed with H3K9ac and H3K9me2 during differentiation (Figure 3-9). These findings suggest that H3K4me3 and H3K27me3 enrichment act as indicators of the transcriptional state of pluripotent genes. Also given that the genes are more enriched for H3K4me3 than H3K9ac, it can be deduced that the former mark has a greater influence on gene transcription.

For Hoxb1 and 5 it was observed that changes in histone modifications during differentiation correlated with the temporal and spatial patterning of gene expression. Hoxb1 expression was upregulated at day 3 (Figure 3-4) of differentiation and this was accompanied by high levels of H3K4me3 at the promoter and low levels of H3K27me3 (Figure 3-10). However, this pattern of modifications was not observed at Hoxb1.2 and 1.3. At all three regions of the gene however, changes in H3K9ac and H3K9me2 levels were negligible (Figure 3-11) indicating

that the levels of these marks at the promoter do not significantly influence Hoxb1 transcription. Conversely, the increase in Hoxb5 expression observed at day 5 of differentiation was accompanied by a progressive increase in H3K9ac enrichment during differentiation (Figure 3-11). The levels of H3K9me2 and H3K27me3 were negligible while H3K4me3 levels declined during differentiation. This suggests that only the levels of the active H3K9ac influenced the transcription of the target gene. Therefore, while Hoxb1 and 5 are in the same cluster, the expression of the genes is influenced by different histone modifications. The pattern of histone modifications observed on the Hoxb9 gene did not correlate with the changes in gene expression observed during differentiation. Hoxb9 should be expressed at a later stage of differentiation (~day 7), however in this study the gene was found to be upregulated at day 2 (Figure 3-4). This is unusual since Hoxb9 is located at the 5' end of the cluster and should be expressed later than Hoxb5. The levels of histone modifications were not consistent with the changes in gene expression observed. Although an increase in H3K9ac enrichment was observed at day 2 of differentiation when gene expression was found to increase however the enrichment remained high at day 3 when expression rapidly declined suggesting that this mark did not influence Hoxb9 transcription.

Interestingly, changes in fold enrichment of the histone marks on the Hoxb genes did not correspond with changes in levels on the Hoxa genes despite the genes having similar expression patterns during differentiation (Figure 3-12). This suggests that these genes may be enriched with a different set of modifications which in turn influence the transcription. Analysis of histone marks on the Gapdh gene revealed that the epigenetic state of the gene is not maintained during differentiation. The levels of active marks were found to be higher downstream of the promoter compared with the repressive marks. This is expected since the gene is constitutively expressed during differentiation (Figure 3-13B). H3K4me3 levels

declined during differentiation while H3K9ac levels increased which indicates that the presence of a particular active mark may vary but high levels of active mark are always present. This correlates with the maintenance of expression observed during differentiation (Figure 3-13A).

During the study it was observed that the enrichment of H3K4me3 on all genes was much higher than the other modifications. However, when comparing absolute levels of histone modifications it is important to take into consideration the differences in antibody pull down efficiencies. The difference is controlled for by ensuring that the same concentration of bound and unbound DNA is amplified during quantitative PCR. Nevertheless, differences in pull down efficiencies must be considered when comparing absolute levels.

The results indicate that the changes in histone modification during differentiation correlate with the changes in gene expression observed but did not appear to be predictive of the patterning of gene expression. The presence of high levels of H3K4me3 and H3K27me3 on the Hoxb5 and 9 genes in undifferentiated cells indicates that a bivalent chromatin signature was present on these genes that kept them in a transcriptionally poised state. RA may have induced the expression of these genes by reducing H3K27me3 enrichment. Given that these genes are less sensitive to RA it would explain why they are expressed later on during differentiation [18].

The patterning of H3K4me3 and H3K27me3 were found to correlate with each other on most genes. This is where an increase in levels of active mark coincided with a decrease in the levels of repressive mark and vice versa. These modifications have opposing effects on gene expression by recruiting different protein complexes which regulate expression. On the Hox genes, components of the Polycomb repressor complex bind to regions enriched with

H3K27me3 and repress Hox gene expression [34]. Conversely regions of genes with H3K4me3 enrichment recruit Trithorax proteins which act by promoting gene expression [34]. These complexes have opposing effects on Hox gene expression therefore, the balance between the activity of these complexes dictates the transcriptional status of the gene.

The data showed that the enrichment of the histone modifications at the promoter of the genes correlates with the patterning of gene expression during differentiation to a greater extent than the levels downstream of the promoter; with the exception of Gapdh. This indicates that marks which regulate transcriptional initiation are more relevant than those that regulate elongation. Furthermore, it was found that enrichment of a particular mark correlated with changes in transcription of certain genes but not others. This indicates that while a certain mark may be enriched on target genes it does not necessarily mean that it will influence its expression. This is because the effects of other marks may counteract its action. Therefore, analysing the enrichment of individual modifications is not sufficient for understanding how gene expression is regulated.

In conclusion, the data indicates that changes in pluripotent and Hox gene expression correlates with variations in the enrichment of specific histone modifications. It was observed that changes in H3K4me3 and H3K27me3 enrichment were more relevant than changes in H3K9ac and H3K9me2 levels. However, the data suggests that while these marks were not predictive of the patterning of gene expression, the levels reflect the transcriptional status of genes.

Hox genes provide a good model system for analysing epigenetic regulation of gene transcription in embryonic stem cells (ESCs) given that the pattern of expression is coordinated. However, in this study a mouse ESC line was used to analyse enrichment of

marks on Hox genes during differentiation. There are limitations in the extent to which ESC lines mimic embryonic development *in vivo*. Furthermore, although Hox genes are highly conserved, the actions of the proteins that deposit histone marks on the genes and those that regulate gene transcription in response to the presence of these marks are vary between mouse and human. Therefore, enrichment of enrichment of these marks should also be tested in human embryonic stem cells. In addition, to determine whether changes in epigenetic marks observed in this study occur during development, the presence of these marks should be analysed in embryos.

Analysis of epigenetic regulation of Hox gene expression can be used to understand how gene expression is tightly regulated in cells. This is important since changes in histone modifications have been implicated in the development of a range of diseases, namely cancer. Histone modifying enzymes are often mutated in cancers. Consequently, understanding how histone modifications are altered in the diseased state and the effect that it has on the disease progression will enable novel diagnostic markers and treatment targets to be identified. Therefore, characterising the function of different histone modifications in regulating gene expression can be used to identify which marks are involved with tumourigenesis.

Furthermore, elucidating the way in which histone modifications alter gene transcription may be used in induced pluripotent stem cell (iPSC) technology. These cells are generated by introducing exogenous pluripotency factors into the cell which causes cells to be reprogrammed into a pluripotent state. It is currently unclear how the introduction of these transgenes into the cell leads to the reactivation of endogenous pluripotent genes [35]. Given that addition of histone deacetylase inhibitors has been shown to enhance the efficiency of reprogramming it is apparent that changes in histone modifications on the pluripotent genes may promote reactivation of endogenous pluripotent genes [35]. Therefore, analysing changes

in histone modifications on pluripotent genes during differentiation may explain how the genes are reactivated during reprogramming.

5. BIBLIOGRAPHY:

(1) O'Shea KS (2004). Self renewal vs. differentiation of mouse embryonic stem cells. Biology of Reproduction; 71: p1755-1765.

(2) Chambers I (2004). The molecular basis of pluripotency in mouse embryonic stem cells. Cloning Stem Cells; 6: p386-391.

(3) McKiernan E, O'Driscoll L, Kasper M, Barron N, O'Sullivan F and Clynes M (2007). Directed differentiation of mouse embryonic stem cells into pancreatic-like or neuronal- and glial-like phenotypes. Tissue Engineering; 13(10): p2419-2430.

(4) Murry CE, Keller G (2008). Differentiation of embryonic stem cells to clinically relevant populations: lessons from embryonic development. Cell; 132(4): p661-680.

(5) Hamazaki T, Oka M, Yamanaka S, Terada N (2004). Aggregation of embryonic stem cells induces Nanog repression and primitive endoderm differentiation. Journal of Cell Science; 117: p5681-5686.

(6) Bernstein BE, Mikkelsen TS, Xie X, Kamal M, Schreiber SL, Lander ES (2006). A Bivalent Chromatin Structure Marks Key Developmental Genes in Embryonic Stem Cells. Cell; 125(2): p315-326.

(7) Ivanova N, Dobrin R, Lu R, Levorse J, Lemischka IR et al. (2006). Dissecting self-renewal in stem cells with RNA interference. Nature; 442(712): p533-538.

(8) Takahashi K, Yamanaka S (2006). Induction of pluripotent stem cells from mouse and adult fibroblast cultures by defined factors. Cell; 126: p663-676.

(9) Lowry WE, Quan WL. Roadblocks en route to the clinical application of induced pluripotent stem cells. Journal of Cell Science. 2010; 123(5): 643-651.

(10) Graf U, Casanova EA, Cinelli P (2011). The Role of the Leukemia Inhibitory Factor (LIF) — Pathway in Derivation and Maintenance of Murine Pluripotent Stem Cells. Genes; 2: p280-297.

(11) Frischer LE, Hagen FS, Garber RL (1986). An inversion that disrupts the Antennapedia gene causes abnormal structure and localisation of RNAs. Cell; 47(6): p1017-1023.

(12) Shah N, Sukumar S (2010). The Hox genes and their role in oncogenesis. Nature Reviews Cancer; 10: p361-371.

(13) Castelli-Gair J (1998). Implications of the spatial and temporal regulation of Hox genes on development and evolution. International Journal of Developmental Biology; 42: p437-444.

(14) McGinnis W Krumlauf R (1992). Homeobox genes and axial patterning. Cell; 68(2): p283-302.

(15) Daftary GS, Taylor HS (2006). Endocrine regulation of HOX genes. Endocrine Reviews; 27(4): p331-355.

(16) Barber RA, Rastegar M (2010). Epigenetic control of Hox genes during neurogenesis, development and disease. Annals of Anatomy; 192(5): p261-274.

(17) Roelen BA, de Graaff W, Forlani S, Deschamps J (2002). Hox cluster polarity in early transcriptional availability: a high order regulatory level of clustered Hox genes in the mouse. Mechanisms of Development; 119(1): p81-90.

(18) Chamberyron S, Bickmore WA (2004). Chromatin decondensation and nuclear reorganisation of the HoxB locus upon induction of transcription. Genes and development; 18: p1119-1130.

(19) Loden M, van Steensel B (2005). Whole genome views of chromatin structure. Chromosome Research; 13(3): p289-298.

(20) Marino-Ramirez L, Kann MG, Shoemaker BA, Landsman D (2005). Expert Review Proteomics; 2(5): p719-729.

(21) Li E (2002). Chromatin modification and epigenetic reprogramming in mammalian development. Nature Review Genetics; 3: p662-673.

(22) Riester D, Hildmann C, Grunewald S, Beckers T, Schwienhorst A (2007). Factors affecting the substrate specificity of histone deacetylases. Biochemical and Biophysical Research Communications; 357(2): p439-445.

(23) Bannister AJ, Kouzarides T (2005). Reversing histone methylation. Nature; 436: p1103-1106.

(24) Henikoff S (2005). Histone modifications: Combinatorial complexity or cumulative simplicity? PNAS; 102(15): p5308-5309.

(25) Thorne JL, Campbell MJ, Turner BM (2009). Transcription factors, chromatin and cancer. International Journal of Biochemistry and Cell Biology; 41(1): p164-175.

(26) Barski A, Cuddapah S, Cui K, Roh TY, Schones DE, Zhao K (2007). High-Resolution Profiling of Histone Methylations in the Human Genome. Cell; 129(4): p823-837.

(27) Hartzog GA, Tamkun JW (2007). A new role for histone tail modifications in transcriptional elongation. Genes and development; 21(24): p3209-3213.

(28) Meshorer E, Misteli T (2006). Chromatin in pluripotent embryonic stem cells and differentiation. Nature Reviews Molecular Cell Biology; 7(7): p540-546.

(29) Hyslop LA, Armstrong L, Stojkovic M and Lak M (2005). Derivation of a human embryonic stem cell line, and differentiation strategies. Expert Reviews in Molecular Medicine; 7(19).

(30) http://www.mun.ca/biology/desmid/brian/BIOL2060/BIOL2060-18/CB18.html - The nucleosome structure.

(31) Felsenfeld G, Groudine M (2003). Controlling the double helix. Nature; 42: p448-453.

(32) Spotswood HT, Turner BM (2002). An increasingly complex code. Journal of Clinical Investigation; 110: p577-582.

(33) Li B, Carey M, Workman JL (2007). The role of chromatin during transcription. Cell; 128: p707-719.

(34) Schuettengruber B, Ganapath M, Leblanc B, Portoso M, Jaschek R, Cavalli G et al. (2009). Functional Anatomy of Polycomb and Trithorax Chromatin Landscapes in Drosophila Embryos. PLoS Biology; 7(1): e1000013.

(35) Maherali N, Sridharan R, Xie W, Utikal J, Tchieu J, Hochedlinger K et al. (2007). Directly Reprogrammed Fibroblasts Show Global Epigenetic Remodeling and Widespread Tissue Contribution. Cell Stem Cell; 1: p55-70.